CO-PRODUCTION OF YEAST OIL AND β-CAROTENE BY BIODIESEL-BASED CRUDE GLYCEROL FROM POLYURETHANE FOAM AND BIOACTIVE INGREDIENT SYNTHESIS

SASITORN KHUNTONG

A THESIS SUBMITTED IN PARTIAL FULLFILLMENT OF THE REQUIREMENT FOR THE DEGREE OF MASTER OF SCIENCE PROGRAM IN APPLIED BIOLOGY

FACULTY OF SCIENCE AND TECHNOLOGY

RAJAMANGALA UNIVERSITY OF TECHNOLOGY THANYABURI

ACADEMIC YEAR 2024

CO-PRODUCTION OF YEAST OIL AND β-CAROTENE BY BIODIESEL-BASED CRUDE GLYCEROL FROM POLYURETHANE FOAM AND BIOACTIVE INGREDIENT SYNTHESIS

SASITORN KHUNTONG

A THESIS SUBMITTED IN PARTIAL FULLFILLMENT OF THE REQUIREMENT FOR THE DEGREE OF MASTER OF SCIENCE PROGRAM IN APPLIED BIOLOGY

FACULTY OF SCIENCE AND TECHNOLOGY

RAJAMANGALA UNIVERSITY OF TECHNOLOGY THANYABURI

ACADEMIC YEAR 2024

Thesis Title	Co-Production of Yeast Oil and β-Carotene from Biodiesel-Based Crude Glycerol for Polyurethane Foam and Bioactive Ingredient Synthesis
Name – Surname	Miss Sasitorn Khuntong
Program	Applied Biology
Thesis Advisor	Associate Professor Atsadawut Areesirisuk, Ph.D.
Academic Year	2024

THESIS COMMITTEE

Kamonchai Cha-aim ..... Chairman

(Assistant Professor Kamonchai Cha-aim, Ph.D.)

Thanasak Lomthong ..... Committee

(Associate Professor Thanasak Lomthong, Ph.D.)

Jantima Teeka ..... Committee

(Assistant Professor Jantima Teeka, Ph.D.)

Atsadawut Areesirisuk ..... Committee

(Associate Professor Atsadawut Areesirisuk, Ph.D.)

Approved by the Faculty of Science and Technology, Rajamangala University of Technology Thanyaburi in Partial Fulfillment of the Requirements for the Master's Degree

Nipat Jongsawat .....Dean of Faculty of Science and Technology

(Assistant Professor Nipat Jongsawat, Ph.D.)

30 April 2025

Thesis Title	Co-Production of Yeast Oil and β-Carotene by Biodiesel-Based Crude Glycerol from Polyurethane Foam and Bioactive Ingredient Synthesis
Name – Surname	Miss Sasitorn Khuntong
Program	Applied Biology
Thesis Advisor	Associate Professor Atsadawut Areesirisuk, Ph.D.
Academic Year	2024

Abstract

Co-producing yeast oil (YO) and β-carotene from biodiesel-derived crude glycerol (BCG) offers a promising approach for high-value bioproduct synthesis and sustainable waste valorization. This study aimed to: 1) investigate the effect of surfactant and osmotic pressure on YO and β-carotene co-production by *Rhodosporidium toruloides* using BCG-based medium, 2) improve production efficiency through an integrated cell retention system, and 3) explore practical applications of polyurethane foam production and β-carotene encapsulation.

The effects of various inducer on YO and β-carotene co-production were systematically evaluated. *R. toruloides* cultivation was conducted using continuous fermentation integrated with cell retention (CF-CR) system to enhance production efficiency. The produced YO and β-carotene were subsequently applied to manufacture polyurethane (PU) foam and encapsulated powder, respectively.

Results revealed that Tween 20 and ethephon significantly increased total yeast oil and total β-carotene production, with their combined use yielding 2.0 and 2.6-fold increases, respectively, in bioreactor conditions compared to flask cultivation. The CF-CR process enhanced total biomass and total oil by 1.55 and 1.86-fold compared to continuous fermentation alone. The YO primarily consisted of C16 and C18 long-chain fatty acids. YO was successfully transformed into both rigid and semi-rigid PU foams. Additionally, the encapsulated β-carotene extract exhibited notable antimicrobial activity and stability under light conditions.

Keywords: co-production process, oil, β-carotene, polyurethane foam, encapsulation

Acknowledgments

This research was fully supported by Fundamental Fund scholarship from the Thailand Science Research and Innovation (TSRI) Promotion Funding.

Secondly, I would like to express sincere gratitude to my advisor, Associate Professor Dr. Atsadawut Areesirisuk, for the superb tutorial, the valuable guidance, encouragement, help, and all support throughout this thesis.

Thirdly, I acknowledge my co-advisor, Assistant Professor Dr. Jantima Teeka for also making suggestions and supporting my thesis.

Fourth, I would like to thank the thesis committee, Assistant Professor Dr. Kamonchai Cha-aim and Associate Professor Dr. Thanasak Lomthong for valuable comments and helpful suggestions.

Subsequently, I would especially like to thank my friends, sister, Bioengineering lab members, and the Division of Biology, Faculty of Science and Technology, RMUTT, for their help and support throughout this research.

Finally, I am especially thankful to my parents and family for their major encouragement, sincere love, and support of everything.

Sasitorn Khuntong

Table of Content

Page

List of Tables

Page

List of Figures

Page

List of Figures (Continued)

Page

List of Abbreviations

Nomenclature

ACL	: ATP:citrate lyase
ACC	: Acetyl-CoA carboxylase
BCG	: Biodiesel-derived crude glycerol
BCG-M	: Biodiesel-derived crude glycerol based medium
BF	: Batch fermentation
BPU	: Bio-polyurethane foams
CF	: Continuous fermentation
CF-CR	: Continuous fermentation integrated with cell retention system
CTP	: Citrate transport protein
D	: Dilution rate
EC	: Extracellular β carotene
EE	: Encapsulation efficiency
EO	: Extracellular oil
EP	: Ethephon
FA	: Fatty acid
FD-G	: Freeze-dried with gum Arabic
FD-GM	: Freeze-dried with gum Arabic and maltodextrin
GK	: Glycerol kinase
IC	: Intracellular β-carotene
IO	: Intracellular oil
OAA	: Oxaloacetate
OLE1	: Δ9-fatty acid desaturase
PBCG	: Purified biodiesel-derived crude glycerol
PBCG-M	: Purified biodiesel-derived crude glycerol based medium
PU	: Polyurethane foam
PYC	: Pyruvate carboxylase
Q_{TC}	: Total β-carotene productivity
Q_{TO}	: Total oil productivity

List of Abbreviations (Continued)

Nomenclature

Q_X	: Biomass productivity
ΔS	: Consumed glycerol
SO	: Sodium oleate
SC	: Sodium chloride
SD-G	: Spray-dried with gum Arabic
SD-GM	: Spray-dried with gum Arabic and maltodextrin
TAG	: Triglyceride or triacylglycerol
TC	: Total β-carotene
TCA	: Tricarboxylic acid
TGL	: Triacylglycerol lipase
TMP	: Trimethylolpropane
TO	: Total oil
TW	: Tween 20
WCO	: Waste cooking oil
WCO-based BPU	: Waste cooking oil-based bio-polyurethane
WCYO	: Waste cooking oil mixed with yeast oil
WCYO-based BPU	: Waste cooking oil mixed yeast oil-based bio-polyurethane
X_{max}	: Maximum biomass
YO	: Yeast oil
YO-based BPU	: Yeast oil-based bio-polyurethane
$Y_{TC/S}$	: Total β-carotene yield
$Y_{TO/S}$	: Total oil yield
$Y_{X/S}$	: Biomass yield

Greek letters

μ_{max}	: Maximum specific growth rate (h^{-1})
α	: Growth-associated production coefficient (g oil/g cell)
β	: Non-growth associated production coefficient (g/g h)

CHAPTER 1
INTRODUCTION

1.1 Background and Statement of Problems

Previous research has discovered that some microorganisms can produce and store more than 20% of oil in cells by dry weight. They are called oleaginous microbes. The oil is produced and accumulated tiny oil droplets inside microbial cells. The microbial oil composition is triglyceride or triacylglycerol (TAG) for 95% approximately. The TAG has properties similar to vegetable oil which has a high potential feedstock for bio-lubricant production. Some yeast strains have as high as 50% of the oleaginous yeasts, such as *Pseudozyma parantarctica*, *Cryptococcus albidus*, *Rhodosporidium toruloides*, *Rhodotorula glutinis*, and *Yarrowia lipolytica* [1]. Also, the raw material employed as the culture's carbon supply affected how each strain of yeast accumulated and produced lipids [2].

Currently, microorganisms have been cultivated to produce oil to replace fossil and vegetable oils. The oils are used to produce readily biodegradable oil-based products which are environmentally friendly. Agricultural waste and biodiesel-based glycerol could be used as carbon sources for oleaginous cultivation [1]. Glycerol has been studied as a carbon source for microorganisms that create a variety of crucial compounds, including malic acid, 1,3-propanediol, and bioethanol [3]. In addition, biodiesel-based glycerol has been applied for yeast growth and oil formation. Additionally, glycerol utilization increases its value and reduces the burden of glycerol to be disposed of in the environment. The cost of various product formations is also diminished.

The interest in natural goods of customers is rising in the present day. β-carotene, specific microbes can produce a high-value natural product. It is a yellow-orange-red pigment and oil-soluble substance [4]. β-carotene is a significant compound frequently employed as food coloring, premium additives, and antioxidant compounds [5, 6]. Consumer interest in natural goods is also rising in the present day. The generation of β-carotene using microorganisms is a realistic and more sustainable option due to concerns about using synthetic colors [7, 8]. The synthesis of microbial β-carotene is a natural and more sustainable option due to concerns about using artificial colors.

This study aimed to: 1) investigate the effect of surfactant and osmotic pressure on YO and β-carotene co-production by *Rhodosporidium toruloides* using BCG-based medium, 2) improve production efficiency through an integrated cell retention system, and 3) explore practical applications of polyurethane foam production and β-carotene encapsulation.

1.2 Purpose of the Study

1.2.1 To study the effect of induceron co-production of yeast oil (YO) and β-carotene by *R. toruloides* using biodiesel-derived glycerol (BCG) as a main carbon source.

1.2.2 To develop YO and β-carotene co-production by *R. toruloides* cultivation integrated cell retention system.

1.2.3 To study bio-polyurethane foam formation and antimicrobial activity of β-carotene.

1.3 Scope of thesis

The scope of this research is to improve the co-production of YO and β-carotene by *R. toruloides* TISTR 5186 from biodiesel-derived glycerol (BCG). These applications can increase the value of glycerol by reducing the burden of disposing of glycerol in the environment. In addition, it can reduce the raw material cost of YO to produce bio-lubricants by using glycerol as a main carbon source. The influence of surfactants and osmotic pressure as inducer on the release of extracellular oil and co-production with β-carotene is also investigated. Then, the cell retention system connected with continuous cultivation is performed to enhance the co-production efficiency. The YO is then used to produce bio-polyurethane foam and then the β-carotene are spray-dried to use as aquatic active ingredients.

1.4 Expectations of thesis

This thesis, I have the scope and limitations of studying which are concerned to the previous works which are:

1.4.1 Known the effect of inducer on co-production of YO and β-carotene by *R. toruloides* using BCG as a main carbon source.

1.4.2 Known the effectiveness of YO and β-carotene co-production by *R. toruloides* cultivation integrated cell retention system.

1.4.3 Known the application of YO for bio-polyurethane foam production and bioactive properties of β-carotene.

CHAPTER 2
RESEARCH OF THE LITERATURE

2.1 Energy crisis

The energy crisis, one of the main problems, makes the world violent and dangerous. Energy resources are being used quickly, and all indications indicate their eventual disappearance. In such cases, renewable energy sources need to be given more thought. Although fossil fuels are widely used worldwide, they are not sustainable since they damage the ecology by increasing greenhouse gas and CO_2 levels. To preserve sustainability and a clean environment, it is necessary to produce environmentally responsible and renewable fuels [9].

The current energy crisis is brought on by the limited amount of energy produced from accessible fossil resources. Resources that can be used to produce energy are running out quickly. The need for energy is still there and is likely to keep growing. Recognize the possibility that it might pass. This is a critical problem [10, 11]. Due to the disadvantage that these energies cannot be reproduced, the economy needs to improve. The increase in CO_2 caused by using petroleum fuels influences the environment and global energy supply [12]. Fossil fuels are the best energy source, except for the issues they create. They provide highly concentrated, transportable energy that can be converted into essentials for civilization, like heat, electricity, and propulsion. As a result, be prepared for the benefits of fossil fuels, the usefulness and convenience of renewable alternatives must be equal. Furthermore, fossil fuels have the capacity to produce enormous amounts of energy. Therefore, alternatives must equal such a massive scale while lowering the level of ambient CO_2 [13]. Fossil fuels are used in the creation of energy, the running of transportation networks, and the synthesis of plastics and polymers. Numerous socioeconomic and environmental problems have been exacerbated by reliance on these resources and the substances they produce. This includes topics like international conflicts, global warming, deforestation, the accumulation of non-biodegradable materials, and pollution of natural resources [13, 14]. Therefore, renewable resource utilization is essential in this situation.

2.2 Oleaginous microorganism

It has been proposed that single-cell oil made by oleaginous yeasts could be a replacement feedstock for producing oleochemicals and biodiesel. Oleaginous yeasts are particularly attractive for industrial applications because they can produce up to 70% of dry cell weight. Additionally, the lipids that these yeasts accumulate have characteristics that are similar to those of vegetable oils. The synthesis of these lipids by yeasts does not compete with food production for example, vegetable oil), and it depends on the time of year or a different region [15, 16].

According to earlier studies, some microorgainsmhave been found to create and preserve more than 20% of intracellular oil by dry weight. It is a member of the class of oleaginous microorganisms, which also includes bacteria, yeast, and algae. Oil is produced inside the cells of microorganisms and builds up as tiny oil droplets or microdroplet oils. When microbial cells are fed a medium rich in carbon sources, microbial fat synthesis is most frequently seen. Furthermore, restricting the amount of nitrogen and other nutrients impacts how much oil builds up in microbial cells [17, 18]. TAG, which possesses qualities similar to vegetable oil and has excellent potential for the advancement of the production of bio-lubricants, makes up around 95% of all oil. Oleaginous yeasts, including *P. parantarctica*, *C. albidus*, *R. toruloides*, *R. glutinis*, and *Y. lipolytica* have also been capable of accumulating up to 50% oil by weight. Small oil droplets assemble in the cytoplasm. The type and culture of the yeast affect how much oil accumulates. One factor affecting how various yeast strains retain and create oil is the origin of the raw materials employed as a carbon source in the culture. The raw materials used as a carbon source in culture are one of several variables affecting YO production and accumulation [2].

2.3 Applications of microbial oil

2.3.1 Biolubricant

Earlier research on microbial culture aimed to create biodegradable oils and goods. For instance, Ma *et al*. also investigated the effectiveness of making bio-lubricants from high oleic acid content oils produced from *Rhodotorula glutinis* yeast creating an ester compound. Under the appropriate conditions, it was shown that YO could be

converted into lubricants by yeast lipase and trimethylolpropane (TMP), which have the same qualities as lubricants derived from fossil fuels. Its effectiveness at low temperatures is comparable to conventional lubricants [19]. According to a recent study, YO can replace fossil and vegetable oils as feedstock to produce bio-lubricants.

2.3.2 Biodiesel

Biodiesel is typically produced through the chemical process of transesterification, converting fatty acids into fatty acid methyl esters using a catalyst. While various factors influence biodiesel quality, including process parameters and purification, feedstock selection is paramount. Traditionally, biodiesel production has relied heavily on energy crops like palm oil and soybean. However, recent research highlights the potential of waste sources, such as animal fat and used vegetable oils [20]. Studies indicate that biodiesel derived from waste materials like vegetable oils, beef tallow, poultry fat, and sewage sludge exhibits lower environmental impacts across metrics like global warming, acidification, and eutrophication compared to conventional diesel and even soybean or rapeseed biodiesel. Furthermore, investigations into grease trap waste demonstrate environmental savings when lipid concentrations exceed 10% compared to soybean-based biodiesel [21]. Although waste cooking oil is widely utilized, the efficiency and characteristics of the collection system significantly influence the final product's environmental footprint [22].

2.4 β-carotene

β-carotene are a class of yellow, orange, and red pigments soluble in oil [23]. β-carotene is widely known as a significant chemical commonly used as a food coloring and premium food additive. Additionally, antioxidants are very important in protecting ovarian, cervical, breast, colon, and vascular malignancies, along with cardiovascular and ocular issues [5, 6]. In 2017, the market for β-carotene was anticipated to be worth $1.5 billion. It is projected to reach $2.0 billion by 2022 [24]. Due to concerns over synthetic colors, consumers are showing a growing interest in natural products nowadays. Producing carotenoid-rich microorganisms becomes a viable and sustainable option as a result [7, 8]. According to earlier studies, yeast has the potential to produce β-carotene that may be used in the food, feed, and pharmaceutical sectors [35–38]. The production

of oil and β-carotene from yeast has been thoroughly examined, and productivity is related to dietary consumption, environmental factors, and carbon and nitrogen sources [29].

β-carotene is a lipophilic isoprenoid, categorized chemically into carotenes (hydrocarbons) and xanthophylls (oxygenated derivatives) [40–43]. Carotenoids are also classified based on pro-vitamin A activity, including pro-vitamin A forms like β-carotene, β-cryptoxanthin, and α-carotene, and non-provitamin A forms such as lycopene, lutein, and zeaxanthin [44, 45], alongside ketocarotenoids like canthaxanthin and astaxanthin [36]. The β-carotene synthesis from acetyl CoA, derived from fatty acids via the β-oxidation pathway presented in Figure 2.2.

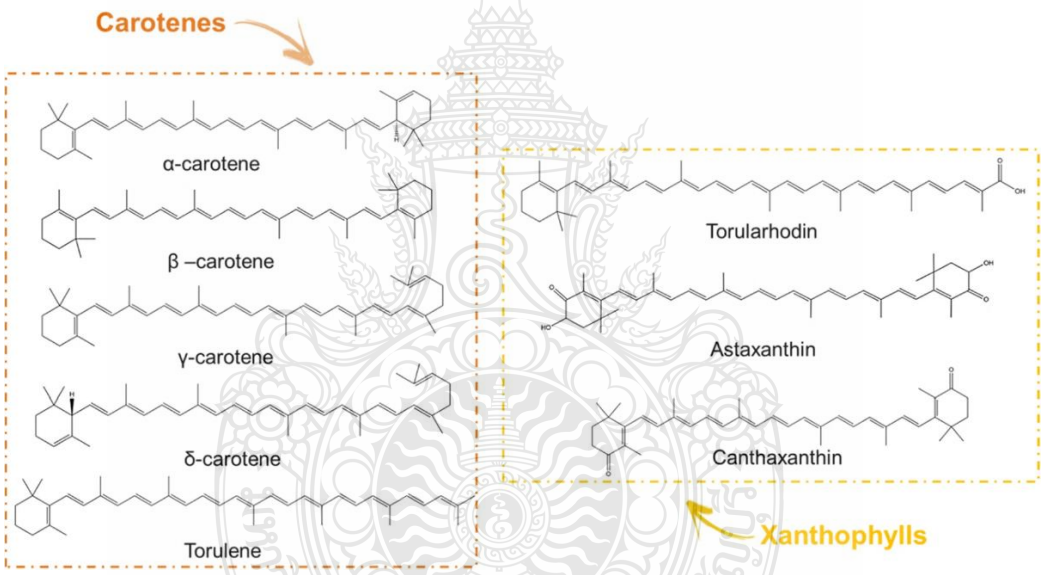

Figure 2.1 Structures of microbial β-carotene [24].

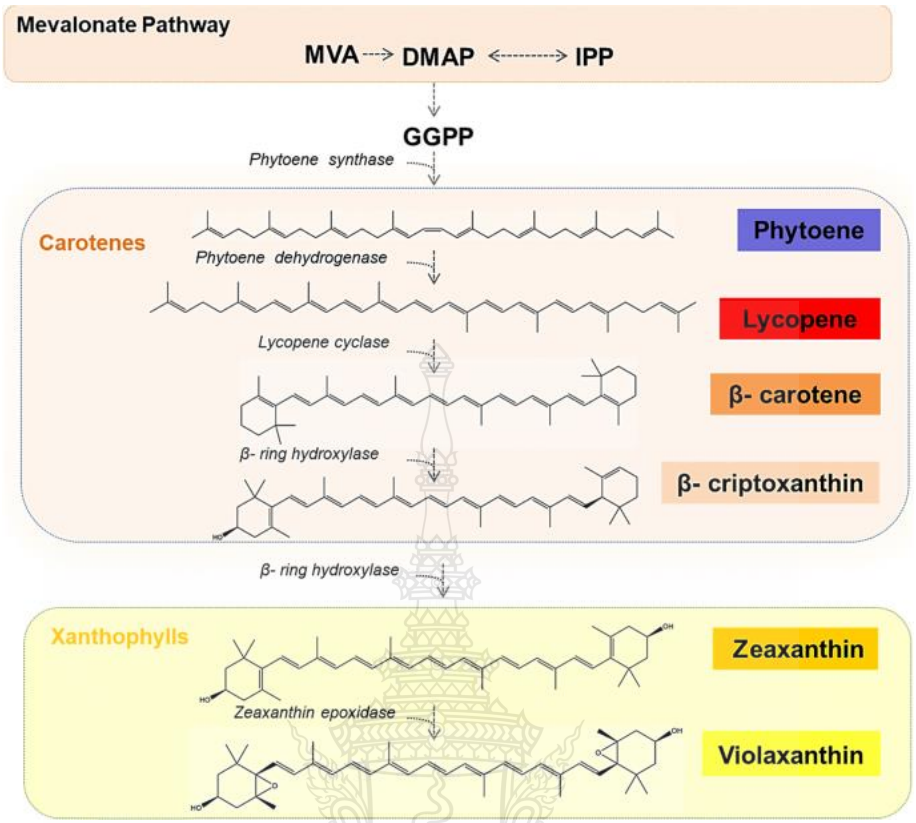

Figure 2.2 Carotenoid biosynthesis through the MVA pathway in microorganisms [39].

2.5 Applications of β-carotene

Carotenoids, a class of natural pigments exhibiting a spectrum of colors from yellow to red, hold substantial significance across the chemical, pharmaceutical, food, and feed industries. Beyond their well-established role in pigmentation and as precursors to vitamin A [40], these compounds have garnered considerable attention for their inherent antibacterial, antioxidant, and tumor-inhibiting properties. Consistent with these attributes, prior investigations have documented the antibacterial and antioxidant activities of natural carotenoids [28–30], prompting ongoing research into their potential application as antimicrobial and antioxidant agents, thus extending their utility beyond their coloring function.

2.6 Biodiesel-based crude glycerol

Glycerol, a significant by-product of biodiesel production with an approximate yield of 100 kg per ton of biodiesel [1], presents opportunities for value addition through microbial conversion into products such as bioethanol, malic acid, and 1,3-propanediol [27, 28]. Such biotransformations not only mitigate the environmental burden associated with crude glycerol disposal but also hold the potential to reduce the cost of yeast cultivation for biolubricant production by serving as an alternative carbon source. The economic viability and sustainability of biotechnological processes are further enhanced by the utilization of inexpensive and renewable carbon feedstocks for microbial growth [46]. Lignocellulosic biomass, rich in fermentable sugars like glucose and xylose [47] and derivable from agricultural waste, forestry residues, and energy crops, represents a promising alternative. Notably, wheat straw constitutes a substantial portion of agricultural waste in Europe, accounting for 109 million tons annually, or 42.2% of the total [48], highlighting its potential as a fermentation substrate. While oleaginous yeasts exhibit metabolic versatility, capable of utilizing diverse carbon-based materials [16], the inherent structural complexity and polymerization of sugars in lignocellulosic biomass necessitate pretreatment to facilitate their assimilation [49].

2.7 Characteristics of *Rhodosporidium toruloides*

The oleaginous yeast *Rhodotorula toruloides* exhibits significant potential for microbial oil synthesis due to its oil-producing capacity, various substrate utilization ranges, and ability to co-produce valuable pigments [50]. Prior studies have demonstrated the successful cultivation of *R. toruloides* on diverse raw materials, including sugar-based biomass, lignocellulosic-based biomass, and waste and by-products from industries, for microbial oil generation [22, 49]. Furthermore, certain crude glycerol-derived soaps possessing conventional surfactant chemical structures have been observed to enhance both biomass and oil synthesis in *R. toruloides* oleaginous yeast [50]. Similarly, Na-lignosulfonate, a byproduct of lignocellulosic biomass acid hydrolysis, has shown some positive effects on *R. toruloides* growth. However, comprehensive research and reporting the impacts of various surfactant types on *R. toruloides* remain limited. Consequently, this study investigates the impact of non-ionic, and ionic surfactants on the yeast growth

and oil accumulation. Elucidating these effects on lipid synthesis could significantly advance the bioconversion of diverse resources into biodiesel.

2.8 Microbial oil and β-carotene production pathway of *Rhodosporidium toruloides*

Acetyl-CoA is a crucial precursor in lipid biosynthesis, primarily derived from pyruvate decarboxylation and the citric acid cycle. Several key enzymes are involved in this process: acetyl-CoA carboxylase (*ACC1*), stearoyl-CoA desaturase (*SCD1*), and diacylglycerol acyltransferase (*DGAT1*), which catalyze the initial, middle, and final steps of triacylglycerol synthesis, respectively [52, 53]. The oxidative pentose phosphate pathway, along with cytosolic NADP+-dependent malic enzyme activity, serves as a major source of NADPH, a reducing power essential for fatty acid acyl carrier protein production [54, 55]. Acetyl-CoA also contributes to the formation of dimethylallyl diphosphate and its isomer 3-isopentenyl diphosphate, precursors of terpenoids such as lycopene and β-carotene. Furthermore, peroxisomal β-oxidation of free fatty acids generates acetyl-CoA, which can then enter the glyoxylate cycle to produce succinate [57], as illustrated in Figure 2.3.

Pyruvate is converted to acetyl-CoA, a central metabolite in oleaginous yeast that plays a crucial role in the tricarboxylic acid (TCA) cycle. Acetyl-CoA also serves as a key precursor for both the fatty acid and mevalonate biosynthesis pathways, the latter of which ultimately leads to carotenoid biosynthesis (Figure 2.4), suggesting a potential metabolic link between lipid and carotenoid production. Within carotenoid biosynthesis, the synthesis of phytoene and its subsequent desaturation represent two critical steps [58].

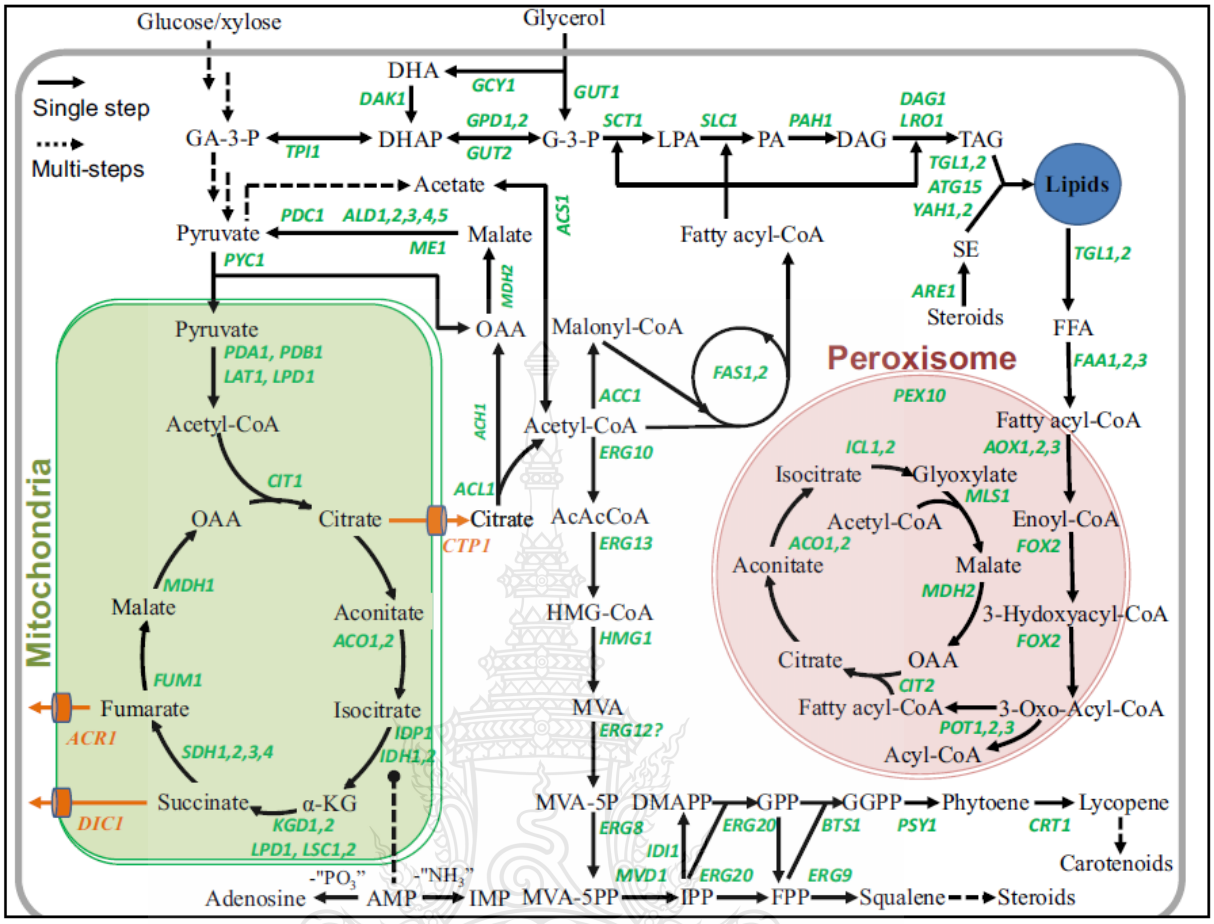

Figure 2.3 The primary metabolic pathways oil and β-carotene of *R. toruloides* [59].

2.9 Gene expression

Gene expression is the process by which the information encoded in a gene is translated into a functional product, most commonly through the transcription of RNA molecules that code for proteins or non-coding RNAs with diverse roles. The timing, location, and levels of protein and RNA production are tightly regulated, varying significantly in response to environmental cues and cell type. Many genes encode RNAs and proteins that, in turn, regulate the expression of other genes. Gene expression can be assessed by measuring the functional activity of a gene product or by observing a phenotype associated with a specific gene.

2.10 Effect of surfactant to yeast oil

It is practice classifying surfactants into two categories: ionic and non-ionic. Non-ionic surfactants are further divided into ether and ester kinds, whereas ionic surfactants are further divided into cationic, anionic, and zwitterionic types. The hydrophilic head group and the hydrophobic tail constitute non-ionic surfactants. When producing niosomes, it is a non-ionic, generally non-toxic substance [60]. Natural steroids, alkyl (T), or fluoroalkyl can be found in the hydrophobic tail of surfactants. Comparatively, a large range of vesicle-forming surfactants are available to the hydrophilic head groups. These include Brij, Spans (sorbitan esters), and Tweens (polysorbates). The generally recognized as safe (GRAS) category niosomes may be prepared using them, and they are safe to use [61]. A variety of amphibious molecules known as non-ionic surfactants are absorbed at the contact to lower the tension in the skin. Both a hydrophobic portion and a hydrophobic section make up surfactant molecules. This characteristic enables them to absorb via the interface that forms when two phases with opposite polarities are mixed [62]. Especially when added to microbial growth medium, they permeabilize cell membranes, increasing the release of enzymes and intracellular metabolites outside of cells [63]. The production of biological products has made use of surfactants having an amphipathic molecular structure, which improve electron transport. The activity of important metabolic enzymes and other factors have been shown to regulate the permeability of cell membranes. The non-ionic surfactants are less likely to froth, have a higher surface activity, and are water resistant. It may increase the pace at which microbial metabolites are produced and enhance the way that microbes secrete their products [64].

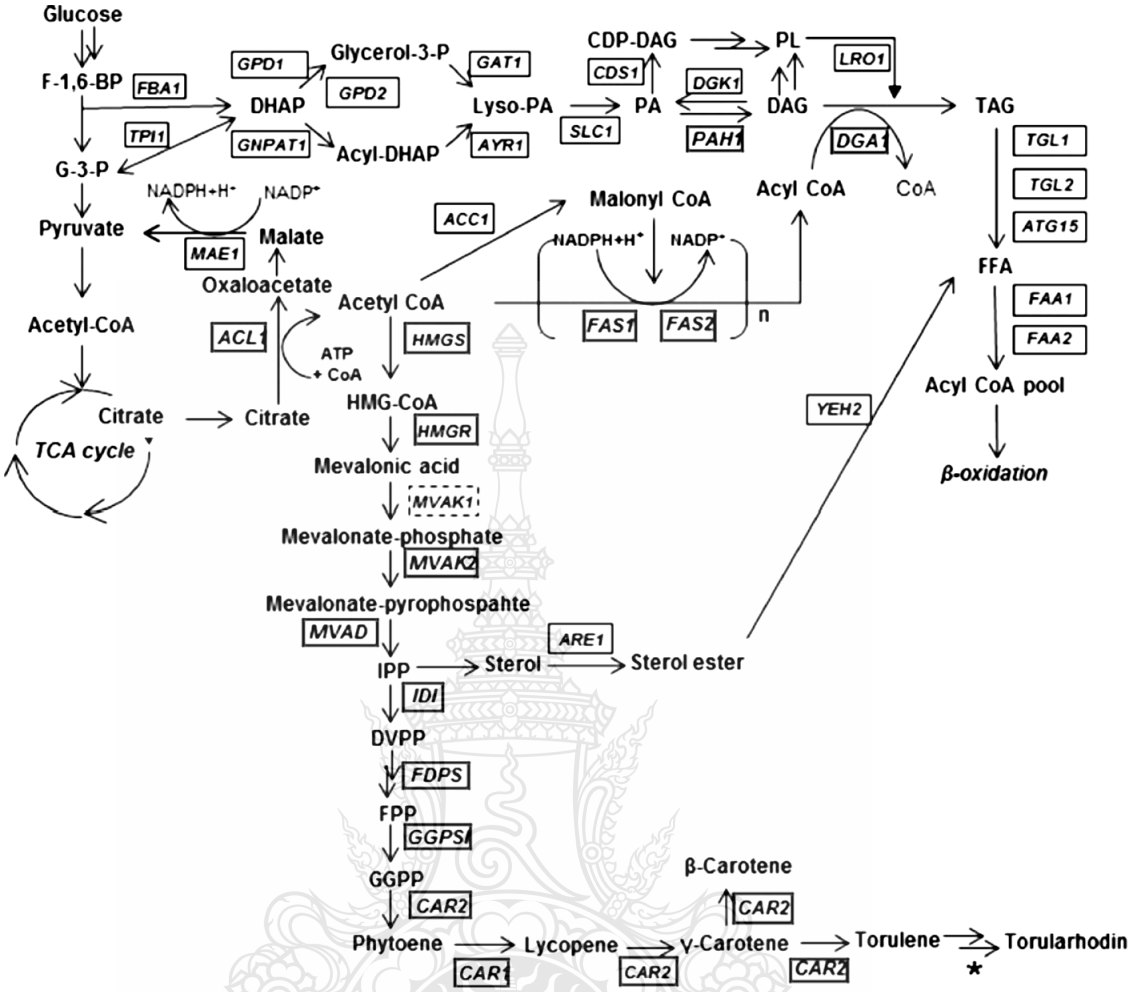

Figure 2.4 Biosynthesis pathway of β-carotene in *R. toruloides* [58].

2.11 Effect of osmotic pressure to β-carotene

Increasing osmotic stress can increase the efficiency of carotenoid production. Conditions with high salinity cause the cell walls of the yeast to be destroyed due to osmotic pressure. and affects the internal metabolism of cells at various levels Since the inhibition transcription This affects the level of transcription in the cell. In culture media with complex components, complex interactions may occur between them. Complex changes in culture conditions and nutrients accelerate microbial growth and metabolism in a synergistic manner. This is because cells do not need to produce large amounts of nutrients. Cell adaptation and growth therefore proceed rapidly [65].

2.12 Fermentation process integrated cell retention system

Fermenter is connected to a hollow fiber membrane to recirculate the cell to fermenter using a peristaltic pump, while fresh culture media was continuously pumped into the fermenter. Simultaneously, hollow-fiber membrane technology was applied to extract the cell-free broth. To regulate cell density within the fermenter, some cell broth was consistently withdrawn via the effluent port. The cell broth from the effluent and the cell-free broth from the hollow-fiber membrane system were collected in a harvesting container. In order to maintain a stable state during continuous culture, the total influent flow rate was adjusted to match the total effluent flow rate [66].

2.13 Literature reviews

Taoka et al. reported that non-ionic surfactants increase the growth of *Thraustochytrium aureum,* and oil content increased by 1.15-fold [67]. Tween 80 has a beneficial effect since it makes cell walls more permeable and can be used as a carbon source. However, Tween was unable to accelerate the growth and *R. toruloides* oil accumulation, suggesting that the effects may vary depending on the type of yeast involved. The permeability of cell wall can be raised by cationic surfactants, though. Therefore, dispersing the created materials outside encourages the growth of microbes. However, cationic surfactant damages *R. toruloides* by dissolving the cell membranes. Then, materials inside the cell exit and enter the culture medium. It prevents cells from dividing. Additionally, anionic surfactant was discovered to be advantageous for *R. toruloides* growth and oil production due to the potential of substance similarity to a cell membrane structure and the hydrophobic component is the key role. Yeast multiplies and makes oil [68].

Prior research has highlighted that elevating osmotic stress can enhance carotenoid production efficiency. High salinity in microbial cultivation exerts considerable osmotic pressure, which disrupts yeast cell walls and influences their internal metabolism. Consequently, transcription inhibition can impact cellular transcription levels. In complex culture media with various components, complex interactions are occurring. Minor changes in the culture environment and the availability of nutrients work together to speed up microbial growth and metabolism. This is

attributed to the reduced need for substantial nutrient production, facilitating rapid cell adaptation and growth [61, 62].

Mussagy et al. (2020) detailed a method for the selective recovery of both fatty acids and carotenoids (specifically β-carotene and torularhodin, initially also torulene) from *R. glutinis* CCT-2186 biomass using bio-based solvent mixtures [71]. Their optimized ternary mixture of ethanol, ethyl acetate, and water (67:33:0% w/w/w) applied to pre-treated dry biomass achieved over 75% recovery. Interestingly, while initial analysis showed torulene, it was absent after extending the bioreactor growth to 120 hours, indicating its complete conversion to torularhodin. This simplification to two primary carotenoids offers advantages for industrial downstream processing.

Taoka et al. (1998) studied *Thraustochytrium aureum* ATCC 34304 growth with and without Tween 80 supplementation. Their results showed that TW 80 significantly enhanced *T. aureum* growth, with biomass yield increasing with TW 80 concentration. At 1.0% TW 80, total lipid and fatty acid content were considerably higher than in the control. Fatty acid analysis indicated a substantial rise in C18:1n-9 (oleic acid) with TW 80 addition. The authors proposed two potential mechanisms: direct uptake of oleate from TW 80 into cellular lipids, or the utilization of TW 80 as a supplementary carbon source for metabolism [72].

Liu et al. investigated the capacity of *L. starkeyi* AS 2.1560 to produce microbial oil using crude glycerol as the sole carbon source. Their optimization studies determined the following optimal conditions for lipid formation: crude glycerol concentration of 70 g/L, yeast extract combined with peptone as nitrogen sources, a carbon-to-nitrogen (C/N) ratio of 60, inoculum concentration of 10.0%, cultivation temperature of 30°C, and pH of 6.0. Under these optimized conditions, the researchers achieved maximal biomass of 21.1 g/L, lipid content of 35.7%, lipid production of 7.5 g/L, and a lipid coefficient of 17.3%. Notably, the methanol present in crude glycerol exhibited a moderate inhibitory effect on lipid synthesis [73].

Xu et al. (2012) explored carboxylate surfactants, structurally similar to natural fats and often derived from oleochemicals. Their study examined sodium oleate and sodium n-octanoate, differing in their hydrophobic chains, regarding their impact on the growth and oil synthesis of *R. toruloides*. SO features a polar carboxylate head and a long-

chain alkane tail. Sodium n-octanoate has a shorter hydrophobic chain. The researchers found that sodium oleate (0.5–2.0 g/L) boosted both lipid accumulation and cell growth in *R. toruloides* using crude glycerol. The structural similarity between carboxylate surfactants and cell membranes might facilitate interactions, with the surfactants' hydrophobic properties potentially enhancing membrane permeability and nutrient uptake [74].

Choudhari et al. identified several stimulators that enhance β-carotene synthesis in B. trispora. Their research demonstrated that both natural oils (including palm, sunflower, and soybean oils) and non-ionic surfactants (such as Span 20, Span 40, Tween 20, and Tween 60) can effectively promote the β-carotene biosynthetic pathway in this organism. These findings establish potential strategies for optimizing β-carotene production through supplementation with specific lipid-based additives [75].

He et al. investigated *Blakeslea trispora* as a natural source of β-carotene production. Their research demonstrated that ethylene treatment (ET) significantly enhanced β-carotene yields by 52 ± 0.20%, reaching 1.87 ± 0.11 g/L. The study employed comprehensive analytical approaches, combining two-dimensional electrophoresis-based proteomics via MALDI-TOF/TOF with gas chromatography/mass spectrometry-based metabolomics. Their findings revealed that ethylene enhances β-carotene synthesis through two primary mechanisms: reducing tricarboxylic acid (TCA) cycle flux, thereby promoting acetyl-CoA accumulation, and upregulating transcription of key genes in the mevalonate pathway, including *hmgR, ipi, carG, carRA,* and *carB* [76].

Uprety et al. demonstrated that crude glycerol utilization resulted in 2-fold increase in biomass and a threefold enhancement in oil concentration compared to pure glycerol applications. Their research revealed that the methanol component of crude glycerol significantly influenced both biomass formation and oil production. Additionally, the organism exhibited tolerance to salt concentrations up to 1.5% (w/v) in the culture medium. The study further established that soap and FAMEs present in crude glycerol exerted positive effects on biomass generation and lipid accumulation [7].

Bansal et al. investigated the cultivation of *Rhodotorula mucilagenosa* IIPL32 MTCC 25056 using crude glycerol as the primary carbon source under nitrogen-limiting conditions. The study achieved oil and biomass yields of 5.6 g/L and 19.7 g/L,

respectively. Fatty acid profile analysis revealed the predominance of oleic acid (61.88%), linoleic acid (16.17%), and linolenic acid (1.03%), collectively constituting approximately 80% of the total monounsaturated fatty acids (MUFA) and polyunsaturated fatty acids (PUFA) in the extracted oil. The researchers further conducted comparative evaluations between this MUFA-rich YO and various plant-derived edible oils, calculating nutritional indices to assess the potential application of the YO as an edible product [78].

Guerfali et al. (2013) employed biodiesel-derived crude glycerol, characterized as 64.5% glycerol, 5.9% methanol, 11% water, and 5.8% other impurities, as their substrate. Under optimized conditions (166 h fermentation), they achieved 26.6 g/L biomass with a 51.9% oil content (13.6 g/L fat yield). Their comparative analysis highlighted significant differences in fatty acid composition and lipid profiles between cultures grown on pure versus crude glycerol. Notably, lipids from crude glycerol were predominantly long-chain fatty acids, rich in linoleic acid (45%), and property analysis suggested their suitability for efficient biodiesel production [79].

Villegas-Méndez et al. investigated the significance of volumetric mass transfer coefficient (k_La) studies for oleaginous yeasts, which, being aerobic microorganisms, require such analyses to facilitate bioreactor scale-up and operational optimization for industrial applications. Their research compared to batch and fed-batch cultivation of *Sporobolomyces roseus* CFGU-S005 in a 7 L bioreactor using hydrolysates as substrate. Results demonstrated that oxygen availability significantly influences metabolite production patterns. Maximum lipid production (3.4 g/L) was achieved at a k_La value of 22.44 h^{-1}. At the same time, carotenoid accumulation reached its peak (2.58 mg/L) when agitation speed was increased to 350 rpm (corresponding to k_La 32.16 h^{-1}) in fed-batch mode, resulting in a twofold increase in productivity compared to batch cultivation [80].

Kot et al. utilized potato wastewater and glycerol as culture medium components in their research. The study examined growth at 20 °C and 28 °C in a bioreactor system, achieving biomass yields of up to 20 g/L after 72 h of cultivation. Oil content in the yeast biomass reached its maximum (19 g/100 g dry weight) on the 3rd and 4th days of cultivation, with the highest linoleic acid content (~28%) observed after 96 h. Carotenoid biosynthesis continued throughout 120 h of cultivation; however, maximum volumetric

production (6.24 mg/L) occurred at 96 h. At this time point, β-carotene (~47%) and torulene (~51%) were present in similar proportions, while torularhodin was detected in minimal amounts (<1%). The study demonstrated that *R. gracilis* cultivated in bioreactor conditions could serve as a viable source of microbial lipids and carotenoids. Additionally, the researchers observed reduced oxygen demand in the culture medium, suggesting that this cultivation approach may offer environmental benefits by utilizing biofuels and spent industrial starch waste [81].

Sarantou et al. investigated *Y. lipolytica* ACA-DC 5033 for lipid production using a nitrogen-limited medium derived from crude glycerol. Notably, lipid extraction with a chloroform/methanol mixture yielded higher lipid recovery without requiring dry cell weight (DCW) acidification or boiling. The strain exhibited rapid lipid accumulation during early growth phases, followed by subsequent degradation as fermentation progressed, leading to the production of polyols and citric acid. Fatty acid analysis revealed oleic acid as the predominant lipid component, with palmitic acid in minor quantities [82].

Liu et al. investigated optimal fermentation conditions to enhance lipid and carotenoid production in *R. toruloides* cultivated on wheat straw hydrolysate. An evolved strain with improved tolerance to hydrolysate-derived inhibitors was employed. The study evaluated the effects of temperature and inoculum size on lipid and carotenoid yields. Results demonstrated that a combination of 3.5 g/L inoculum and a fermentation temperature of 17 °C synergistically increased the accumulation of both lipids and carotenoids [83].

Gong et al. (2015) explored the impact of light on *R. glutinis* to concurrently boost lipogenesis and β-carotene production using sodium acetate. Optimal sodium acetate levels (10-20 g/L) enhanced cell growth, intracellular lipid synthesis, and carotenoid yield. However, high light intensity (8000 lux) inhibited cell growth and lipid production but increased β-carotene accumulation. Fatty acid analysis showed light exposure increased PUFA and linoleic acid content, suggesting a protective role against oxidative stress. Transcriptional analysis revealed significant upregulation of genes in acetate metabolism, lipid biosynthesis, and carotenoid production under illumination, indicating

light effectively enhances lipid and β-carotene synthesis in *R. glutinis* on sodium acetate [84].

Previous studies have shown that the addition of appropriate stimulants can increase the production of YO. Culture under stress will help the microorganisms produce higher levels of carotenoids. Therefore, it was expected that culturing yeast under conditions with stimulants and osmotic pressure simultaneously would promote yeast production of oil and carotenoids. They can be used together in high quantities, and applying cell retention systems should help achieve higher cell concentrations.

CHAPTER 3
RESEARCH METHODOLOGY

3.1 Chemicals, Apparatus and Equipments

	Company / Brand
3.1.1 Acetonitrile (C_2H_3N) Chemicals™	Macron Fine
3.1.2 Ammonium sulfate ($(NH_4)_2SO_4$)	UNIVAR
3.1.3 Analytical balance	OHAUS
3.1.4 Autoclave	N-BIOTEC/NB-1080
3.1.5 Beaker	SCHOOT
3.1.6 β-carotene ($C_{40}H_{56}$)	TLC
3.1.7 Biosafety cabinet (BSC)	ESCO/Singapore
3.1.8 Centrifuge	SIGMA / 2-16PK
3.1.9 Centrifuge tube	Nalgene
3.1.10 Chloroform ($CHCl_3$)	RCI Labscan
3.1.11 Duran bottle	SCHOOT
3.1.12 Ethephon ($C_2H_6ClO_3P$)	TLC
3.1.13 Flask	PYREX
3.1.14 Gas chromatography-mass spectroscopy (GC-MS)	Shimadzu/ Japan
3.1.15 Glucose ($C_6H_{12}O_6$)	SRL
3.1.16 High-Performance Liquid Chromatography (HPLC)	Shimadzu/ Japan
3.1.17 Hot air oven	Binder/ Germany
3.1.18 Hydrochloric acid (HCl)	QRëC
3.1.19 Incubator and shaker	N-BIOTEK / NB-205V
3.1.20 Magnesium sulfate heptahydrate ($MgSO_4 \cdot 7H_2O$)	UNIVAR
3.1.21 Malt extract powder	SRL
3.1.22 Methanol (CH_3OH) AR Grade	KEMAUS
3.1.23 Methanol (CH_3OH) HPLC grade	RCI Labscan

3.1.24	Microtube	Nalgene
3.1.25	Peptone	SRL
3.1.26	Plastic plate	Hycon
3.1.27	Potassium dihydrogen phosphate (KH_2PO_4)	SRL
3.1.28	Sodium chloride (NaCl)	SRL
3.1.29	Sodium Oleate ($C_{18}H_{33}NaO_2$)	TCL
3.1.30	Spectrophotometer	SHIMADZU / UV-1800
3.1.31	Microplate reader	BMG/SPECTROstar Nano
3.1.32	Sulfuric acid (H_2SO_4)	UNIVAR
3.1.33	Test tube	PYREX
3.1.34	Tween 20 ($C_{58}H_{114}O_{26}$)	Thermo Scientific
3.1.35	Volumetric flask	PYREX
3.1.36	Vortex mixture	Scientific Industries / G560E
3.1.37	Yeast extract	IYEAST

3.2 Microorganism

3.2.1 *Rhodosporidium toruloides* TISTR 5186

The source of *R. toruloides* TISTR 5186 was obtained from culture collection of Thailand Institute of Scientific and Technological Research (TISTR)

3.2.2 Pathogen

3.2.2.1 *Aeromonas hydrophila* TISTR 1321

3.2.2.2 *Staphylococcus aureus* TISTR 746

3.2.2.3 *Vibrio parahaemolyticus* TISTR 1596

3.2.2.4 *Escherichia coli* TISTR 527

3.2.2.5 *Bacillus subtilis* TISTR 1248

3.3 Materials and Methods

3.3.1 Yeast maintenance and inoculum preparation

R. toruloides TISTR 5186, obtained from the Thailand Institute of Scientific and Technological Research (TISTR), was employed in this study. Initial cultures were established in yeast-malt (YM) broth and incubated at 30 °C with agitation at 200 rpm (NB-205V, N-Biotek, South Korea) for 24 hours. Subsequently, 800 µL of this culture was aseptically transferred to 200 µL of sterile glycerol solution (75% v/v) for cryopreservation at -80 °C, serving as the master stock [85], [86]. The yeast master stock was revived in YM broth and cultured for 24 h. The activated yeast was then inoculated into yeast potato dextrose (YPD) medium and cultured under identical conditions. Yeast cells were harvested by centrifugation and resuspended in sterile water to serve as the inoculum for subsequent experiments.

3.3.2 Purification of biodiesel-derived crude glycerol

The BCG, a byproduct of poultry processing oil-based biodiesel production utilizing NaOH as an alkaline catalyst, was obtained from the CPF Plc. biodiesel production plant at the Saraburi Chicken Processing Industry, Thailand. The inherent alkalinity of this BCG (pH 10), attributed to the biodiesel production process, rendered it suboptimal for yeast cultivation [86], [87]. Therefore, a partial purification of the BCG was necessary prior to its use as the primary carbon source. The BCG was treated by an acidification process to eliminate contaminants following Rakkitkanphun et al.[87]. The purified BCG (PBCG) was used as the carbon source for this study.

3.3.3 Influence of inducer supplementation on co-production of yeast oil and β-carotene from purification of biodiesel-derived crude glycerol

3.3.3.1 Effect of individual inducers on YO and β-carotene production

An inoculum volume of 15 mL was introduced into 135 mL of PBCG-based medium (PBCG-M), which was composed of 50 g/L PBCG, 0.4 g/L $(NH_4)_2SO_4$, 0.8 g/L $MgSO_4 \cdot 7H_2O$, 0.16 g/L KH_2PO_4, 0.2 g/L yeast extract. Yeast cultivation was performed in triplicate at 30 °C with agitation at 200 rpm. At 24 h of cultivation, individual inducers—Tween 20 (TW), sodium oleate (SO), ethephon (EP), and sodium chloride (SC)—were supplemented into separate yeast cultures at varying concentrations. Samples

were collected at regular intervals throughout the cultivation period to determine biomass, YO, β-carotene, and glycerol concentrations.

The yields of biomass ($Y_{X/S}$), total oil ($Y_{TO/S}$), and β-carotene ($Y_{TC/S}$) were described by Eqs. (3.1) to (3.3), respectively.

$$Y_{X/S} = \frac{X}{\Delta S} \quad (3.1)$$

$$Y_{TO/S} = \frac{TO}{\Delta S} \quad (3.2)$$

$$Y_{TC/S} = \frac{TC}{\Delta S} \quad (3.3)$$

where X, TO, TC, and ΔS are biomass (g/L), total oil (TO; g/L), total β-carotene (TC; mg/L), and consumed substrate (g/L), respectively.

The productivity of biomass (Q_X; g/L·h), TO (Q_{TO}; g/L·h), and TC (Q_{TC}; mg/L·h) were presented in Eqs. (3.4) to (3.6), respectively.

$$Q_X = \frac{X}{t} \quad (3.4)$$

$$Q_{TO} = \frac{TO}{t} \quad (3.5)$$

$$Q_{TC} = \frac{TC}{t} \quad (3.6)$$

where t is fermentation time (h).

The content of TO (g_{TO}/g_{cell}) and TC (mg_{TC}/g_{cell}) were described in Eqs. (3.7) to (3.8), respectively.

$$\text{TO content} = \frac{TO}{X} \quad (3.7)$$

$$\text{TC content} = \frac{TC}{X} \quad (3.8)$$

3.3.3.2 Combined effect of Tween 20 and ethephon on YO and β-carotene in flask and bioreactor scales

The synergistic effect of Tween 80 (TW) and ethyl propionate (EP) on the co-production of yeast oil (YO) and β-carotene was evaluated in Erlenmeyer flasks and a 10-L bioreactor. In flask experiments, *R. toruloides* cultures in PBCG-M were simultaneously treated with TW (1% w/v) and EP (10 ppm) after 24 hours of growth and incubated under previously established conditions. YO and β-carotene levels were monitored periodically using standard methods. All flask experiments were conducted in

triplicate [86]. For bioreactor studies, a 10-L stirred-tank bioreactor (MDFT-N-10L, B.E. Marubishi, Japan) with a 5 L working volume was used. A 10% starter culture was inoculated into the fermenter, which was operated at 30 °C with agitation at 200 rpm and aeration at 1 vvm [86].

3.3.4 Enhancing yeast oil and β-carotene co-production by *R. toruloides* cultivation integrated cell retention system

Yeast cultivation with an integrated cell retention system was conducted in 5-L bioreactors. Initially, 500 mL of *R. toruloides* TISTR 5186 starter was inoculated into 4500 mL of PBCG-M within the bioreactor. The cultivation operates at 30°C, 200 rpm, and an aeration rate of 1 vvm. Non-ionic surfactant and Sodium chloride (SC) were added based on previous results. The bioreactor was connected to a cell retention system employing a cross-flow filter to retain yeast cells within the bioreactor. As glycerol was depleted, add medium at 24 h. the cultured medium was drawn out of the bioreactor through the cell retention system. The high yeast cell suspension was returned to the bioreactor, while the cell-free medium was transferred to an external reservoir. Subsequently, 5,000 mL of fresh culture media was introduced into the bioreactor, and the subsequent fermentation cycle begins under the same conditions. The cell retention system continues to operate until glycerol was not fully utilized. Samples were periodically collected to measure biomass, intracellular and extracellular oils, glycerol, and β-carotene [66].

3.3.5 Gene expression analysis

RNA extraction from *R. toruloides* was performed after cultivation in PBCG-M medium with Tween 20 and ethephon induction at 24 h. Cells were harvested at 36 h (10,000 rpm, 9168 × g, 4°C, 10 min) and processed using a bead mill yeast RNA purification kit (OMNI International, USA). Quality assessment utilized agarose gel electrophoresis and nanodrop spectrophotometry (Eppendorf BioSpectrometer). Vishuo Biomedical conducted library preparation, including poly(A) mRNA isolation, fragmentation, cDNA synthesis, end repair, dA-tailing, adaptor ligation, size selection, and PCR amplification with P5/P7 primers. Sequencing employed an Illumina NovaSeq platform with 2×150 paired-end configuration. Raw data underwent quality filtering via

Cutadapt (v1.9.1) with parameters: error rate 0.1, adapter overlap 1 bp, minimum read length 75 bp, maximum N proportion 0.1. Clean reads were aligned to *R. toruloides* NP11 reference genome using Hisat2 (v2.2.1). Gene expression analysis utilized transcript sequences derived from GFF annotation files, with HTSeq (v0.6.1) estimating expression levels. Differential expression analysis implemented DESeq2 Bioconductor package with negative binomial distribution modeling, incorporating data-driven prior distributions for dispersion and log-fold change estimates. Differentially expressed genes were identified using adjusted p-value ≤ 0.05 [86].

3.3.6 Yeast oil-based bio-polyurethane foams production

The YO was converted to bio-polyurethane (BPU) foams through a modified method from Samranrit et al. [88]. The process began with oil epoxidation, combining 10 g of YO with 11 g ethyl acetate and 0.9 g formic acid in a 250 mL glass container. YO was epoxidized with hydrogen peroxide at 60°C for 6 h, then washed and dried to obtain epoxidized YO (EYO). EYO was converted to polyol by heating with phosphoric acid at 85°C for 1 h. The resulting polyol was used to synthesize rigid and semi-rigid bio-polyurethane foams with toluene di-isocyanate and water as a blowing agent.

3.3.7 Production of yeast cell powder by spray dryer

The yeast wet cells were collected by centrifugation at 10,000 rpm for 10 min at 4 °C. The collected yeast cells were cleaned twice with water and re-centrifuged to remove water. The cleaned yeast cells were resuspended in water and mixed with 10% maltodextrin as the binder. The yeast suspension was fed to a spray dryer at approximately 120 °C inlet temperature. The moisture, oil, and β-carotene of the achieved yeast powder were determined.

3.3.8 Antimicrobial properties of extracted β-carotene.

The antimicrobial properties of extracted β-carotene were determined by disc diffusion technique and microdilution method [1, 2]. The β-carotene was extracted and purified following the method of Mussagy et al. [89]. The bacterial pathogens, namely *B. subtilis*, *S. enterica*, *P. vulgaris,* and *E. coli*, were activated in nutrient broth for 24 h. The

activated bacteria was smeared on nutrient agar (NA). Then, the sterile disc was put on the smeared NA, and 200 uL of extracted yeast β-carotene was dropped. The agar plate was incubated at 37 °C for 24-48 h and observed in the clear zone. Standard antibiotic penicillin β-carotene was taken as the positive control [89].

3.3.9 Kinetic modeling of yeast oil and β-carotene production.

3.3.9.1 Yeast growth

The yeast growth rate ($\frac{dX}{dt}$) was described according to the logistic growth model [90] in Eq. (3.9):

$$\frac{dX}{dt} = \mu_{max} X\left(\frac{X\text{-}X_{max}}{X_{max}}\right) \qquad (3.9)$$

where μ_{max} is the maximum specific growth rate (h-1); X and X_{max} are the biomass and the maximum biomass concentration (g/L); S is the substrate concentration (g/L), and t is the cultivation time (h). In Eq. (3.9), μ_{max} and X_{max} are the model constants.

3.3.9.2 Substrate consumption

The substrate consumption rate ($\frac{dS}{dt}$) was importantly related to cell growth and product formation. The kinetic model for glycerol consumption was established [91] as Eq (3.10):

$$\frac{dS}{dt} = \frac{1}{Y_{x/s}}\left(\frac{dX}{dt}\right) + m_s X \qquad (3.10)$$

where $Y_{x/s}$ is the biomass yield on the consumed substrate, and m_s is the biomass maintenance coefficient (g/g h).

3.3.9.3 Product formation

The product production rate ($\frac{dP}{dt}$) which depends on the yeast growth, was described by the Luedeking–Piret equation [90] as Eqs. (3.11) and (3.12):

$$\frac{dP}{dt} = \alpha\frac{dX}{dt} + \beta X \qquad (3.11)$$

$$Y_{p/s} = \alpha Y_{x/s} \qquad (3.12)$$

Eq. (3.11) defines product formation using α, the growth-associated coefficient, and β, the non-growth-associated coefficient. If α is non-zero and β is zero, product synthesis directly correlates with yeast growth. If both are non-zero, product

formation is partly linked to growth. Conversely, if α is zero and β is non-zero, product formation is independent of growth. Eq. (3.12) defines $Y_{p/s}$ as the yield of product per unit of substrate consumed.

The kinetic parameters of the mathematical models (i.e., μ_{max}, X_{max}, $Y_{x/s}$, m_s, α, and β) were defined as the required values to best fit the model (Eqs. (3.9) – (3.12)) with actual results, achieving the fitting result using the Berkeley Madonna™ software version 8.3.18 (Berkeley Madonna Inc., USA).

3.3.10 Analysis

3.3.10.1 Glycerol concentration

Glycerol concentration was determined via HPLC (LC-20AD, Shimadzu, Japan) using an isocratic mobile phase of 85% (v/v) acetonitrile at a flow rate of 1 mL/min. Separation was achieved on a Pinnacle II Amino 3 µm column (150 mm × 4.6 mm) (Restek, USA) maintained at 35 °C, with detection by a refractive index detector (RID-20A, Shimadzu, Japan) [85].

3.3.10.2 Biomass concentration

Biomass concentration was quantified according to the methodology described by Ngernsombat et al. [85].

3.3.10.3 Yeast oil concentration

The produced YO was analyzed in its intracellular (IO) and extracellular (EO) forms. Intracellular oil (IO) was quantified following the Bligh and Dyer extraction method [92]. Extracellular oil (EO) determination was performed according to the method outlined by Ngernsombat et al. [85].

3.3.10.4 Fatty acid profile

The fatty acids of IO and EO were determined as fatty acid methyl ester (FAME) using gas chromatography with mass spectrometry (GC-MS) following Rakkitkanphun et al. [93].

3.3.10.5 β-carotene

β-carotene was measured by spectrophotometry using microplate reader at 450 nm.

3.3.10.6 FTIR

Fourier transform infrared spectroscopy (FTIR) analysis of extracted and standard β-carotene using Fourier transform infrared spectroscopy. Pelleted with potassium bromide. The spectrum ranges between 400 and 4000 cm^{-1} were available. Two major and strong peaks at 3417 cm^{-1} (aromatic O-H) and 1659 cm^{-1} (aromatic C = C) dominate the FTIR absorption spectra of extracted pigments of β-carotene and standard β-carotene by analyzing the typical epoxy group in the 823–915 cm^{-1} region [94].

3.3.11 Statistical analysis

Statistical significance among groups was determined using one-way ANOVA (*p*-value < .05). Duncan's multiple range test (DMRT) was used for post-hoc analysis of significant ANOVA results using SPSS version 15.0 (SPSS Inc., USA).

3.4 Experimental place

This research was conducted at the Biotechnology Laboratory, Division of Biology, Faculty of Science and Technology, Rajamangala University of Technology Thanyaburi (RMUTT), Pathum Thani, Thailand.

CHAPTER 4
RESULTS AND DISCUSSION

4.1 Effect of individual inducers on yeast oil and β-carotene production

4.1.1 Effect on growth, glycerol consumption, and yeast oil production

A schematic overview of YO and β-carotene co-production process by *R. toruloides* under the influence of four individual inducers is presented in Figure 4.1. Yeast growth exhibited a rapid increase during the initial 48 h, followed by a stationary phase across all conditions (Figure 4.1A). Notably, the addition of SO at concentrations ranging from 0.7% to 1% (w/v) significantly enhanced oleaginous biomass accumulation, indicating its potential as an effective inducer for biomass production. Glycerol, the primary carbon source, was rapidly consumed within the first 24 h of cultivation under all tested conditions, with a steady decline thereafter (Figure 4.1B). The SC supplementation enhanced glycerol consumption in the oleaginous yeast, peaking at 10% (w/v), consistent with the principle that external solutes increase osmotic pressure, driving solute uptake for cellular equilibrium [95]. The highest IO concentration was observed with sodium oleate (SO) (Figure 4.1C), significantly boosting IO biosynthesis efficiency and suggesting the effectiveness of SO in stimulating YO production by *Rhodosporidium toruloides*.

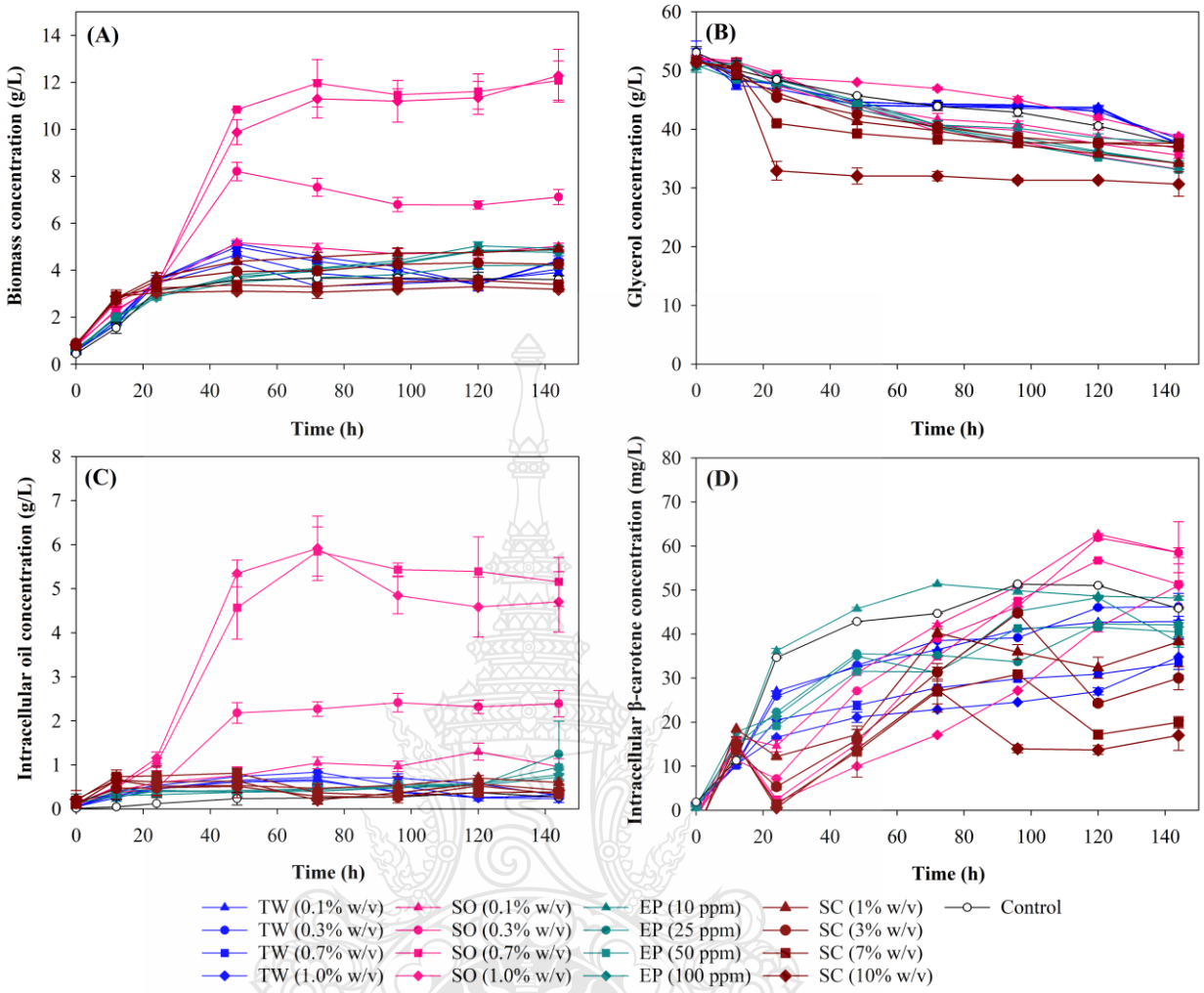

Figure 4.1 Growth kinetics and metabolite production by *R. toruloides* under various inducers: (A) biomass, (B) glycerol utilization, (C) intracellular oil (IO) accumulation, and (D) intracellular β-carotene (IC) formation. Values represent means ± standard deviation (SD). TW = Tween 20, SO = sodium oleate, EP = ethephon, SC = sodium chloride.

Figure 4.2 illustrates the impact of various inducers on YO production by *R. toruloides* cultivated in PBCG-M for 144 h. SO demonstrated the most significant effect on IO accumulation, with peak IO concentrations of 5.15 ± 0.55 g/L and 4.70 ± 0.68 g/L observed at SO concentrations of 0.7% and 1% (w/v), respectively (Figure 4.2A). Conversely, EP resulted in considerably lower IO production, ranging from 0.72 ± 0.08 to 1.24 ± 0.75 g/L. TW induced the highest level of EO secretion, reaching 6.85 ± 0.48

g/L at a concentration of 1% (w/v) (Figure 4.2B), while the other inducers led to minimal EO production. Regarding TO production (the sum of IO and EO), the highest yield of 7.08 ± 0.59 g/L was achieved with 1% (w/v) TW, followed by 0.7% (w/v) SO (Figure 4.2C). EP and SC consistently resulted in comparatively lower YO production across all tested concentrations.

The observed enhancement of EO secretion by TW is consistent with previous studies highlighting the amphiphilic nature of surfactants, which can improve nutrient solubility, promote growth and metabolite synthesis, and facilitate transport across cell membranes [96]. Similarly, Ngernsombat et al. (2016) [85] demonstrated that TW stimulated both the production and release of YO, achieving the highest TO synthesis and oil content. The mechanism by which TW enhances overall YO production may involve alleviating product inhibition caused by high IO accumulation by promoting its secretion as EO. Furthermore, transcriptomic studies have shown significant upregulation of genes associated with YO biosynthesis, such as acetyl-CoA carboxylase (ACC) and diacylglycerol acyltransferase (DGA), under TW-supplemented conditions [85], further supporting its positive impact on YO production.

Significant IO accumulation was observed within the cytoplasm of *R. toruloides* cells upon the addition of SO (Figure 4.2A), a finding consistent with the observations of Xu et al. (2012) [68]. Their study reported that supplementing the culture medium with 0.05% (w/v) SO led to a 45.4% increase in oil concentration and a 31.3% rise in the IO content of *R. toruloides* AS 2.1389, alongside enhanced cell growth and glycerol consumption. In the present study, SO supplementation also resulted in a reduction of EO content (Figure 4.2B). In contrast to SO, cultures treated with TW exhibited lower IO levels but significantly elevated EO levels, leading to an overall enhancement in TO production compared to other inducers (Figure 4.2C). These observations suggest that TW effectively alleviated potential product inhibition in *R. toruloides* TISTR 5186 cultivation utilizing glycerol-rich PBCG, thereby facilitating increased TO production. The addition of SC at all tested concentrations resulted in higher YO production compared to the control conditions (Figure 4.2A–C). This finding corroborates the work of Singh et al. (2016) [97] demonstrating that supplementation with 5% (w/v) SC enhanced YO production when utilizing 5 g/L glucose as the substrate.

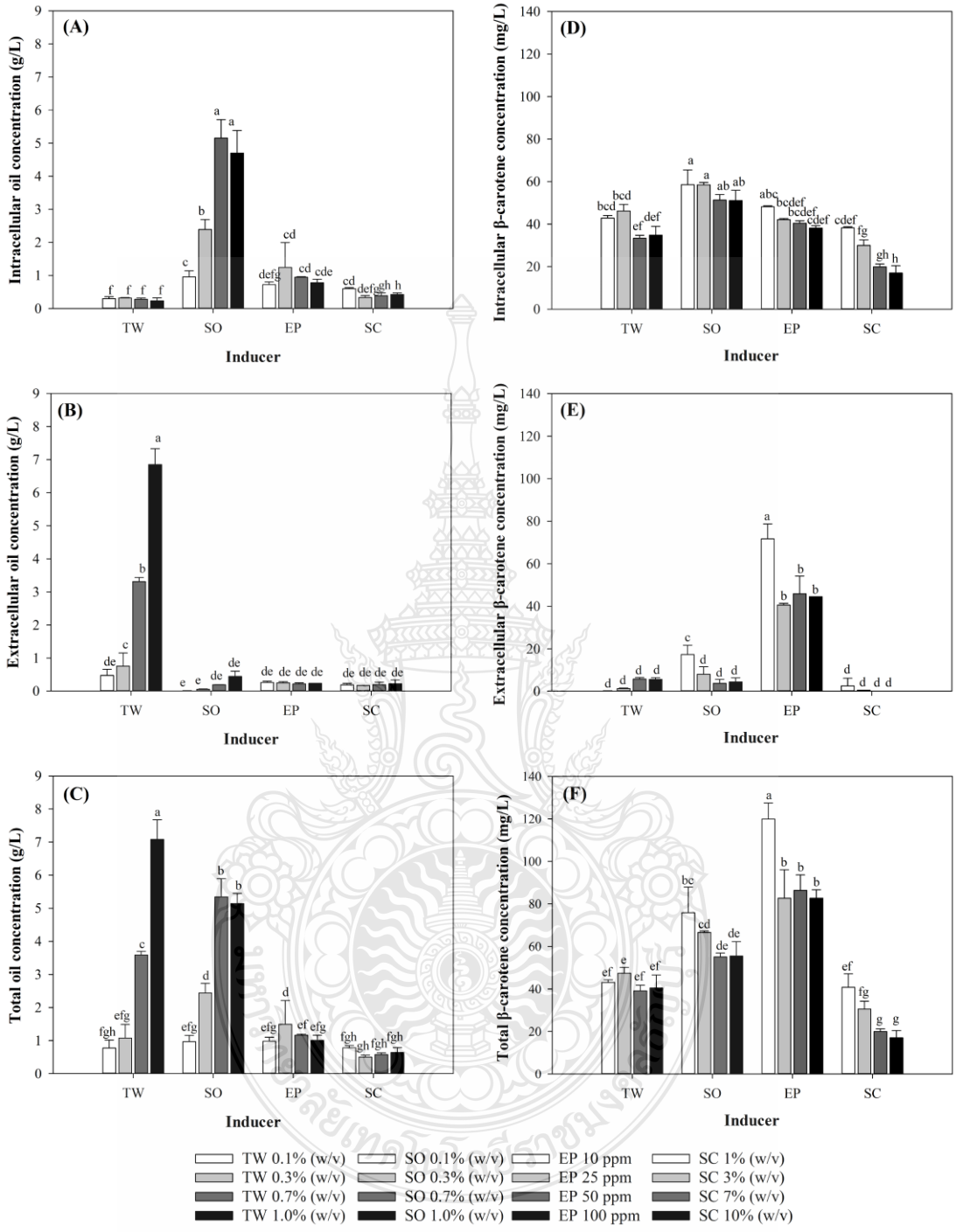

Figure 4.2 YO and β-carotene produced by *R. toruloides* cultured in PBCG-M containing different inducers at 144 h. (A) IO, (B) EO, (C) TO, (D) IC, (E) EC, and (F) TC. Data are exhibited as mean values ±SD bar. Different lowercase superscripts indicate significant differences at p-value ≤ .05. TW = Tween 20, SO = sodium oleate, EP = ethephon, SC = sodium chloride.

4.1.2 Effect on β-carotene production

The profile of IC production is depicted in Figure 4.1D. *R. toruloides* exhibited rapid IC synthesis under EP and control conditions, while TW and SC appeared to impede IC accumulation. After 144 h, the highest IC concentrations were observed with SO at 0.1% (58.52 ± 6.97 mg/L) and 0.3% (w/v) (58.49 ± 1.12 mg/L), followed by TW and EP. SC consistently resulted in the lowest IC levels (Figure 4.2D). Notably, EP was the most effective in promoting EC secretion, peaking at 71.75 ± 7.04 mg/L with 10 ppm EP (Figure 4.2E), leading to the highest total carotenoid (TC) concentration (119.91 ± 7.56 mg/L) at this EP concentration (Figure 4.2F). TW and SC resulted in lower overall TC production. These findings suggest that 10 ppm EP was the optimal inducer concentration for enhancing TC production by *R. toruloides* utilizing PBCG-M.

The observed influence of non-ionic surfactants on carotenoid production is consistent with Choudhari et al. (2008) [98], reporting that 0.1% Span 20 optimally enhanced β-carotene yield in *Blakeslea trispora*. Furthermore, the concurrent enhancement of lipid and carotenoid accumulation by SO observed in this study corroborates the findings of Vijay et al. (2011) [99] in *Chlorella vulgaris*, suggesting that SO can act as an active modulator, promoting pigment production up to specific threshold concentrations [99].

This study aligns with prior report [100] showing ethyl propionate (EP) enhances β-carotene production in *Blakeslea trispora*, mirroring increased accumulation in *R. toruloides* [100]. EP, or 2-chloroethylphosphonic acid, releases ethylene, which influences glycolysis by reducing its flux [101]. Furthermore, ethylene has been shown to upregulate key enzymes within the mevalonate pathway, the primary biosynthetic route for β-carotene synthesis [100]. Singh et al. [97] have also reported the co-production of oil and carotenoids in *R. toruloides* under osmotic stress induced by SC. Their study showed that 5-10% SC in glucose medium (5 g/L) aided metabolite co-production. While SC is a significant abiotic stressor affecting microbial metabolism [102], our findings contrast, as SC-induced osmotic stress seemed to inhibit β-carotene metabolism in *R. toruloides* on PBCG-M. This suggests the effect of SC on carotenoid synthesis may depend on the substrate or medium composition.

4.1.3 Kinetic parameters of yeast oil and β-carotene co-production

The impact of various inducers on key fermentation parameters for YO and β-carotene co-production by *R. toruloides* from PBCG at 144 h is detailed in Table 4.1. The highest biomass yield was achieved with 1.0% (w/v) SO (12.29 ± 1.12 g/L), closely followed by 0.7% (w/v) SO (12.08 ± 0.83 g/L). TW moderately increased biomass, while EP's effect varied with concentration. SC at 3% (w/v) promoted biomass, but higher levels (≥ 7% w/v) caused a reduction. Glycerol consumption by *R. toruloides* under TW and EP supplementation was comparable to the control, whereas SO (at 0.7% w/v) and SC (at 10% w/v) significantly enhanced glycerol consumption, with the highest consumption observed at 10% (w/v) SC (20.66 ± 0.11 g/L). SO supplementation at higher concentrations significantly improved the biomass yield per substrate consumed ($Y_{X/S}$), with a peak $Y_{X/S}$ of 0.94 ± 0.13 g biomass/g glycerol at 1.0% (w/v) SO. Increasing concentrations of TW and SO significantly increased the total oil yield per substrate consumed ($Y_{TO/S}$) (p-value ≤ .05), with the highest YTO/S of 0.52 ± 0.04 g oil/g glycerol achieved at 1.0% (w/v) TW. EP addition significantly enhanced the total carotenoid yield per substrate consumed ($Y_{TC/S}$) to 9.19 ± 0.36 mg/g glycerol at 10 ppm. The maximum biomass production rate (Q_X) was observed at 0.7% and 1.0% (w/v) SO. The maximum total oil production rate (Q_{TO}) was 0.049 ± 0.003 g/L·h at 1.0% (w/v) TW, and the maximum total carotenoid production rate (Q_{TC}) was 0.833 ± 0.037 mg/L·h at 10 ppm EP. The inducers significantly influenced the TO and TC content per gram of biomass, with the highest TO content (1.60 ± 0.05 g/g cell) observed at 1.0% (w/v) TW and the highest TC content (28.53 ± 2.16 mg/g cell) at 10 ppm EP. The high TO content, comprising both intracellular and extracellular oil, relative to cellular biomass under TW supplementation indicates its effectiveness in stimulating the secretion of intracellular oil, a phenomenon that can enable sustained oil production in oleaginous yeasts beyond typical intracellular accumulation limits [85].

The TW enhanced nutrient availability for *R. toruloides*, promoting YO production as energy storage and facilitating IO secretion, thus reducing product inhibition and sustaining YO production. EP effectively induced β-carotene production at low concentrations, likely influencing carotenoid biosynthesis pathways via stress responses. These inducers show potential for enhancing valuable metabolite co-

production in *R. toruloides,* leading to the selection of TW and EP for synergistic co-production studies of YO and β-carotene.

Table 4.1 Effect of inducers on yeast oil and β-carotene co-production by *R. toruloides* from PBCG at 144 h.

Condition	X_{max} (g/L)	ΔS (g/L)	$Y_{X/S}$	$Y_{TO/S}$	$Y_{TC/S}$	Q_X (g/L·h)	Q_{TO} (g/L·h)	Q_{TC} (mg/L·h)	TO content (g_{TO}/g_{cell})	TC content (mg_{TC}/g_{cell})
Control	3.61 ± 0.15^{fgh}	16.54 ± 0.44^{bcd}	0.23 ± 0.07^{h}	0.02 ± 0.00^{h}	3.01 ± 0.18^{ef}	0.025 ± 0.001^{ghi}	0.002 ± 0.0^{h}	0.331 ± 0.011^{e}	0.09 ± 0.00^{j}	13.23 ± 0.09^{cd}
TW (% w/v)										
0.1	3.91 ± 0.57^{efgh}	16.32 ± 0.89^{bcd}	0.24 ± 0.02^{gh}	0.05 ± 0.02^{fgh}	2.94 ± 0.02^{ef}	0.027 ± 0.004^{fgh}	0.005 ± 0.002^{fgh}	0.299 ± 0.018^{ef}	0.20 ± 0.07^{ghi}	11.20 ± 2.02^{de}
0.3	4.06 ± 0.27^{defg}	16.31 ± 1.05^{bcd}	0.25 ± 0.03^{fgh}	0.06 ± 0.01^{fgh}	3.02 ± 0.29^{ef}	0.028 ± 0.002^{efgh}	0.007 ± 0.003^{efg}	0.329 ± 0.094^{e}	0.26 ± 0.09^{efg}	11.80 ± 3.86^{cde}
0.7	4.38 ± 0.08^{cdef}	15.33 ± 0.18^{cde}	0.29 ± 0.00^{defgh}	0.23 ± 0.01^{d}	2.78 ± 0.15^{fg}	0.030 ± 0.001^{cdef}	0.025 ± 0.001^{c}	0.272 ± 0.015^{ef}	0.82 ± 0.02^{b}	8.93 ± 0.34^{efg}
1.0	4.42 ± 0.20^{cdef}	13.69 ± 0.09^{de}	0.32 ± 0.02^{def}	0.52 ± 0.04^{a}	2.57 ± 0.31^{fg}	0.031 ± 0.001^{cdef}	0.049 ± 0.003^{a}	0.281 ± 0.065^{ef}	1.60 ± 0.05^{a}	9.09 ± 1.74^{efg}
SO (% w/v)										
0.1	5.02 ± 0.13^{c}	15.40 ± 0.73^{cde}	0.33 ± 0.00^{def}	0.06 ± 0.02^{fgh}	5.42 ± 0.62^{cd}	0.035 ± 0.001^{c}	0.007 ± 0.001^{efg}	0.527 ± 0.131^{bc}	0.19 ± 0.03^{ghi}	15.05 ± 3.37^{bc}
0.3	7.12 ± 0.32^{b}	16.67 ± 0.17^{bcd}	0.43 ± 0.01^{c}	0.15 ± 0.02^{e}	4.00 ± 0.06^{de}	0.049 ± 0.002^{b}	0.017 ± 0.002^{d}	0.462 ± 0.083^{cd}	0.34 ± 0.04^{de}	9.40 ± 2.06^{ef}
0.7	12.08 ± 0.83^{a}	19.06 ± 0.30^{ab}	0.63 ± 0.05^{b}	0.28 ± 0.01^{c}	2.89 ± 0.00^{ef}	0.084 ± 0.006^{a}	0.037 ± 0.004^{b}	0.382 ± 0.013^{de}	0.44 ± 0.05^{c}	4.57 ± 0.32^{i}
1.0	12.29 ± 1.12^{a}	13.76 ± 1.03^{e}	0.94 ± 0.13^{a}	0.39 ± 0.08^{b}	4.29 ± 0.82^{d}	0.085 ± 0.008^{a}	0.036 ± 0.004^{b}	0.385 ± 0.070^{de}	0.42 ± 0.02^{cd}	4.54 ± 0.92^{i}
EP (ppm)										
10	4.21 ± 0.17^{defg}	13.70 ± 0.63^{de}	0.31 ± 0.01^{defg}	0.07 ± 0.01^{fg}	9.19 ± 0.36^{a}	0.029 ± 0.001^{defg}	0.007 ± 0.001^{efg}	0.833 ± 0.037^{a}	0.23 ± 0.02^{fgh}	28.53 ± 2.16^{a}
25	4.86 ± 0.13^{cd}	16.38 ± 2.15^{bcd}	0.30 ± 0.03^{defgh}	0.09 ± 0.00^{f}	5.12 ± 1.46^{bcd}	0.034 ± 0.001^{cd}	0.010 ± 0.005^{e}	0.574 ± 0.074^{b}	0.30 ± 0.14^{ef}	17.03 ± 2.22^{b}
50	4.93 ± 0.12^{cd}	14.79 ± 1.80^{de}	0.36 ± 0.05^{cd}	0.09 ± 0.02^{f}	6.27 ± 0.42^{b}	0.034 ± 0.001^{cd}	0.008 ± 0.0^{ef}	0.600 ± 0.099^{b}	0.24 ± 0.01^{fgh}	17.47 ± 2.52^{b}
100	4.77 ± 0.03^{cde}	14.02 ± 1.87^{de}	0.35 ± 0.01^{de}	0.07 ± 0.01^{fg}	6.04 ± 0.73^{bc}	0.033 ± 0.0^{cde}	0.007 ± 0.001^{efg}	0.574 ± 0.020^{b}	0.21 ± 0.02^{fghi}	17.35 ± 0.58^{b}
SC (% w/v)										
1	4.91 ± 0.08^{cd}	17.47 ± 0.55^{bc}	0.28 ± 0.01^{efgh}	0.04 ± 0.01^{fgh}	2.22 ± 0.13^{fg}	0.034 ± 0.001^{cd}	0.005 ± 0.001^{fgh}	0.283 ± 0.031^{ef}	0.16 ± 0.02^{hij}	8.30 ± 0.86^{efgh}
3	4.26 ± 0.16^{defg}	14.50 ± 0.81^{cde}	0.29 ± 0.01^{defgh}	0.03 ± 0.00^{gh}	2.10 ± 0.20^{fg}	0.030 ± 0.001^{defg}	0.003 ± 0.0^{gh}	0.212 ± 0.031^{fg}	0.12 ± 0.02^{ij}	7.16 ± 0.87^{fghi}
7	3.40 ± 0.10^{gh}	13.98 ± 0.26^{de}	0.24 ± 0.01^{gh}	0.04 ± 0.00^{fgh}	1.43 ± 0.15^{gh}	0.024 ± 0.001^{hi}	0.004 ± 0.0^{fgh}	0.139 ± 0.009^{g}	0.17 ± 0.01^{ghij}	5.87 ± 0.37^{ghi}
10	3.19 ± 0.11^{h}	20.66 ± 0.11^{a}	0.15 ± 0.01^{i}	0.03 ± 0.01^{gh}	0.83 ± 0.10^{h}	0.022 ± 0.001^{i}	0.004 ± 0.001^{fgh}	0.118 ± 0.034^{g}	0.20 ± 0.04^{ghi}	5.37 ± 1.70^{hi}

TW = Tween 20, SO = sodium oleate, EP = ethephon, SC = sodium chloride, X_{max} = maximum biomass, ΔS = consumed glycerol, $Y_{X/S}$ = biomass yield, $Y_{TO/S}$ = total oil yield, $Y_{TC/S}$ = total β-carotene yield, Q_X = biomass productivity, Q_{TO} = total oil productivity, Q_{TC} = total β-carotene productivity, TO content = total oil content, TC content = total β-carotene content. Different lowercase superscripts in the same column indicate significant differences at p-value ≤ .05

4.2 Synergistic effect of Tween 20 and ethephon on yeast oil and β-carotene production in flask and bioreactor scales

The time profiles for yeast cultivation and product formation by *Rhodosporidium toruloides* with the simultaneous addition of 1% (w/v) TW and 10 ppm EP in both flask and bioreactor systems are depicted in Figure 4.3A and 4.3B. In flask-scale cultivation (Figure 4.3A), glycerol was continuously consumed, exhibiting a steady decline throughout the 144-h experimental period. Concurrently, biomass rapidly increased during the initial 48 h, reaching 4.97 ± 0.06 g/L, and further increased to 5.92 ± 0.14 g/L by 144 hours. The IO concentration increased throughout the cultivation, reaching 1.37 ± 0.28 g/L at the end. Interestingly, IC production showed an initial enhancement at 24 hours, followed by a gradual increase until it stabilized after 72 h of cultivation. These results indicate that *R. toruloides* efficiently utilized glycerol to produce biomass, IO, and IC under the combined influence of TW and EP in flask cultures.

Figure 4.3B displays the results of the 5-L bioreactor scale-up. Glycerol consumption patterns were similar to those in flasks, indicating consistent substrate use across different volumes. In the bioreactor, biomass showed an increase, reaching a plateau after 120 h, possibly indicating more stable growth conditions. The production of IO and IC in the bioreactor also showed a gradual rise over time, reaching 0.84 ± 0.12 g/L and 50.21 ± 2.28 mg/L at 144 h, suggesting that the bioreactor environment was more favorable for the sustained simultaneous production of both IO and IC. While flask cultures showed a faster initial accumulation of IO and IC, the bioreactor exhibited a more uniform and extended increase in their co-production throughout the entire cultivation.

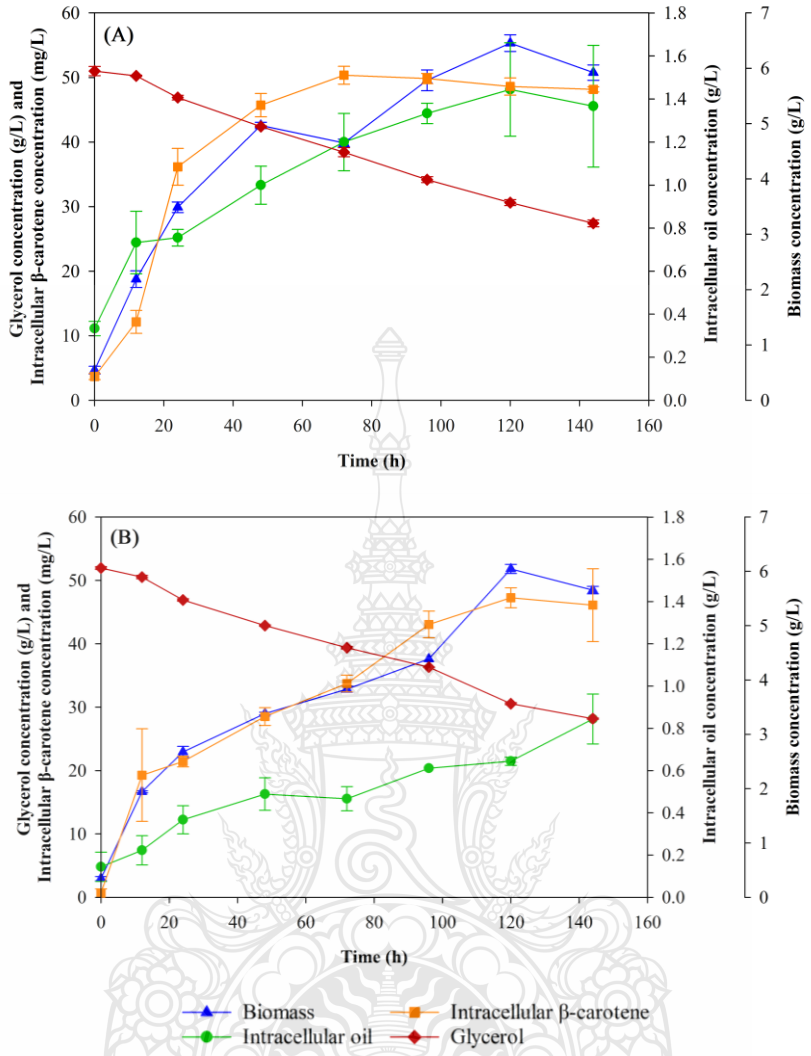

Figure 4.3 Time profiles of biomass production, glycerol consumption, IO accumulation, and β-carotene production by *R. toruloides* under 1% (w/v) TW and 10 ppm EP dual addition in (A) flask and (B) bioreactor. Data are represented as mean values ± SD bar.

Table 4.2 details the 144-h fermentation parameters for YO and β-carotene co-production under dual induction (1% w/v TW and 10 ppm EP) in flasks and a bioreactor. The highest biomass concentration was significantly observed in flasks (5.92 g/L) compared to the bioreactor (5.66 g/L) (p-value ≤ .05). A notable decrease in oleaginous biomass production occurred in the bioreactor relative to flask cultivation with dual inducers. This was attributed to TW-enhanced nutrient solubility in the aqueous phase, facilitating IO and IC transport across cell membranes [96]. EO adherence to cell surfaces potentially hindered nutrient and metabolite transport [103]. In the bioreactor, strong mechanical forces caused EO detachment, increasing IO release and reducing total oleaginous biomass [85].

Table 4.2 Fermentation parameters of yeast oil and β-carotene co-production under dual inducers in flask and bioreactor at 144 h.

Parameter	Flask		Bioreactor	
	Control	Dual inducer	Control	Dual inducer
X_{max} (g/L)	3.61 ± 0.15^{d}	5.92 ± 0.14^{b}	10.23 ± 0.06^{a}	5.66 ± 0.07^{c}
ΔS (g/L)	16.54 ± 0.41^{b}	23.58 ± 0.89^{a}	24.68 ± 0.08^{a}	23.75 ± 0.19^{a}
$Y_{X/S}$	0.23 ± 0.07^{b}	0.25 ± 0.25^{b}	0.41 ± 0.00^{a}	0.24 ± 0.00^{b}
Q_X (g/L·h)	0.025 ± 0.001^{c}	0.041 ± 0.001^{b}	0.071 ± 0.0^{a}	0.039 ± 0.0^{b}
IO (g/L)	0.27± 0.00^{c}	1.37 ± 0.28^{b}	4.28 ± 0.05^{a}	0.84 ± 0.12^{b}
EO (g/L)	0.07 ± 0.01^{c}	5.74 ± 0.30^{b}	0.27 ± 0.03^{c}	8.26 ± 0.49^{a}
TO (g/L)	0.33 ± 0.01^{d}	6.90 ± 0.44^{b}	4.50 ± 0.20^{c}	9.10 ± 0.43^{a}
$Y_{TO/S}$	0.02 ± 0.02^{d}	0.29 ± 0.03^{b}	0.18 ± 0.01^{c}	0.38 ± 0.20^{a}
Q_{TO} (g/L·h)	0.002 ± 0.0^{d}	0.048 ± 0.003^{b}	0.031 ± 0.001^{c}	0.063 ± 0.003^{a}
TO content (g_{TO}/g_{cell})	0.09 ± 0.02^{d}	1.17 ± 0.06^{b}	0.44 ± 0.00^{c}	1.61 ± 0.04^{a}
IC (mg/L)	45.81 ± 0.20^{a}	48.17 ± 0.41^{a}	34.37 ± 2.38^{b}	46.87 ± 5.75^{a}
EC (mg/L)	1.90 ± 0.53^{b}	3.00 ± 2.26^{b}	1.28 ± 0.0^{b}	35.05 ± 0.0^{a}
TC (mg/L)	47.71 ± 0.33^{b}	50.20 ± 2.33^{b}	35.65 ± 2.38^{c}	81.15 ± 5.75^{a}
$Y_{TC/S}$	3.01 ± 0.18^{a}	2.13 ± 0.20^{b}	1.44 ± 0.12^{b}	3.42 ± 1.81^{a}
Q_{TC} (mg/L·h)	0.331 ± 0.011^{b}	0.349 ± 0.013^{b}	0.248 ± 0.017^{c}	0.564 ± 0.040^{a}
TC content (mg_{TC}/g_{cell})	13.23 ± 0.09^{a}	8.48 ± 0.48^{b}	3.48 ± 0.04^{c}	14.24 ± 0.81^{a}

X_{max} = maximum biomass, ΔS = consumed glycerol, $Y_{X/S}$ = biomass yield, Q_X = biomass productivity, IO = intracellular oil, EO = extracellular oil, TO = total oil, $Y_{TO/S}$ = total oil yield, Q_{TO} = total oil productivity, IC = intracellular β-carotene, EC = extracellular β-carotene, TC = total β-carotene, $Y_{TC/S}$ = total β-carotene yield, and Q_{TC} = total β-carotene productivity. Data are represented as mean values ± SD bar. Different lowercase superscripts in the same row indicate significant differences at p-value ≤ .05.

Glycerol consumption and the biomass yield per substrate ($Y_{X/S}$) showed no significant difference (p-value > .05) between flask and bioreactor cultivations. However, the IO concentration was notably higher in flasks (1.37 ± 0.28 g/L) compared to the bioreactor (0.84 ± 0.12 g/L). Conversely, the bioreactor exhibited a higher EO concentration (8.26 ± 0.49 g/L) than flasks (5.74 ± 0.30 g/L), indicating more effective IO secretion in the bioreactor, likely due to the presence of TW.

The amphiphilic nature of surfactants like TW can alter cell membrane integrity, increasing permeability via hydrogen and van der Waals interactions [104]. Increased surfactant levels modify the lipid interface, improving the solubility and dispersion of compounds in the aqueous phase. Research suggests that removing surfactants can create pores in the cell membrane, gradually increasing permeability and facilitating the release of intracellular metabolites into the surrounding medium [104]. This led to a greater total oil (TO) concentration in the bioreactor (9.10 ± 0.43 g/L) and a higher oil yield per substrate ($Y_{TO/S}$) of 0.38 ± 0.20 g oil/g glycerol compared to 0.29 ± 0.03 g oil/g glycerol in flasks. The enhanced mixing in the bioreactor likely increased surfactant penetration, promoting efficient metabolite release [85]. The oil content was significantly higher (1.38-fold) in the bioreactor, while the highest biomass production rate (Q_X) was seen in the bioreactor under control conditions, potentially due to high IO buildup. The dual inducer addition in the bioreactor enhanced the total oil production rate (Q_{TO}) and total carotenoid production rate (Q_{TC}) by 1.31 and 1.62-fold, respectively, compared to flasks. Furthermore, the initial pH levels decreased significantly in the bioreactor under both control and dual treatments, suggesting that pH may significantly influence the growth and oil production efficiency of oleaginous yeast. Consistent with previous research [105], biomass concentration generally increased with increasing pH, but an acidic environment appeared more conducive to oil accumulation, indicating varying pH sensitivities among different oleaginous microorganisms.

In flask experiments, β-carotene production parameters (IC, EC, TC) showed no significant differences between the dual inducer treatment and the control (Table 4.2), indicating a lack of strong upregulation of related genes (Figure 4.4). Conversely, the bioreactor setup showed more efficient co-production of YO and β-carotene compared to flasks. This aligns with Villegas-Méndez et al. (2023) [106], founding that increased

agitation enhanced carotenoid synthesis in *Sporobolomyces roseus* CFGU-S005. Elevated free oxygen radicals during yeast cultivation can induce oxidative stress, prompting upregulation of carotenoid biosynthesis as an antioxidant defense [106], [107]. The enhanced carotenoid accumulation in the bioreactor likely resulted from optimal oxygen availability, controllable via working volume or agitation. These findings demonstrate that using TW and EP as synergistic inducers in a bioreactor for *R. toruloides* on PBCG significantly improved YO and β-carotene co-production efficiency and economic viability, offering a sustainable and cost-effective production strategy.

4.3 Metabolic pathways related to yeast oil and β-carotene production by *R. toruloides* under dual treatment conditions

Transcriptomic analysis of *R. toruloides* TISTR 5186 grown on PBCG-based medium, comparing control and dual inducer (TW and EP) conditions, revealed key metabolic pathway alterations (Figure 4.4). Upregulation of glycerol kinase (*GK*) and pyruvate carboxylase (*PYC*) genes under dual induction correlated with increased glycerol consumption (Table 2). Several triacylglycerol lipase (*TGL*) genes, crucial for storage lipid synthesis, also showed enhanced expression. The citrate transport protein (*CTP*) gene was induced, facilitating citrate movement from the mitochondrial TCA cycle to the cytosol, where ATP:citrate lyase (*ACL*) likely cleaved it into oxaloacetate (OAA) and acetyl-CoA. Acetyl-CoA conversion to malonyl-CoA by upregulated acetyl-CoA carboxylase (*ACC*) was also observed. Furthermore, the elongation and desaturation of fatty acyl-CoA chains, catalyzed by upregulated Δ9-fatty acid desaturase (*OLE1*), were enhanced. These findings suggest that dual inducer treatment significantly boosted yeast oil (YO) synthesis in flask experiments (Table 4.2), while genes directly involved in β-carotene biosynthesis showed no significant expression changes.

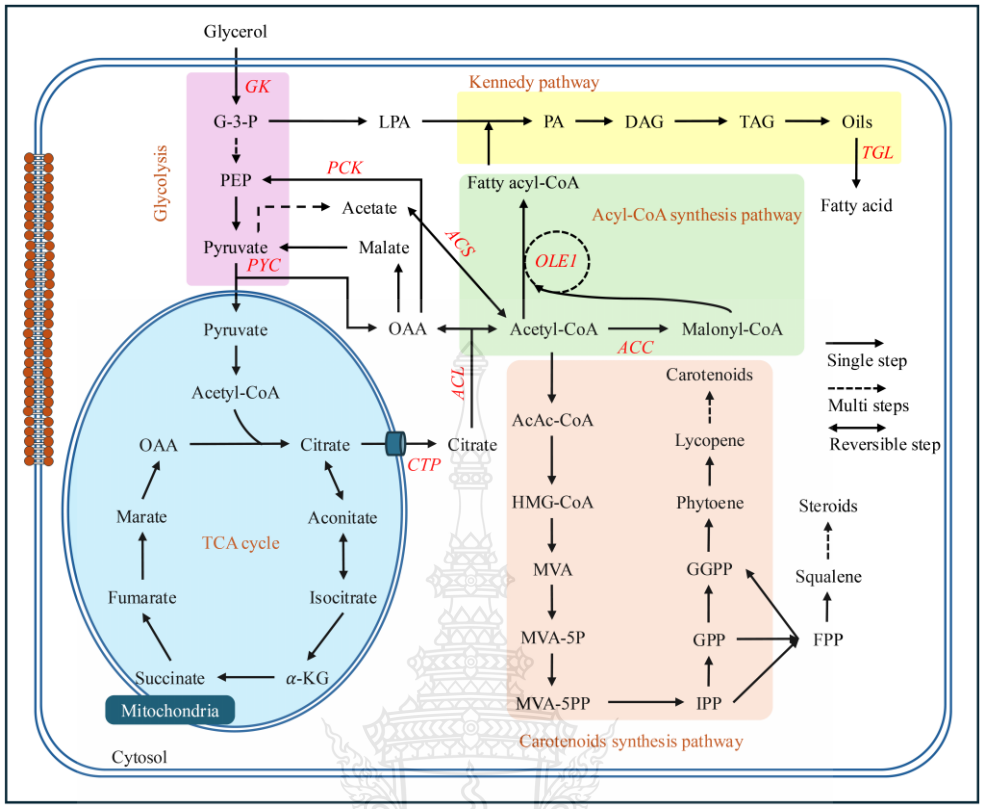

Figure 4.4 Metabolic pathways of *R. toruloides* under dual inducer treatment in flask-scale experiments using PBCG as a carbon source. Abbreviations: G-3-P, glyceraldehyde 3-phosphate; PEP, phosphoenolpyruvate; α-KG, alpha-ketoglutarate; OAA, oxaloacetic acid; LPA, lysophosphatidic acid; PA, phosphatidic acid; DAG, diacylglycerol; TAG, triacylglycerol; TCA cycle, tricarboxylic acid cycle; AcAc-CoA, aceto-acetyl-CoA; HMG-CoA, hydroxymethylglutaryl-CoA; MVA, mevalonate; MVA-5P, mevalonate-5-phosphate; MVA-5PP, mevalonate-5-diphosphate; IPP, isopentenyl diphosphate; GPP, geranyl diphosphate; GGPP, geranylgeranyl diphosphate; FPP, farnesyl diphosphate. The pathway map was adapted from Wen et al. [111] and Ngernsombat et al. [88].

4.4 Mathematic modeling of yeast oil and β-carotene co-production

Mathematical modeling (Eqs. (3.1) to (3.4)) was applied to estimate the kinetic parameters of YO and β-carotene co-production (Table 4.3). This study examined the fermentation behavior of *R. toruloides* under the control condition and with dual inducer supplementation. The experimental and model-predicted profiles during YO and β-carotene co-production under dual inducer addition in flask and bioreactor are illustrated in Figure 4.5A to D. The dynamic Logistic growth equation (Eq. (3.1)) is commonly used to simulate microbial growth data and estimate growth kinetic parameters. As shown in Figure 4.5, the model-predicted growth profile demonstrated good agreement with the experimental data, with R^2 values ranging from 0.78 to 0.93 and *NRMS* values from 0.34 to 1.40. The maximum oleaginous biomass concentration (X_{max}) increased to 6.84 g/L under dual inducer supplementation in the flask-scale experiments. By contrast, the biomass concentration decreased from 9.03 to 6.00 g/L in the bioreactor. These results suggested that IO accumulation in the biomass was significantly promoted under dual inducer conditions, increasing yeast biomass weight. However, in the bioreactor, the IO accumulated in the biomass was transported to EO, resulting in a decrease in oleaginous biomass weight [85].

The maximum specific growth rate (μ_{max}) decreased from 0.103 h^{-1} under control conditions to 0.040 h^{-1} with dual inducer addition in the flask experiments (Table 4.3). In the bioreactor experiments, the decreasing trend in μ_{max} was similar to results observed at the flask scale, with values declining from 0.057 to 0.044 h^{-1}. This result indicated that the estimated μ_{max} was closely related to the secretion of IO in yeast biomass, suggesting that the addition of dual inducers negatively affected the growth rate of *R. toruloides.*

The glycerol consumption rate was primarily influenced by the growth rate of *R. toruloides*, which produced YO and β-carotene, as well as by the substrate uptake rate for cell maintenance (m_S). The experimental data on glycerol consumption were fitted to Eq. (3.2), with the kinetic parameter values for each condition presented in Table 4.3. The R^2 values exceeded 0.72, while *NRMS* values were below 2.75, indicating that the fitting results were satisfactory and closely aligned with the mathematical model (Figure 4.5 and Table 4.3). Results revealed that the oleaginous biomass yield ($Y_{X/S}$) under dual inducer supplementation was lower than in the control experiments in flask and bioreactor

conditions (Table 4.3). However, the EO yield under dual inducer supplementation was higher than in the control experiment, suggesting that the release of IO contributed to the lower estimated $Y_{X/S}$ compared to the control condition. The m_S values were zero across all conditions, demonstrating that glycerol was primarily consumed for growth and product formation rather than for cell maintenance. Energy and carbon sources are used for microbial growth and product formation, with m_S describing the specific substrate consumption rate for cell maintenance. Cellular maintenance requires energy to repair damaged cellular components, transport nutrients and products across the cell membrane, and regulate the osmolarity of microbial cells [109].

The experimental data were fitted to Eqs. (3.3) and (3.4) for YO and β-carotene formation, yielding satisfactory results that well-aligned with the studied product formation models. The R^2 values were above 0.86 and 0.85, while *NRMS* values were below 0.29 and 11.27 for YO and β-carotene formation rates, respectively (Figure 4.5 and Table 4.3). Furthermore, the estimated α values for YO and β-carotene formation were higher than the β values in all experiments, indicating that YO and β-carotene production by *R. toruloides* TISTR 5186 with PBCG as a substrate were growth-associated, consistent with the findings of Ngernsombat et al. [85].

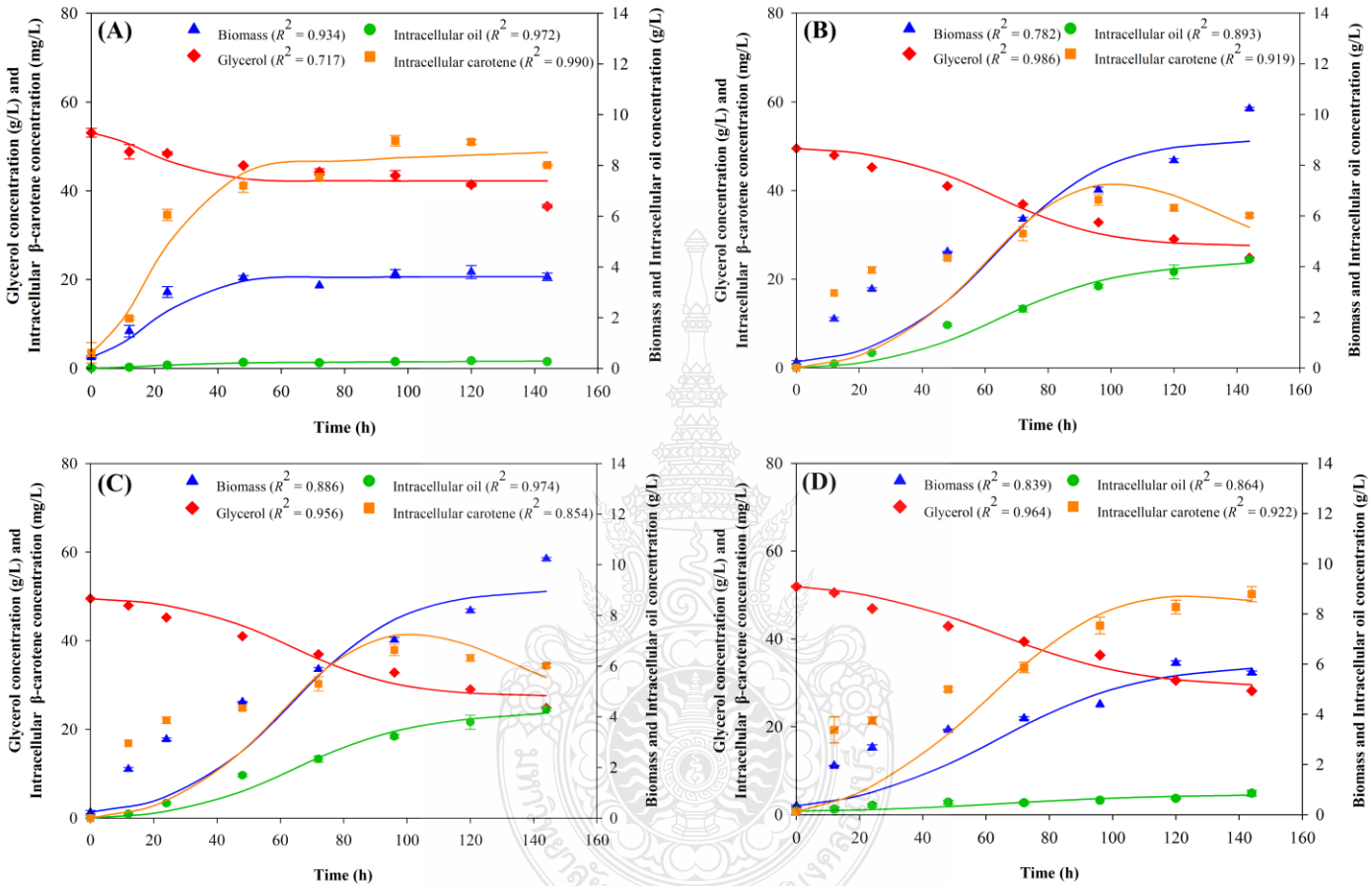

Figure 4.5 Schematic of the experimental observations (symbols) and model predictions (lines) during yeast oil and β-carotene co-production under dual inducer addition. Control (A) and dual inducer (B) condition in flask scale; and control (C) and dual inducer (D) condition in bioreactor scale. Experimental data are represented as mean values ± SD bar.

Table 4.3 Estimated kinetic parameters of intracellular yeast oil and β-carotene co-production by *R. toruloides* TISTR 5186 under dual inducer addition in flask and bioreactor scales.

Model and kinetic parameters	Flask		Bioreactor	
	Control	Dual inducer	Control	Dual inducer
Yeast growth rate				
X_{max} (g/L)	3.611	6.84	9.03	6.00
μ_{max} (1/h)	0.103	0.040	0.057	0.044
R^2	0.9338	0.7821	0.8855	0.8389
NRMS	0.3428	1.3872	1.3954	1.0385
Glycerol consumption rate				
$Y_{X/S}$ (g/g)	0.290	0.273	0.393	0.245
m_S	0	0	0	0
R^2	0.7167	0.9859	0.9557	0.9639
NRMS	2.7544	1.0892	2.0637	1.8071
Yeast oil production rate				
α_{YO} (g/g)	0.0627	0.3150	0.4259	0.1022
β_{YO} (g/gh)	0.0001	0	0.0005	0.0002
$Y_{YO/S}$ (g/g)	0.018	0.086	0.167	0.025
R^2	0.9723	0.8929	0.9744	0.8639
NRMS	0.0177	0.1672	0.2868	0.1038
β-carotene production rate				
α_{CT} (g/g)	0.0133	0.0183	0.0071	0.0115
β_{CT} (g/gh)	0	0	0	0
$Y_{CT/S}$ (g/g)	0.004	0.005	0.003	0.003
R^2	0.9904	0.9187	0.8538	0.9216
NRMS	3.8159	11.2695	9.9256	9.3000

4.5 Enhancing yeast oil and β-carotene co-production by *R. toruloides* cultivation integrated with cell retention system

The time course of YO and β-carotene co-production by batch fermentation (BF) using BCG-based medium is illustrated in Figure 4.6. Glycerol consumption and yeast growth initiated immediately after starter inoculation, with yeast growth proceeding through the log phase without an observable lag phase. Maximum biomass reached 6.38 ± 0.08 g/L at 144 h of cultivation. YO and β-carotene co-production initiated after 24 h of fermentation. β-carotene concentration increased rapidly within the first 72 h, then rose slightly to 35.33 ± 3.33 mg/L at 144 h. In contrast, YO increased continuously, reaching 3.99 ± 0.15 g/L at 144 h. Throughout the process, 12.69 ± 0.86 g/L of glycerol was consumed, which impacts production cost and efficiency. These results indicate that improvement of the fermentation process is necessary to enhance co-production performance, particularly with regard to production rate.

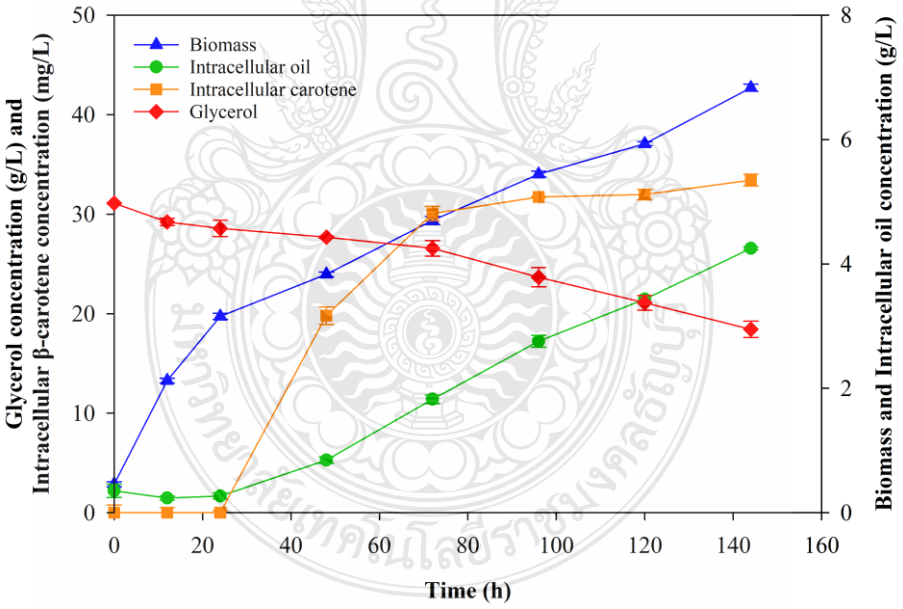

Figure 4.6 Time profiles of yeast oil and β-carotene co-production by *R. toruloides* TISTR 5186 under batch fermentation (BF) in bioreactor. Data are represented as mean values ± SD bar.

In Figure 4.7, increasing dilution rates (D) (0.005 – 0.015 h^{-1}) during continuous fermentation (CF) of *R. toruloides* resulted in distinct trends: residual glycerol accumulated progressively at higher D, while biomass, YO, and β-carotene concentrations declined. This observation reflected the inverse relationship between D and microbial residence time, wherein a faster BCG-based medium flow rate decreased glycerol assimilation efficiency, leaving unconsumed glycerol in the system. Concurrently, a shorter retention period limited biomass accumulation due to cell washout, governed by the steady-state relationship between D, residual glycerol (S), and biomass (X) according to the equation $X \propto D\frac{(S_0\text{-}S)}{\mu}$.

The diminished YO and β-carotene production correlated with restricted yeast growth under high D conditions, as cells had insufficient time to synthesize these metabolites. Thus, elevated D negatively impacted limiting substrate utilization, biomass retention, and metabolite production, significantly affecting overall fermentation efficiency.

The profile of YO and β-carotene co-production under continuous fermentation integrated with cell retention system (CF-CR) at $D = 0.005\ h^{-1}$ in a bioreactor is illustrated in Figure 4.8. Biomass rapidly accumulated in the bioreactor with no outflow, reaching a maximum of 9.64 ± 0.02 g/L at 173 h, before decreasing due to biomass initially remaining in the filter system. Glycerol consumption was higher than in CF, with residual levels maintained at approximately 6.20 to 9.20 g/L during 48 to 144 h. YO production increased continuously, to 5.64 ± 0.13 g/L at 173 h. Additionally, β-carotene concentration increased rapidly to 32.73 ± 6.55 mg/L during the first 72 h and subsequently remained stable with slight fluctuation between 28.50 to 42.90 mg/L until 173 h under this co-production system. These results demonstrate that the cell retention system effectively accumulates biomass to high concentrations, thereby promoting glycerol consumption and enhancing YO and β-carotene co-production.

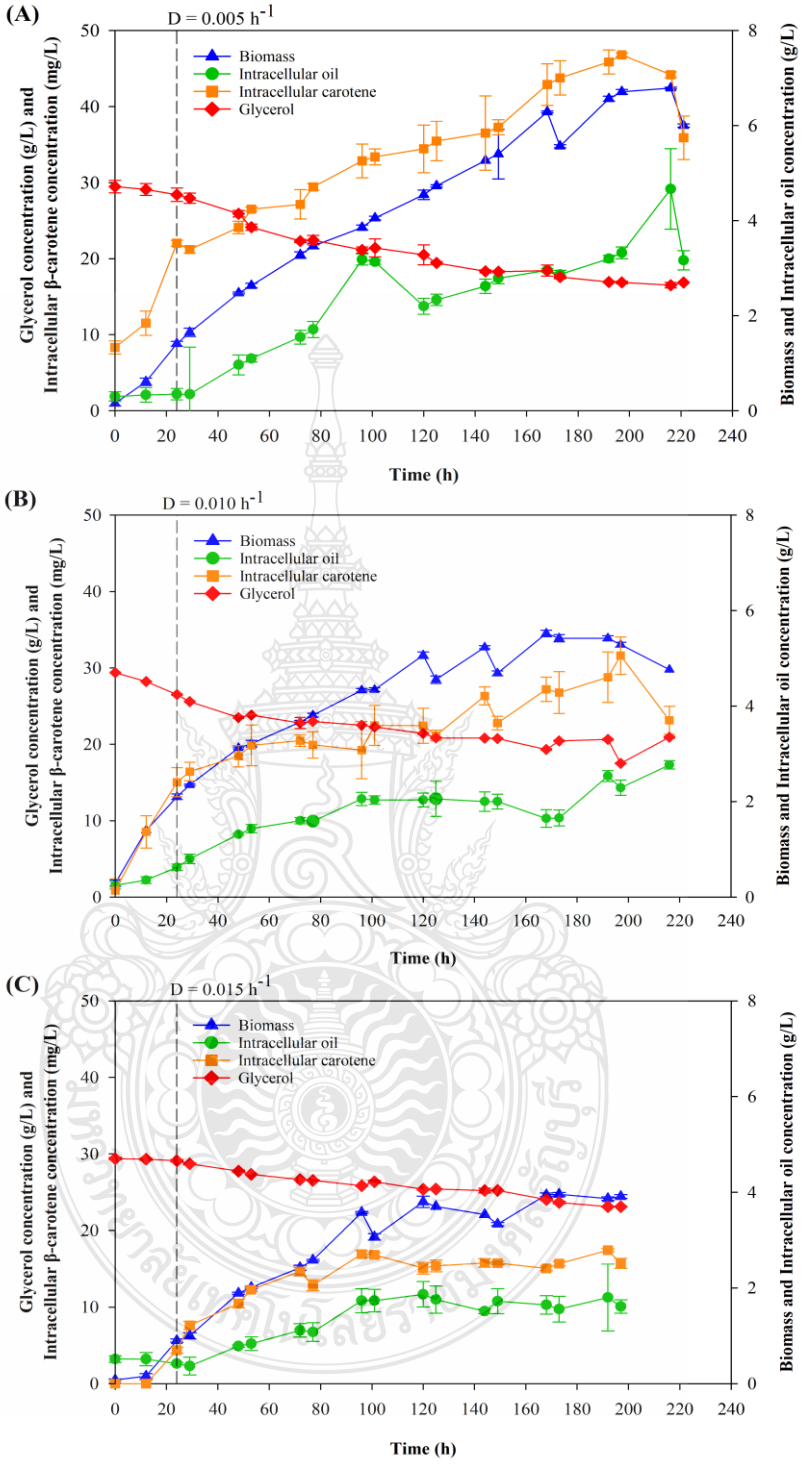

Figure 4.7 Time profiles of yeast oil and β-carotene co-production by *R. toruloides* TISTR 5186 in 10 L bioreactor under continuous fermentation (CF) with dilution rates of (A) 0.005 h^{-1}, (B) 0.010 h^{-1}, and (C) 0.015 h^{-1}. Data are represented as mean values ± SD bar.

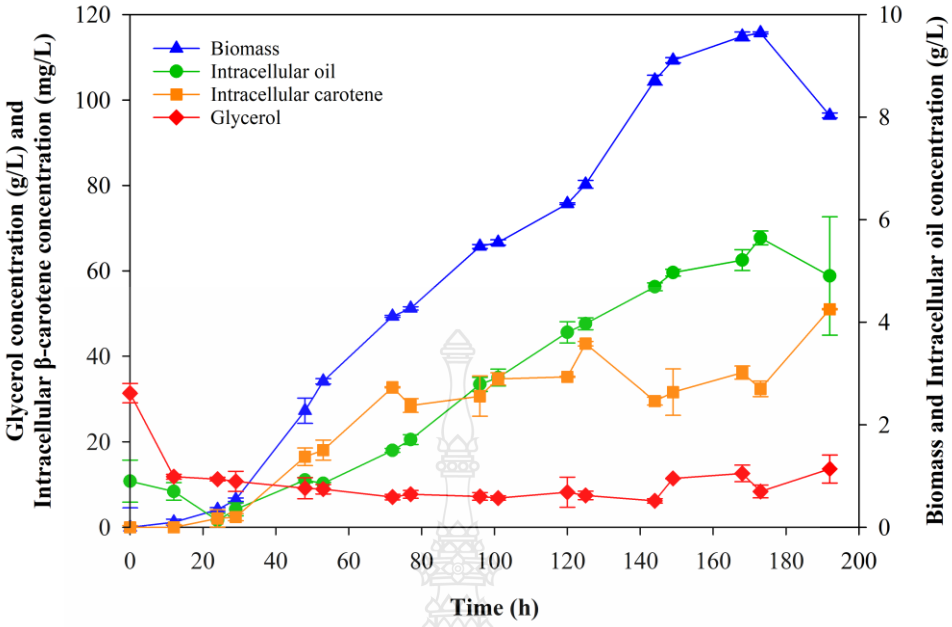

Figure 4.8 Time profiles of yeast oil and β-carotene co-production by *R. toruloides* TISTR 5186 in 10 L bioreactor under continuous fermentation integrated with cell retention system (CF-CR) at D = 0.005 h^{-1} in bioreactor. Data are represented as mean values ± SD bar.

The performance of different fermentation processes on co-production of YO and β-carotene is presented in Table 4.4. Results revealed that volumetric production of biomass, glycerol consumption, and YO dramatically decreased with increasing dilution rate (D) under continuous fermentation (CF). Both TO content and TC content also decreased. This suggests that enhancing D leads to decreased retention time of substrate within the bioreactor [110]. Consequently, the substrate assimilation time for microorganisms was shortened under high D. In contrast, the volumetric production rates of biomass, glycerol consumption, and YO increased with increasing D. Additionally, CF reached steady state more rapidly when D increased. In comparison, the continuously integrated cell retention system (CF-CR) retained biomass containing YO and β-carotene within the bioreactor through a cross-flow filtration unit. Consequently, biomass concentration and its products accumulated in the bioreactor, resulting in improved fermentation parameters

Table 4.4 Fermentation parameters of yeast oil and β-carotene co-production under dual inducers in batch, continuous, and continuous integrated cell retention system in bioreactor.

Parameter	BF	CF			CF-CR
		0.005 h^{-1}	0.010 h^{-1}	0.015 h^{-1}	0.005 h^{-1}
X_{max} (g/L)	6.38 ± 0.08^{b}	6.33 ± 0.45^{b}	5.11 ± 0.02^{c}	3.67 ± 0.02^{d}	9.64 ± 0.02^{a}
ΔS (g/L)	12.69 ± 0.86^{b}	12.27 ± 0.76^{b}	9.10 ± 0.03^{c}	4.65 ± 0.21^{d}	22.97 ± 1.48^{a}
$Y_{X/S}$	0.50 ± 0.04^{b}	0.52 ± 0.04^{b}	0.56 ± 0.0^{b}	0.79 ± 0.04^{a}	0.42 ± 0.03^{c}
Q_X (g/L·h)	0.044 ± 0.001^{c}	0.031 ± 0.002^{d}	0.048 ± 0.001^{b}	0.054 ± 0.0^{b}	0.056 ± 0.0^{a}
YO (g/L)	3.99 ± 0.15^{b}	3.10 ± 0.08^{c}	2.09 ± 0.06^{d}	1.74 ± 0.02^{e}	5.64 ± 0.13^{a}
$Y_{TO/S}$	0.32 ± 0.02^{a}	0.23 ± 0.01^{cd}	0.20 ± 0.01^{d}	0.27 ± 0.03^{b}	0.25 ± 0.01^{bc}
Q_{TO} (g/L·h)	0.028 ± 0.001^{b}	0.014 ± 0.0^{d}	0.018 ± 0.001^{c}	0.018 ± 0.001^{c}	0.033 ± 0.00^{a}
TO content (%)	62.55 ± 2.63^{a}	45.5 ± 4.41^{b}	38.30 ± 0.99^{c}	34.31 ± 2.51^{c}	58.52 ± 1.31^{a}
β-carotene (mg/L)	35.33 ± 3.33^{a}	38.62 ± 2.8^{a}	25.54 ± 0.79^{b}	17.01 ± 1.39^{c}	35.73 ± 0.0^{a}
$Y_{TC/S}$	2.81 ± 0.47^{b}	3.16 ± 0.42^{ab}	2.80 ± 0.10^{b}	3.66 ± 0.37^{a}	1.56 ± 0.10^{c}
Q_{TC} (mg/L·h)	0.245 ± 0.023^{a}	0.193 ± 0.014^{b}	0.255 ± 0.008^{a}	0.255 ± 0.021^{a}	0.207 ± 0.0^{b}
TC content (mg_{TC}/g_{cell})	5.54 ± 0.46^{ab}	6.28 ± 0.69^{a}	5.30 ± 0.26^{b}	4.74 ± 0.38^{b}	3.71 ± 0.01^{c}
Fermentation time (h)	144	–	–	–	173
Steady state period (h)	–	168-221	120-216	96-197	–

Data are shown as mean values ± SD. Different lowercase superscripts in the same row indicate significant differences at *p*-value < .05 BF = batch fermentation, CF = continuous fermentation, CF-CR = continuous fermentation integrated with cell retention system

Total YO and β-carotene co-production under dual inducers in a bioreactor under different processes is presented in Table 4.5. For batch fermentation (BF), the biomass and product formation were lower than in continuous fermentation. In CF, the highest total biomass, YO, and β-carotene production reached 54.40 ± 3.87 g, 26.64 ± 0.67 g, and 332.11 ± 24.47 mg, respectively, at a *D* of 0.005 h^{-1}. Additionally, biomass, YO, and β-carotene significantly decreased with increasing *D*, while the production rates of biomass and yeast products were higher than in BF and enhanced as D increased. Regarding glycerol consumption efficiency, BF demonstrated higher effectiveness than CF. Additionally, high *D* values decreased glycerol consumption efficiency. When comparing the CF-CR at $D = 0.005\ h^{-1}$ to conventional CF at the same D, total biomass and YO increased by 1.55- and 1.86-fold, respectively, while total β-carotene production showed no significant difference (*p*-value ≥ .05). These results demonstrate that CF-CR is an effective process for enhancing fermentation performance, particularly in terms of product concentration and productivity.

Batch fermentation is widely utilized in microbial product formation due to its operational simplicity and low contamination risks. However, batch processes exhibited several limitations, including diminished productivity resulting from inhibitor accumulation and nutrient depletion, limited operational stability, and labor-intensive procedures such as seed culture preparation, fermenter cleaning, and media replacement [111]. On the other hand, continuous fermentation systems offer numerous benefits including enhanced productivity through inhibitor dilution, uninterrupted nutrient supply, and extended operational stability compared to batch methods [111]. The *D*, a key parameter in continuous fermentation calculated as the ratio of medium flow rate to working volume, can be precisely regulated (18). Increasing *D* reduces product concentrations and cell density through dilution while simultaneously improving productivity [112]. Consequently, *D* significantly influences product formation, substrate utilization, productivity, and microbial growth dynamics [113], [114].

The *D* plays a crucial role in substrate utilization efficiency. Studies have consistently demonstrated that increasing the dilution rate leads to a decrease in substrate consumption, primarily due to the reduced residence time of the fermentation medium within the bioreactor. This shortened contact period between microorganisms and substrate prevents complete utilization of available nutrients [110]. Although higher dilution rates diminish overall substrate consumption, the production rate of desired products under specific conditions is enhanced. Under steady state conditions, the dilution rate establishes a critical balance between substrate utilization efficiency and product formation, with higher rates typically resulting in stable but less efficient substrate conversion [115], [116].

Table 4.5 Total yeast oil and β-carotene co-production under dual inducers by batch, continuous, and continuous integrated cell retention system in bioreactor.

Parameter	BF	CF			CF-CR
		0.005 h^{-1}	0.010 h^{-1}	0.015 h^{-1}	0.005 h^{-1}
Fermentation time (h)	144	144*	96*	72*	149*
Production volume (L)**	5.0	8.6	9.8	10.4	8.7
Biomass (g)	31.89 ± 0.42^{e}	54.40 ± 3.87^{b}	50.05 ± 0.20^{c}	38.16 ± 0.22^{d}	84.15 ± 0.17^{a}
YO (g)	19.94 ± 0.77^{c}	26.64 ± 0.67^{b}	20.48 ± 0.58^{c}	18.13 ± 0.24^{d}	49.52 ± 1.18^{a}
β-carotene (mg)	176.65 ± 16.65^{c}	332.11 ± 24.47^{a}	250.25 ± 7.72^{b}	176.95 ± 14.44^{c}	311.77 ± 0.0^{a}
Q_X (g/h)	0.22 ± 0.0^{d}	0.38 ± 0.03^{c}	0.52 ± 0.0^{b}	0.53 ± 0.0^{b}	0.56 ± 0.0^{a}
Q_{TO} (g/h)	0.14 ± 0.01^{e}	0.19 ± 0.0^{d}	0.21 ± 0.01^{c}	0.25 ± 0.0^{b}	0.33 ± 0.01^{a}
Q_{TC} (mg/h)	1.23 ± 0.12^{d}	2.31 ± 0.17^{bc}	2.61 ± 0.08^{a}	2.46 ± 0.20^{ab}	2.09 ± 0.0^{c}
Glycerol consumption efficiency (%)	42.30 ± 2.88^{b}	40.91 ± 2.52^{b}	30.35 ± 0.11^{c}	15.51 ± 0.70^{d}	76.56 ± 4.94^{a}

Data are shown as mean values ± SD. Different lowercase superscripts in the same row indicate significant differences at *p*-value < .05. BF = batch fermentation, CF = continuous fermentation, CF-CR = continuous fermentation integrated with cell retention system.

*Fermentation time of CF and CF-CR is stated from initial feeding time until a steady state was observed.

**Production volume of CF and CF-CR is included initial working volume and feeding volum

4.6 Fatty acid compositions

4.6.1 Fatty acid under synergistic of Tween 20 and ethephon addition

Gas chromatography-mass spectrometry (GC-MS) analysis (Figure 4.9A and B) revealed that the FA compositions of both IO and EO extracts, obtained under varying cultivation conditions, were primarily composed of myristic acid (C14:0), palmitic acid (C16:0), stearic acid (C18:0), oleic acid (C18:1), and linoleic acid (C18:2). This observation aligns with prior studies, such as Ngernsombat et al. (2024) [85], reporting that C16-C18 FAs as the major constituents in *Rhodosporidium toruloides* grown on pure glycerol. Similarly, Polburee et al. (2015) [117] and Duarte et al. (2014) [118] identified C16:0, C18:1, and C18:2 as the dominant FAs in other oleaginous yeasts cultivated on crude glycerol. Our findings corroborate that C16 and C18 FAs are the predominant components of the produced YO, although their relative proportions differed depending on the specific cultivation parameters. It is a recognized fact that the FA profile of microbial oils is susceptible to influences from factors including the carbon source, the specific microbial strain employed, and the operational conditions of the cultivation process [119]. Notably, the long-chain C16 and C18 FAs identified in the *R. toruloides* oil in this study exhibit similarities to those found in commercially significant vegetable oils like palm, sunflower, jatropha, and rapeseed oils [120].

The consistency of the FA composition observed in this study with previous reports on oil produced from both pure and crude glycerol underscores the robustness of *R. toruloides* TISTR 5186 for valorizing this industrial byproduct [85], [118], [121]. Notably, the FA profile of the oil derived from crude glycerol in our study closely resembles that of conventional bio-oil feedstocks utilized for the production of biodiesel, biolubricants, and bio-polyurethane foam [19], [122], [123]. The utilization of such bio-oils in the synthesis of biodegradable and environmentally friendly products has garnered increasing attention in recent years. For instance, Bhatia et al. (2017) [122] demonstrated the feasibility of using YO from *Yarrowia lipolytica* for biodiesel synthesis, while Papadaki et al. (2017) [124] explored the production of bio-wax esters using *Rhodosporidium toruloides*, *Cutaneotrichosporon curvatus*, and *Lipomyces starkeyi*. Furthermore, methodologies for synthesizing polyols from YO to serve as precursors for bio-polyurethane foam production have also been developed [123]. Ma et al. (2021)

investigated the production of bio-lubricants from *Rhodotorula glutinis* YO, successfully converting ester compounds into biolubricants under optimized conditions [19]. These examples highlight the significant potential of microbial oils, including the YO produced in this study from PBCG, as sustainable alternatives for a range of industrial applications, contributing to a more circular bioeconomy.

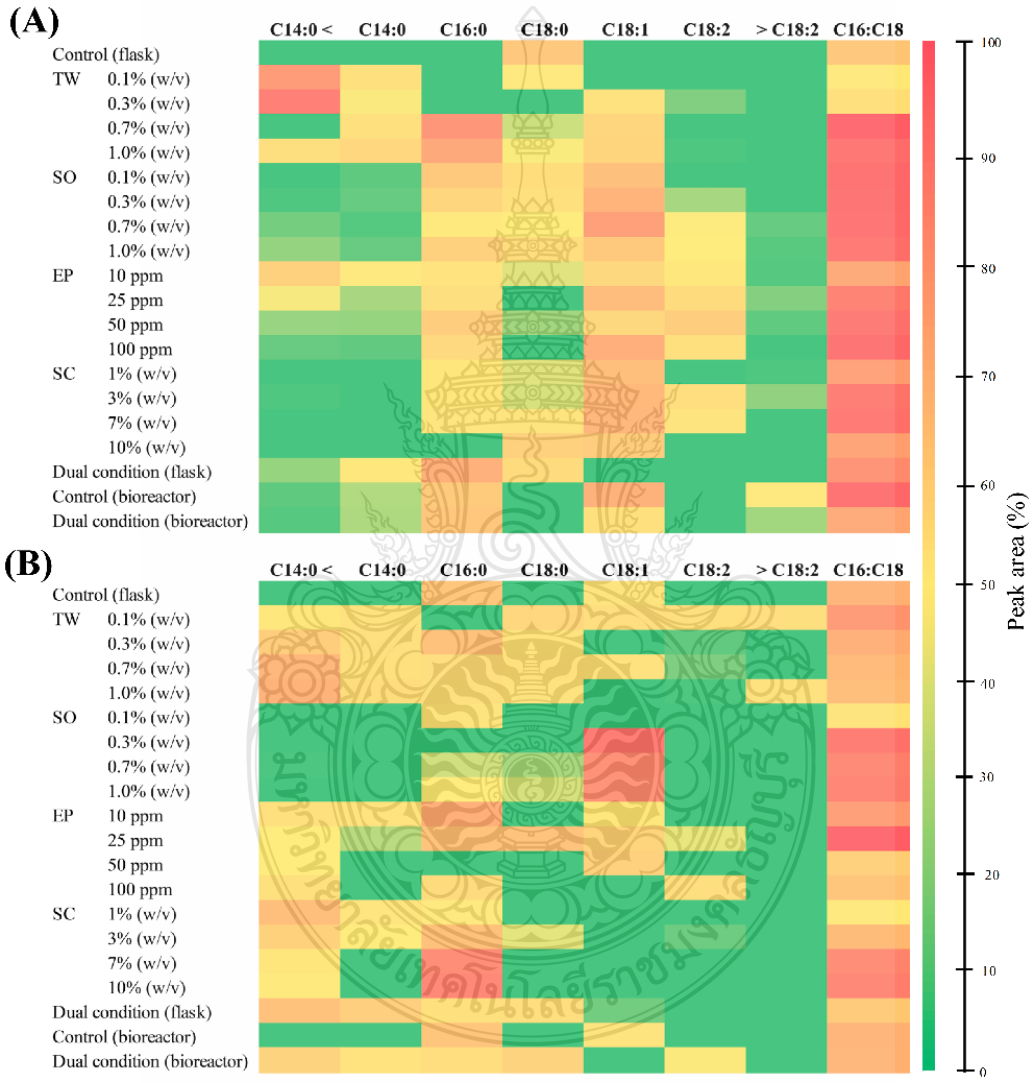

Figure 4.9 Heat map of FA profiles of IO (A) and EO (B) produced under different conditions.

4.6.2 Fatty acid in batch, continuous and continuous with cell retention process

The long-chain C16-18 FAs were the major compositions in YO produced by batch fermentation (BF) (glycerol 30 g/L), continuous fermentation (CF), and continuous fermentation integrated with cell retention (CF-CR) (Figure 4.10). The C16:C18 FA content of YO produced using PBCG-based medium exceeded 80%, similar to vegetable oils. The C16 and C18 long-chain FA profile of *R. toruloides* oil seem like those found in palm, sunflower, jatropha, and rapeseed oils [120], [125], [126], [127]. Furthermore, these findings indicate that the fermentation process did not alter the FA synthesis pathway of *R. toruloides*.

The FA composition significantly influences biodiesel, biolubricant, and bio-polyurethane foam properties. For biodiesel, FA chain length and unsaturation are critical; higher saturated FA content improves viscosity and cetane number, while elevated monounsaturated FA content enhances specific gravity and heating value [120]. For bio-polyurethane foam synthesis, Uprety et al. and Samranrit et al. demonstrated that YO containing C16 and C18 FAs could be successfully converted to bio-polyurethane foams [123], [128]. Furthermore, YO has been utilized in bio-lubricant synthesis through esterification, with formulations potentially replacing conventional lubricants [129]. Ma et al. reported that unsaturated FAs in *R. glutinis* YO enhance the lubricating properties of bio-lubricants [19]. Previous research reveals that YO containing C16 and C18 long-chain FAs significantly influences the characteristics of derived oil-based products. Our study demonstrates that YO synthesized by *R. toruloides* TISTR 5186 using glycerol as the sole carbon source under various fermentation conditions represents a promising feedstock for diverse oil-based applications.

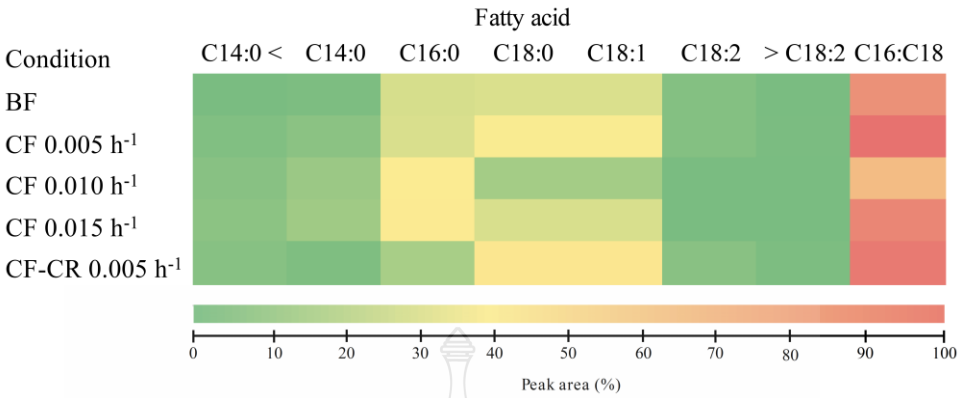

Figure 4.10 Heat map of FA profiles of yeast oil in the bioreactor. BF = batch fermentation, CF = continuous fermentation, and CF-CR = continuous fermentation integrated with cell retention system

4.7 FTIR analysis of yeast β-carotene extract

The FTIR spectra of pure β-carotene, yeast-derived β-carotene, and YO were investigated within the range of 4000–400 cm^{-1} (Figure 4.11). The spectrum of pure β-carotene exhibited distinct bands corresponding to characteristic functional groups. Bands at 2933, 1458, and 1366 cm^{-1} indicated C–H vibrations associated with alkyl groups [130]. The vibration band at 1718 cm^{-1} in the pure β-carotene spectrum was assigned to C=O stretching, a key wavenumber for β-carotene identification [131]. In comparison, the FTIR spectrum of yeast-derived β-carotene displayed peaks at 2914, 1701, and 1468 cm^{-1}, closely resembling those of pure β−carotene. The band at 2847 cm^{-1} represented C–H vibrations, further confirming the presence of alkyl groups, while the peak at 1701 cm^{-1} corresponded to C=O stretching [132]. These results confirmed that the chemical structure of β-carotene produced by *R. toruloides* TISTR 5186 was similar to that of pure β-carotene standards. The FTIR spectrum of YO exhibited a peak at 2914 cm^{-1} indicative of C–H stretching, similar to that observed in yeast−derived β−carotene [130]. The peaks at 1737 and 1699 cm^{-1} in the YO spectrum corresponded to C=O stretching, suggesting the presence of carboxylic acids or ester linkages [130]. The presence of alcoholic functional groups was correlated with C–O stretching bands at 1295, 1099, and 932 cm^{-1}, while the peaks ranging from 720–546 cm^{-1} depicted O–H bending vibrations, potentially indicating the presence of phenols, esters, and aromatic compounds [130].

Notably, the YO spectrum exhibited peaks at 2914, 1737, 1463, 1295, 932, 720, 688, and 546 cm^{-1}, showing some resemblance to the FTIR spectrum of yeast−derived β−carotene. However, the prominent C=O stretching band in YO at a slightly different wave number (1737 cm^{-1}) compared to β−carotene (around 1700−1718 cm^{-1}) suggests the presence of other carbonyl−containing compounds besides β−carotene as major constituents of the extracted oil. These findings suggested that the YO of *R. toruloides* was primarily composed of β-carotene.

4.8 Yeast oil-based BPU production

Figure 4.12 displays the visual characterization of BPU foams synthesized using different oil feedstocks and rigidity types. The rigid foams exhibit a more compact and uniform cellular structure (Figure 4.12A to C), whereas the semi-rigid foams appear less dense with larger, more irregular pores (Figure 4.12D to F). Additionally, the semi-rigid foams generally exhibit more irregular surface morphology compared to their rigid counterparts. Notably, the WCYO-based foams (Figure 4.12C and F) display intermediate morphological traits between WCO and YO foams, suggesting that the oil blend influences foam microstructure. These visual differences indicate that both oil type and foam rigidity significantly influence the final appearance and microstructural features of the PU foams.

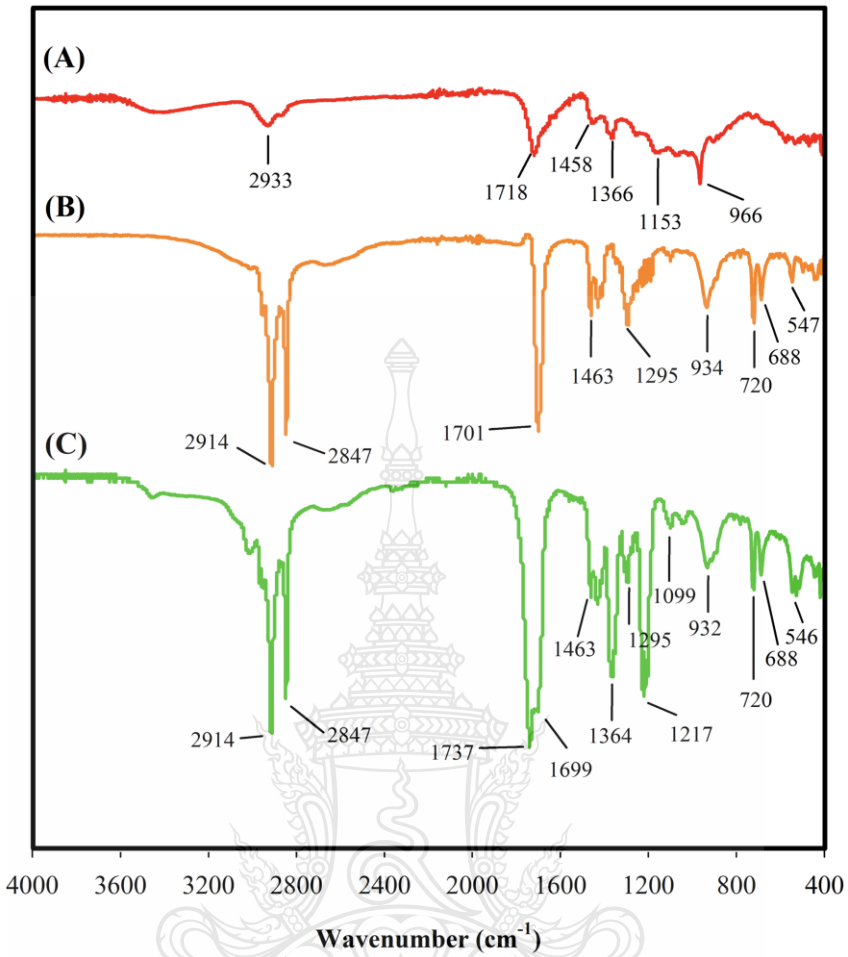

Figure 4.11 FTIR spectra of (A) pure β-carotene, (B) yeast β-carotene, and (C) β-carotene-enriched yeast oil.

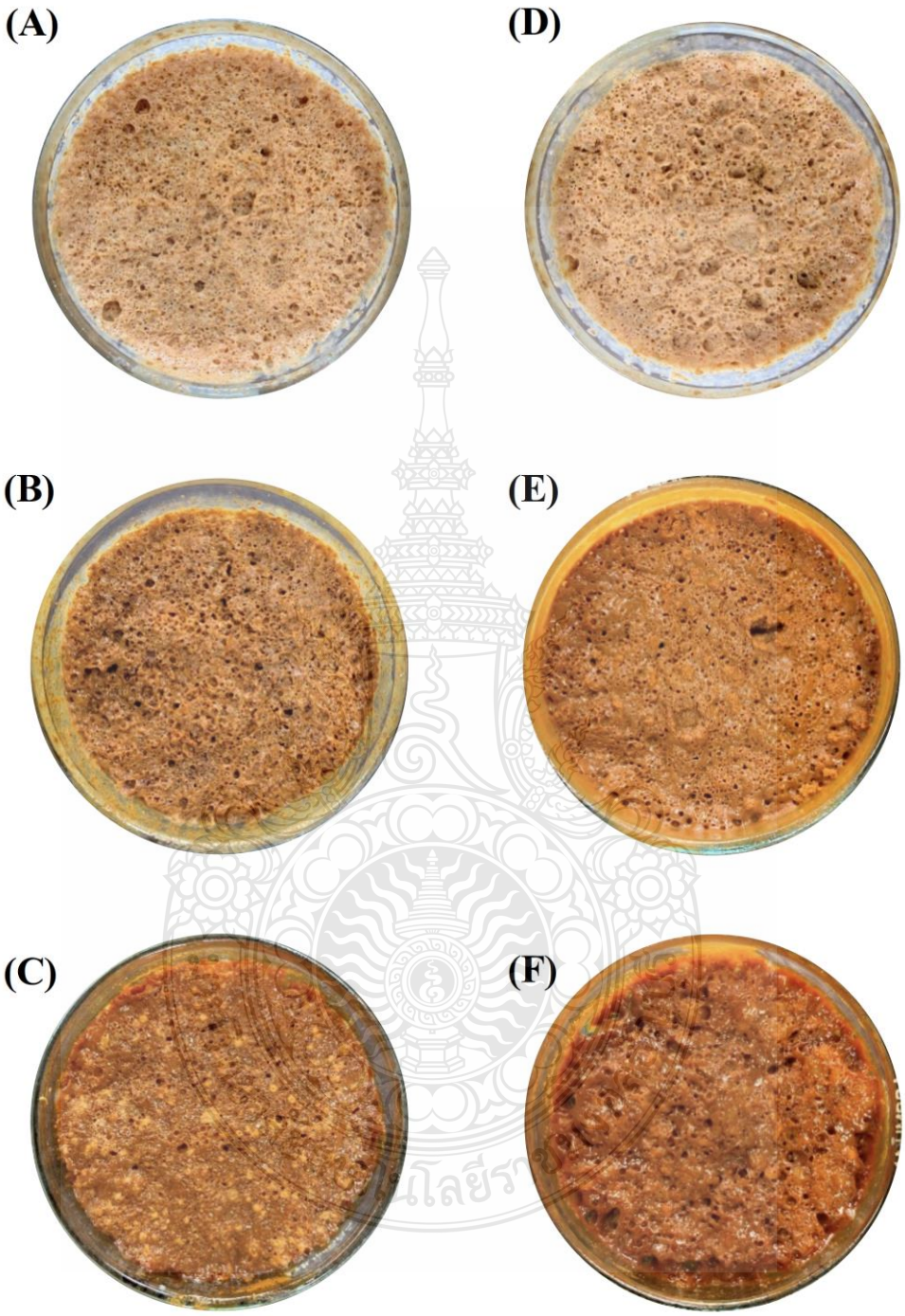

Figure 4.12 Visual characterization of PU foam formed in a 5 cm diameter glass plate. (A) rigid WCO-based PU foam, (B) rigid YO-based PU foam (C) rigid WCYO-based PU foam, (D) semi-rigid WCO-based PU foam, (E) semi-rigid YO-based PU foam (F) semi-rigid WCYO-based PU foam.

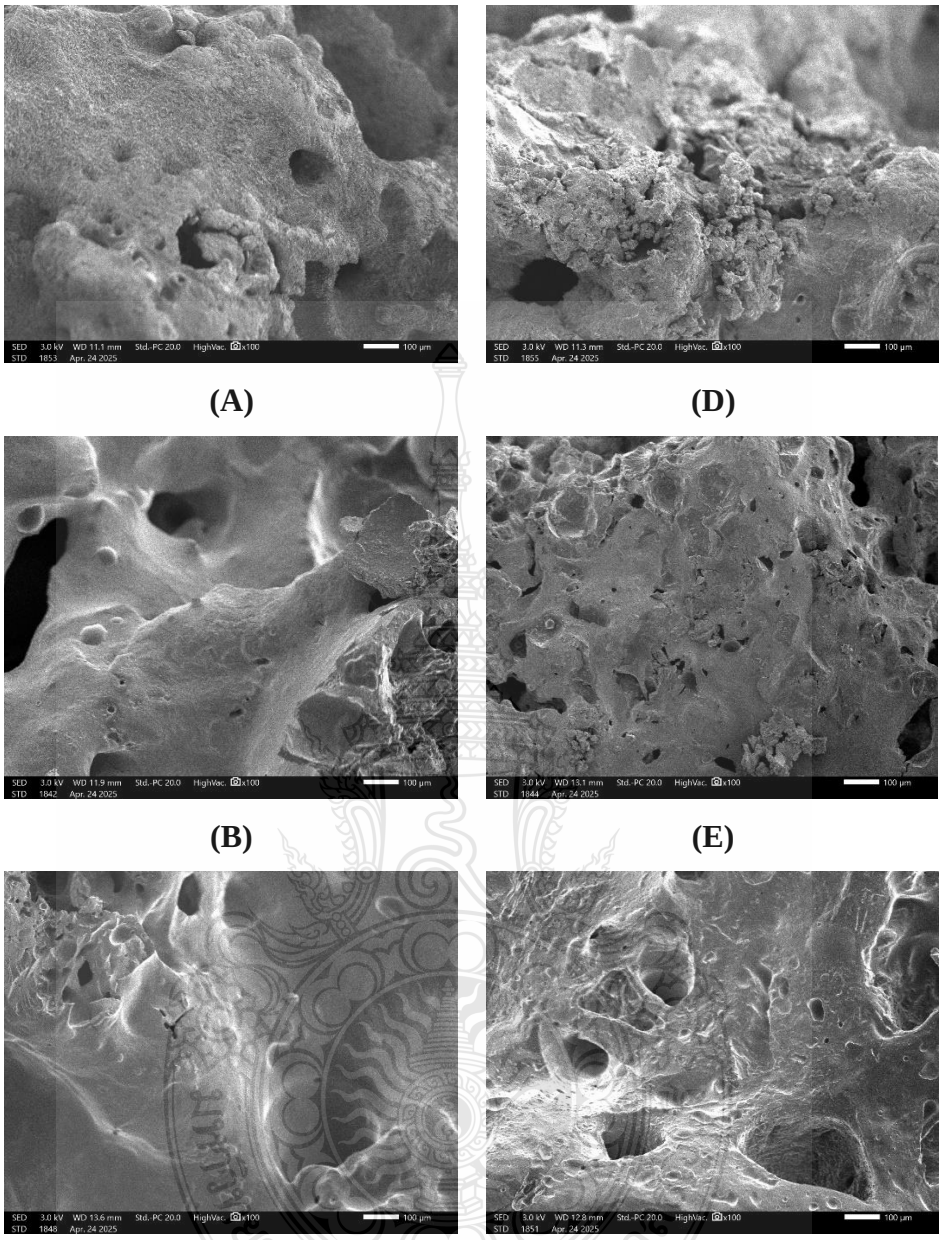

Figure 4.13 SEM images of PU foam. (A) rigid WCO-based PU foam, (B) rigid YO-based PU foam (C) rigid WCYO-based PU foam, (D) semi-rigid WCO-based PU foam, (E) semi-rigid YO-based PU foam (F) semi-rigid WCYO-based PU foam. Magnification = 100X.

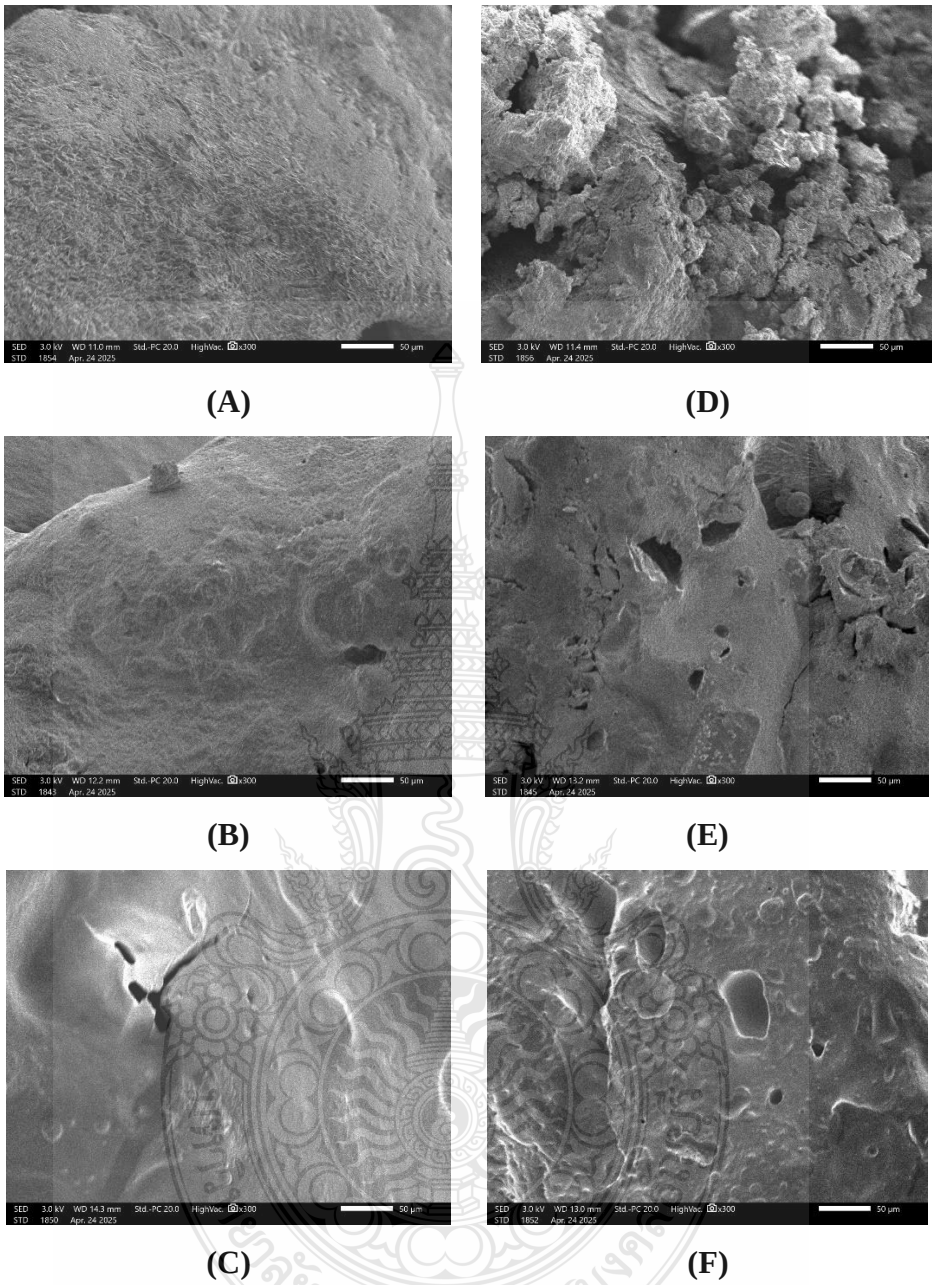

Figure 4.14 SEM images of PU foam. (A) rigid WCO-based PU foam, (B) rigid YO-based PU foam (C) rigid WCYO-based PU foam, (D) semi-rigid WCO-based PU foam, (E) semi-rigid YO-based PU foam (F) semi-rigid WCYO-based PU foam. Magnification = 300X

Scanning electron microscopy (SEM) at 100X and 300X magnifications was employed to analyze the pore morphology of rigid and semi-rigid bio-based polyurethane (BPU) foams synthesized using YO extracted from *Rhodosporidium toruloides* TISTR 5186 (as depicted in Figures 4.13 and 4.14, respectively). Observation of the surface structure revealed a consistent trend across semi-rigid BPU foams derived from waste cooking oil (WCO), yeast oil (YO), and a blend thereof (WYCO): these exhibited a greater abundance of pores compared to their rigid counterparts. This finding aligns with the observations of Samranrit et al., who reported that rigid BPU foams are characterized by a less porous and smoother surface, contrasting with the irregular surface and numerous pores evident in semi-rigid foams. The formation of these pores is attributed to the reaction between water and diisocyanate during the BPU foam production process, which releases carbon dioxide (CO_2) [133].

The density and water absorption properties of rigid and semi-rigid bio-polyurethane (BPU) foams produced from waste cooking oil (WCO), yeast oil (YO), and waste cooking oil mixed with yeast oil (WCYO) were investigated following ASTM D729 and D570 standards, respectively. The results of these analyses are presented in Table 4.6. Results indicate that neither the BPU type (rigid vs. semi-rigid) nor the oil source (WCO, YO, or WCYO) significantly influenced density, as all values ranged narrowly between 0.97 ± 0.03 and 1.01 ± 0.01 g/cm³ without statistically significant differences (p-value ≥ .05). Water absorption showed similar variability without significant differences across samples, with rigid foams exhibiting slightly lower absorption (40.99 ± 3.25% to 42.33 ± 4.90%) compared to semi-rigid foams (43.88 ± 4.64% to 47.60 ± 12.54%). Concurrent with this study, Samranrit et al. reported preliminary BPU synthesis using rice straw hydrolysate, with densities of 0.95 ±0.07 g/cm³ and 0.86 ±0.02 g/cm³ for rigid and semi-rigid BPU, respectively [133]. Bio-based polyurethane (BPU) density varies significantly. Szycher (2011) classified PU foams with densities of 0.5–1.5 g/cm^3 as low-density, consistent with the BPU produced in this study [134]. Conversely, Carriço et al. (2016) reported flexible PU from lignin with density > 1.2 g/cm^3 [135], and Marcovich et al. (2001) described semi-rigid BPU from palm oil with a much higher density of 2.94 ± 0.18 g/cm^3 [136]. These findings demonstrated that BPCG-based YO represents a promising feedstock for BPU production. Using YO and mixed with WCO provided density and water absorption properties comparable to WCO-based foams. Furthermore, YO showed potential as a sustainable replacement for WCO and as a supplementary feedstock for BPU production. Moreover, BCG-based YO exhibited suitable properties for applications such as corrosion barriers, automotive sound absorption materials, and moist medical materials [134]. In this study, the BCG could serve as an alternative inexpensive carbon source for oleaginous yeast cultivation, with the produced YO being highly feasible for BPU synthesis. However, raw material costs remain an obstacle for YO production used in BPU synthesis. Low-cost materials and industrial waste represent alternative resources for sustainable BPU production processes. Additionally, further development of BPU characteristics and manufacturing processes is necessary for practical industrial-scale applications.

Table 4.6 Density and water absorption of BPU foam produced from waste cooking oil (WCO), yeast oil (YO), and waste cooking oil mixed yeast oil (WCYO)

BPU sample	Density (g/cm^3)	Water absorption (%)
Rigid WCO-based BPU	1.01 ± 0.01^{ns}	40.99 ± 3.25^{ns}
Rigid YO-based BPU	0.97 ± 0.03^{ns}	42.33 ± 4.90^{ns}
Rigid WCYO-based BPU	0.98 ± 0.03^{ns}	42.01 ± 2.11^{ns}
Semi-rigid WCO-based BPU	0.98 ± 0.04^{ns}	46.51 ± 2.46^{ns}
Semi-rigid YO-based BPU	0.97 ± 0.05^{ns}	47.60 ± 12.54^{ns}
Semi-rigid WCYO-based BPU	0.99 ± 0.05^{ns}	43.88 ± 4.64^{ns}

Data are shown as mean values ± SD. ns presented no significant differences at *p*-value ≥ .05. WCO-based BPU = waste cooking oil-based bio-polyurethane, YO-based BPU = yeast oil-based bio-polyurethane, and WCYO-based BPU = waste cooking oil mixed yeast oil-based bio-polyurethane.

4.9 Encapsulation of yeast β-carotene extract by spray- and freeze-drying

The yeast β-carotene extract was encapsulated using spray-drying and freeze-drying processes. Gum Arabic alone and Gum Arabic mixed with maltodextrin were employed as the main carriers. Results revealed that the encapsulation efficiency (EE) ranged from 79.90 to 88.25 ± 8.57% (Table 4.7). The EE values obtained from spray drying were not significantly different from those of freeze drying. Similarly, Gum Arabic provided EE comparable to that of Gum Arabic mixed with maltodextrin. When comparing the same encapsulation process, the solubility of encapsulated yeast β-carotene extract showed no significant differences (*p*-value ≥ .05). However, the solubility of freeze-dried with gum Arabic (FD-G) was significantly higher than spray-dried with gum Arabic (SD-G). This result concurs with the reports of Guo et al. and Stabrauskiene et al. [137], [138]. The freeze-drying process generates superior solubility compared to spray-drying encapsulation primarily due to its distinct structural properties. Freeze-drying creates a more porous structure through the lyophilization process, resulting in higher solubility (61.58% versus 60.21%) [138]. This enhanced porosity facilitates quicker release and better distribution of the encapsulated compounds when introduced to solvents. In contrast, the denser structure formed during spray-drying,

despite its efficiency in encapsulating the bioactive compounds, limits immediate availability and dissolution. The freeze-drying method allows for the formation of a more stable structure that effectively enhances solubility, whereas the compact nature of spray-dried particles may restrict the release rate of the encapsulated compounds, consequently affecting overall solubility performance.

Table 4.7 Encapsulation efficiency and solubility of encapsulated β-carotene under different encapsulation processes.

Encapsulation process	Encapsulation efficiency (%)	Solubility (%)
SD-G	81.00±6.57[a]	94.03±0.30[b]
SD-GM	79.90±11.70[a]	96.35±0.57[ab]
FD-G	84.79±0.14[a]	98.98±1.07[a]
FD-GM	88.25±8.57[a]	97.24±2.22[ab]

Data are shown as mean values ± SD. Different lowercase superscripts in the same row indicate significant differences at *p*-value < .05. SD-G = spray-dried with gum Arabic, SD-GM = spray-dried with gum Arabic and maltodextrin, FD-G = freeze-dried with gum Arabic, and FD-GM = freeze-dried with gum Arabic and maltodextrin.

4.10 Properties of encapsulated yeast β-carotene extract

4.10.1 Effect of light on encapsulated yeast β-carotene extract

Figure. 4.13(A) illustrates the effect of light on β-carotene retention in non-encapsulated and encapsulated yeast β-carotene extract under light conditions. β-carotene retention in the non-encapsulated treatment decreased significantly compared to the encapsulated yeast β-carotene extract. In the non-encapsulated samples, β-carotene retention was nearly depleted at 21 days (less than 0.82%) and was undetectable at 28 days. The β-carotene retention in SD-G and SD-GM decreased at a higher rate than in FD-G and FD-GM. Nevertheless, β-carotene retention remained above 15.85% in all encapsulated powders. These results demonstrate that the encapsulation process effectively protects β-carotene from light degradation, enhancing its stability under light exposure. Figure 4.13(B) presents the 50% decreasing time (D50) for different encapsulation conditions. The highest D50 was observed for SD-G (9.42 ± 0.33 days),

followed by SD-GM, FD-G, and FD-GM. In contrast, UE-G and UE-GM exhibited significantly lower D50 values of 2.86 ± 0.33 days and 2.60 ± 0.45 days, respectively. These findings indicate that spray-dried encapsulation provided higher D50 compared to freeze-dried encapsulation, while unencapsulated powders had the shortest D50. The results clearly demonstrate that spray drying encapsulation contributes to greater light stability of β-carotene compared to freeze drying. The encapsulation process protects β-carotene from environmental factors that cause degradation. The dense structure formed during spray drying encapsulates the carotenoids more effectively, shielding them from light and oxygen exposure [139].

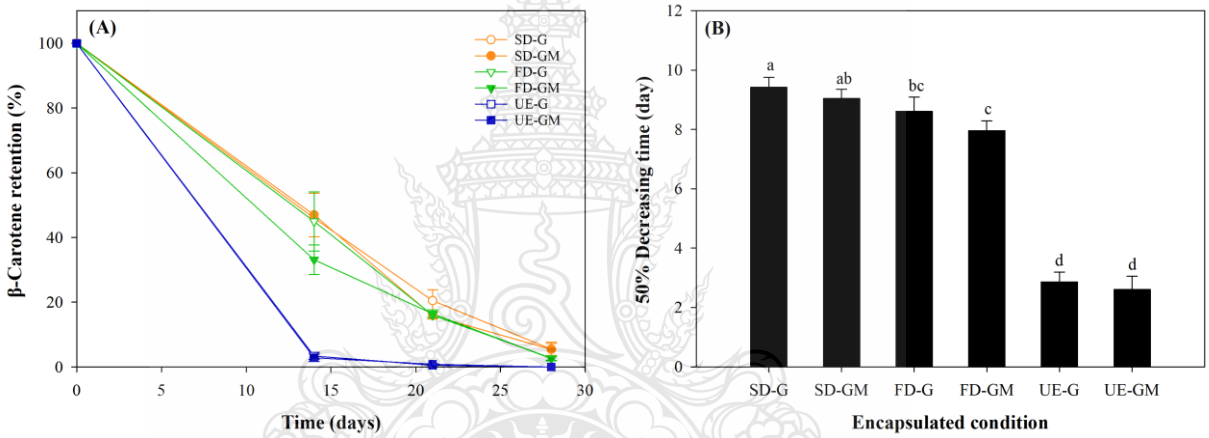

Figure 4.15 Effect of light on encapsulated yeast β-carotene extract retention. (A) β-carotene retention and (B) 50% β-carotene decreasing time. Data are represented as mean values ± SD bar. Different lowercase superscripts indicate significant differences at *p*-value < .05. SD-G = spray-dried with gum Arabic, SD-GM = spray-dried with gum Arabic and maltodextrin, FD-G = freeze-dried with gum Arabic, FD-GM = freeze-dried with gum Arabic and maltodextrin, UE-G = unencapsulated with gum Arabic, and UE-GM = unencapsulated with gum Arabic and maltodextrin.

4.10.3 Antimicrobial property

The antimicrobial properties of β-carotene extracted from *R. toruloides* TISTR 5186 and encapsulated under different conditions were investigated at 100 μg/mL (20 μL/disc). In the spray-drying process, SD-G (spray-dried with gum Arabic) effectively inhibited *B. subtilis* and *A. hydrophila* (Table 4.8), while SD-GM (spray-dried with gum Arabic and maltodextrin) demonstrated inhibitory effects against all tested pathogens. For freeze-dried samples, FD-G (freeze-dried with gum Arabic) exhibited positive inhibition against all experimental pathogens except *S. aureus*, whereas FD-GM (freeze-dried with gum Arabic and maltodextrin) showed antimicrobial activity against all investigated pathogens. This study demonstrated that the addition of maltodextrin enhanced the antimicrobial activity of encapsulated β-carotene extract. Similar findings were reported by Van et al., indicating that maltodextrin addition increases the antimicrobial activity of encapsulation products [140]. This enhancement is attributed to the water-soluble properties of maltodextrin, which facilitate improved diffusion of β-carotene extract, thereby enhancing antibacterial efficacy. The improved formulation allowed β-carotene extract to be more readily released and better distributed to bacterial cells, resulting in enhanced antibacterial properties, particularly against *E. coli*, *S. aureus*, and *V. parahaemolyticus*. Notably, SD-GM and FD-GM demonstrated antimicrobial efficacy comparable to ampicillin and streptomycin, and superior to chloramphenicol. These findings indicated that β-carotene derived from *R. toruloides* TISTR 5186 represents a promising alternative antimicrobial agent. Furthermore, the maltodextrin supplementation during the encapsulation process enhanced the antimicrobial properties of the extracted β-carotene.

Table 4.8 Antimicrobial properties of encapsulated yeast β-carotene extract เพิ่มรหัสเชื้อก่อโรค

Antimicrobial agent	Pathogens				
	E. coli TISTR 527	*S. aureus* TISTR 746	*B. subtilis* TISTR 1248	*V. parahaemolyticus* TISTR 1596	*A. hydrophila* TISTR 1321
	-	+	+	-	-
Amphicilin	+	+	+	+	+
Streptomycin	+	+	+	+	+
Chloramphenicol	−	−	+	+	+
SD-G	−	−	+	−	+
SD-GM	+	+	+	+	+
FD-G	+	−	+	+	+
FD-GM	+	+	+	+	+

SD-G = spray drying with gum Arabic, SD-GM = spray drying with gum Arabic and maltodextrin, FD-G = freeze drying with gum Arabic, FD-GM = freeze drying with gum Arabic and maltodextrin, (+) = positive result, and (−) = negative result

CHAPTER 5
CONCLUSIONS

The TW and EP were found to be potent singular enhancers for boosting the synthesis of YO and β-carotene, respectively, when pretreated black cumin ground served as the main carbon source. Remarkably, the combined use of Tween 80 and ethyl propionate substantially increased the simultaneous production of both YO and β-carotene in both laboratory flasks and larger bioreactor systems. Examination of the generated YO showed it was mainly composed of long-chain fatty acids with 16 and 18 carbon atoms. Moreover, the active chemical parts of the β-carotene obtained from *Rhodosporidium toruloides* displayed features similar to those of commercially available pure β-carotene. Gene expression analysis of *R. toruloides* TISTR 5186 grown in a medium based on black cumin ground showed that several important genes, including *GK*, *PYC*, *TGL*, *CTP*, *ACL*, *ACC*, and *OLE1*-involved in metabolic processes were more active when both inducers were added together.

Consequently, the CF process outperforms BF process in biomass and product yield, with optimal performance observed at D of 0.005 h^{-1}. However, higher D values reduce glycerol consumption efficiency and product formation. The CF-CR further enhances biomass and YO production compared to conventional CF, though β-carotene levels remain unchanged. These findings suggest that CF-CR is a promising strategy for improving fermentation efficiency, particularly for targeted product outputs.

The YO was successfully utilized to synthesize both rigid and semi-rigid BPU foams, demonstrating comparable density and water absorption properties to BPU foams derived from WCO and a blend of WCO and WCYO. These density and water absorption characteristics suggest the feasibility of YO-based BPU foams for specific industrial applications. Furthermore, β-carotene extract was effectively encapsulated via spray drying and freeze drying, employing gum Arabic either alone or in combination with maltodextrin, achieving high encapsulation efficiencies ranging from 79.9% to 88.3%. While the solubility of encapsulated samples was generally similar, FD-G exhibited superior solubility compared to its SD-G. Encapsulation significantly enhanced the light stability of β-carotene, with all encapsulated powders retaining over 15.85% of the

compound after 28 days. Notably, the SD-GM and FD-GM formulations demonstrated antimicrobial activity comparable to ampicillin and streptomycin, and superior to chloramphenicol.

In summary, BCG presents a promising, low-cost raw material for the concurrent production of YO and β-carotene. To ascertain the economic viability of this dual-inducer approach, further research is strongly recommended, focusing on pilot-scale production of YO and β-carotene co-production using *R. toruloides*. Such investigations would provide critical insights into the scalability and cost-effectiveness of this sustainable bioprocess.

PUBLICATION

Khuntong, S., Samranrit, T., Koedprasong, P., Teeka, J., Chiu, C. H., Srila, W., & Areesirisuk, A. (2025). Synergistic effects of Tween20 and ethephon on yeast oil and β-carotene co-production by *Rhodosporidium toruloides* using purified biodiesel-derived crude glycerol as an alternative carbon source. Bioresource Technology, 132211.

List of Bibliography

[1] A. Dobrowolski, P. Mituła, W. Rymowicz, and A. M. Mirończuk, "Efficient conversion of crude glycerol from various industrial wastes into single cell oil by yeast *Yarrowia lipolytica*," *Bioresource Technology*, vol. 207, pp. 237–243, 2016.

[2] C. Huang, M. Zong, H. Wu, and Q. Liu, "Microbial oil production from rice straw hydrolysate by *Trichosporon fermentans*," *Bioresource Technology*, vol. 100, no. 19, pp. 4535–4538, 2009.

[3] E. Fokum *et al.*, "Co-fermentation of glycerol and sugars by *Clostridium beijerinckii*: Enhancing the biosynthesis of 1,3-propanediol," *Food Bioscience*, vol. 41, p. 101028, 2021.

[4] M. M. S. Cabral *et al.*, "Carotenoids production from a newly isolated *Sporidiobolus pararoseus* strain by submerged fermentation," *European Food Research and Technology*, vol. 233, no. 1, pp. 159–166, 2011.

[5] M. D. C. Cerón García, C. V. González López, J. M. Fernández Sevilla, and E. Molina Grima, "Preparative recovery of carotenoids from microalgal biomass," *Methods in Molecular Biology*, vol. 1852, pp. 107–115, 2018.

[6] A. Milani, M. Basirnejad, S. Shahbazi, and B. Bolhassani, "Carotenoids: biochemistry, pharmacology and treatment," *British Journal of Pharmacology*, vol. 174, no. 11, Jun. 2017.

[7] A. Das, S.-H. Yoon, S.-H. Lee, J.-Y. Kim, D.-K. Oh, and S.-W. Kim, "An update on microbial carotenoid production: application of recent metabolic engineering tools," *Applied Microbiology and Biotechnology*, vol. 77, no. 3, pp. 505–512, 2007.

[8] V. M. Ye and S. K. Bhatia, "Pathway engineering strategies for production of beneficial carotenoids in microbial hosts," *Biotechnology Letters*, vol. 34, no. 8, pp. 1405–1414, 2012.

[9] P. M. Schenk *et al.*, "Second generation giofuels: High-efficiency microalgae for biodiesel production," *BioEnergy Research.*, vol. 1, no. 1, pp. 20–43, 2008.

List of Bibliography (Continued)

[10] B.-F. Lin, J.-H. Huang, and D.-Y. Huang, "Experimental study of the effects of vegetable oil methyl ester on DI diesel engine performance characteristics and pollutant emissions," *Fuel*, vol. 88, no. 9, pp. 1779–1785, 2009.

[11] S. Khan *et al.*, "Biodiesel production from algae to overcome the energy crisis," *HAYATI Journal of Biosciences*, vol. 24, no. 4, pp. 163–167, 2017.

[12] M. Ayoub and A. Z. Abdullah, "Critical review on the current scenario and significance of crude glycerol resulting from biodiesel industry towards more sustainable renewable energy industry," *Renewable and Sustainable Energy Reviews*, vol. 16, no. 5, pp. 2671–2686, 2012.

[13] B. E. Rittmann, "Opportunities for renewable bioenergy using microorganisms," *Biotechnology and Bioengineering*, vol. 100, no. 2, pp. 203–212, 2008.

[14] B. K. Uprety, W. Chaiwong, C. Ewelike, and S. K. Rakshit, "Biodiesel production using heterogeneous catalysts including wood ash and the importance of enhancing byproduct glycerol purity," *Energy Conversion and Management*, vol. 115, pp. 191–199, 2016.

[15] Z. Liu, A. M. Feist, G. Dragone, and S. I. Mussatto, "Lipid and carotenoid production from wheat straw hydrolysates by different oleaginous yeasts," *Journal of Cleaner Production*, vol. 249, p. 119308, 2020.

[16] B. Vasconcelos, J. C. Teixeira, G. Dragone, and J. A. Teixeira, "Oleaginous yeasts for sustainable lipid production—from biodiesel to surf boards, a wide range of 'green' applications," *Applied Microbiology and Biotechnology*, vol. 103, no. 9, pp. 3651–3667, 2019.

[17] R. Sparling, D. B. Levin, and N. Cicek, "Lipid production in the under-characterized oleaginous yeasts, *Rhodosporidium babjevae* and *Rhodosporidium diobovatum*, from biodiesel-derived waste glycerol," *Bioresource Technology*, vol. 185, pp. 49–55, 2015.

[18] C. T. Evans, C. Ratledge, and S. C. Gilbert, "A rapid screening method for lipid-accumulating yeast using a replica-printing technique," *Journal of Microbiological Methods*, vol. 4, no. 3, pp. 203–210, 1985.

List of Bibliography (Continued)

[19] X. Ma, Y. Zhang, Z. Song, K. Yu, C. He, and X. Zhang, "Enzyme-catalyzed synthesis and properties of polyol ester biolubricant produced from *Rhodotorula glutinis* lipid," *Biochemical Engineering Journal*, vol. 173, p. 108101, 2021.

[20] J. Dufour and D. Iribarren, "Life cycle assessment of biodiesel production from free fatty acid-rich wastes," *Renewable Energy*, vol. 38, no. 1, pp. 155–162, 2012.

[21] J. Dufour and D. Iribarren, "Life cycle assessment of biodiesel production from free fatty acid-rich wastes," *Renewable Energy*, vol. 38, no. 1, pp. 155–162, 2012.

[22] C. Caldeira, J. Queirós, A. Noshadravan, and F. Freire, "Incorporating uncertainty in the life cycle assessment of biodiesel from waste cooking oil addressing different collection systems," *Resources, Conservation and Recycling*, vol. 112, pp. 83–92, 2016.

[23] M. M. S. Cabral *et al.*, "Carotenoids production from a newly isolated *Sporidiobolus pararoseus* strain by submerged fermentation," *European Food Research and Technology*, vol. 233, no. 1, pp. 159–166, 2011.

[24] C. U. Mussagy, J. Winterburn, V. C. Santos-Ebinuma, and J. F. B. Pereira, "Production and extraction of carotenoids produced by microorganisms," *Applied Microbiology and Biotechnology*, vol. 103, no. 3, pp. 1095–1114, 2019.

[25] B. Latha and K. Jeevaratnam, "Purification and characterization of the pigments from *Rhodotorula glutinis* DFR-PDY isolated from natural source," *Global Journal of Biochemistry and Biotechnology*, vol. 5, Jan. 2010.

[26] F. M. Squina and A. Z. Mercadante, "Influence of nicotine and diphenylamine on the carotenoid composition of *Rhodotorula Strains*," *Journal of Food Biochemistry*, vol. 29, no. 6, pp. 638–652, 2005.

[27] J. Tinoi, N. Rakariyatham, and R. L. Deming, "Simplex optimization of carotenoid production by *Rhodotorula glutinis* using hydrolyzed mung bean waste flour as substrate," *Process Biochemistry*, vol. 40, no. 7, pp. 2551–2557, 2005.

[28] A. M. Kot, S. Błażejak, A. Kurcz, I. Gientka, and M. Kieliszek, "*Rhodotorula glutinis*-potential source of lipids, carotenoids, and enzymes for use in industries," *Applied Microbiology and Biotechnology*, vol. 100, no. 14, pp. 6103–6117, 2016.

List of Bibliography (Continued)

[29] C. U. Mussagy, A. A. C. Guimarães, L. V. F. Rocha, J. Winterburn, V. de C. Santos-Ebinuma, and J. F. B. Pereira, "Improvement of carotenoids production from *Rhodotorula glutinis* CCT-2186," *Biochemical Engineering Journal*, vol. 165, p. 107827, 2021.

[30] J. Avalos and M. Carmen Limón, "Biological roles of fungal carotenoids," *Current Genetics*, vol. 61, no. 3, pp. 309–324, Aug. 2015.

[31] R. Delgado-Pelayo, L. Gallardo-Guerrero, and D. Hornero-Méndez, "Carotenoid composition of strawberry tree (*Arbutus unedo L.*) fruits," *Food Chemistry*, vol. 199, pp. 165–175, 2016.

[32] L. C. Mata-Gómez, J. C. Montañez, A. Méndez-Zavala, and C. N. Aguilar, "Biotechnological production of carotenoids by yeasts: an overview," *Microbial Cell Factories*, vol. 13, no. 1, p. 12, 2014.

[33] M. Colmán-Martínez, M. Martínez-Huélamo, E. Miralles, R. Estruch, and R. M. Lamuela-Raventós, "A new method to simultaneously quantify the antioxidants: carotenes, xanthophylls, and vitamin A in human plasma," *Oxidative Medicine and Cellular Longevity*, vol. 2016, p. e9268531, 2015.

[34] I. R. Maldonade, A. R. P. Scamparini, and D. B. Rodriguez-Amaya, "Selection and characterization of carotenoid-producing yeasts from Campinas region, Brazil," *Brazilian Journal of Microbiology.*, vol. 38, pp. 65–70, 2007.

[35] E. Toti, C.-Y. O. Chen, M. Palmery, D. Villaño Valencia, and I. Peluso, "Non-provitamin A and provitamin A carotenoids as immunomodulators: Recommended dietary allowance, therapeutic index, or personalized nutrition," *Oxidative Medicine and Cellular Longevity*, vol. 2018, p. e4637861, 2018.

[36] J. Jayaraj, R. Devlin, and Z. Punja, "Metabolic engineering of novel ketocarotenoid production in carrot plants," *Transgenic Research*, vol. 17, no. 4, pp. 489–501, 2008.

[37] S. Lovisa and R. Kalluri, "Fatty acid oxidation regulates the activation of endothelial-to-mesenchymal transition," *Trends in Molecular Medicine*, vol. 24, no. 5, pp. 432–434, 2018.

List of Bibliography (Continued)

[38] M.-H. Liang, J. Zhu, and J.-G. Jiang, "Carotenoids biosynthesis and cleavage related genes from bacteria to plants," *Critical Reviews in Food Science and Nutrition*, vol. 58, no. 14, pp. 2314–2333, 2018.

[39] J. Clotault, D. Peltier, V. Soufflet-Freslon, M. Briard, and E. Geoffriau, "Differential selection on carotenoid biosynthesis genes as a function of gene position in the metabolic pathway: a study on the carrot and dicots," *PLoS One*, vol. 7, no. 6, p. e38724, 2012.

[40] E. A. Johnson and W. A. Schroeder, "Microbial carotenoids," in *Downstream* Processing Biosurfactants Carotenoids, in Advances in Biochemical Engineering/Biotechnology. *Berlin, Heidelberg: Springer*, 1996, pp. 119–178.

[41] S. Han and Y. Yang, "Antimicrobial activity of wool fabric treated with curcumin," *Dyes and Pigments*, vol. 64, no. 2, pp. 157–161, 2005.

[42] R. Siva *et al.*, "Evaluation of antibacterial, antifungal, and antioxidant properties of some food dyes," *Food Science and Biotechnology*, vol. 20, no. 1, pp. 7–13, 2011.

[43] M. Yolmeh, M. B. Habibi Najafi, and R. Farhoosh, "Optimisation of ultrasound-assisted extraction of natural pigment from annatto seeds by response surface methodology (RSM)," *Food Chemistry*, vol. 155, pp. 319–324, 2014.

[44] J. Iyyappan, G. Baskar, B. Bharathiraja, and R. Saravanathamizhan, "Malic acid production from biodiesel derived crude glycerol using morphologically controlled *Aspergillus niger* in batch fermentation," *Bioresource Technology*, vol. 269, pp. 393–399, 2018.

[45] M. Martín and I. E. Grossmann, "Design of an optimal process for enhanced production of bioethanol and biodiesel from algae oil via glycerol fermentation," *Applied Energy*, vol. 135, pp. 108–114, 2014.

[46] C. K. Yamakawa, L. Kastell, M. R. Mahler, J. L. Martinez, and S. I. Mussatto, "Exploiting new biorefinery models using non-conventional yeasts and their implications for sustainability," *Bioresource Technology*, vol. 309, p. 123374, 2020.

List of Bibliography (Continued)

[47] S. I. Mussatto and G. M. Dragone, "Chapter 1 - Biomass Pretreatment, Biorefineries, and Potential Products for a Bioeconomy Development," in *Biomass Fractionation Technologies for a Lignocellulosic Feedstock Based Biorefinery*, S. I. Mussatto, Ed., Amsterdam: Elsevier, pp. 1–22, 2016.

[48] N. Scarlat, M. Martinov, and J.-F. Dallemand, "Assessment of the availability of agricultural crop residues in the European Union: Potential and limitations for bioenergy use," *Waste Management*, vol. 30, no. 10, pp. 1889–1897, 2010.

[49] S. I. Mussatto, *Biomass Fractionation Technologies for a Lignocellulosic Feedstock Based Biorefinery*. Elsevier, 2016.

[50] J. Xu, T. Oura, D. Liu, and S. Kajiwara, "Heat-alkaline treatment of excess sludge and the potential use of hydrolysate as nitrogen source for microbial lipid production," *Sheng Wu Gong Cheng Xue Bao*, vol. 27, no. 3, pp. 482–488, 2011.

[51] J. Xu, W. Du, X. Zhao, G. Zhang, and D. Liu, "Microbial oil production from various carbon sources and its use for biodiesel preparation," *Biofuels, Bioproducts and Biorefining*, vol. 7, no. 1, pp. 65–77, 2013.

[52] Y. Morikawa, X. Zhao, and D. Liu, "Biological co-production of ethanol and biodiesel from wheat straw: a case of dilute acid pretreatment," *RSC Advances*, vol. 4, no. 71, pp. 37878–37888, 2014.

[53] L.-B. Yang, X.-B. Zhan, Z.-Y. Zheng, J.-R. Wu, M.-J. Gao, and C.-C. Lin, "A novel osmotic pressure control fed-batch fermentation strategy for improvement of erythritol production by *Yarrowia lipolytica* from glycerol," *Bioresource Technology*, vol. 151, pp. 120–127, Jan. 2014.

[54] Z. Chen, P. Liu, Y. Liu, H. Tang, Y. Chen, and L. Zhang, "Identification and characterization of a type-2 diacylglycerol acyltransferase (DGAT2) from *Rhodosporidium diobovatum*," *Antonie Van Leeuwenhoek*, vol. 106, no. 6, pp. 1127–1137, 2014.

[55] Z. Zhu *et al.*, "A multi-omic map of the lipid-producing yeast *Rhodosporidium toruloides*," *Nature Communications*, vol. 3, p. 1112, 2012.

List of Bibliography (Continued)

[56] S. T. Coradetti *et al.*, "Functional genomics of lipid metabolism in the oleaginous yeast *Rhodosporidium toruloides*," *Elife*, vol. 7, p. e32110, 2018.

[57] M. T. Castañeda, S. Nuñez, F. Garelli, C. Voget, and H. De Battista, "Comprehensive analysis of a metabolic model for lipid production in *Rhodosporidium toruloides*," *Journal of Biotechnology*, vol. 280, pp. 11–18, Aug. 2018.

[58] K. D. Pham *et al.*, "Effect of light on carotenoid and lipid production in the oleaginous yeast *Rhodosporidium toruloides*," *Biosci Biotechnol Biochem*, vol. 84, no. 7, pp. 1501–1512, Jul. 2020.

[59] Z. Wen, S. Zhang, C. K. Odoh, M. Jin, and Z. K. Zhao, "*Rhodosporidium toruloides* - A potential red yeast chassis for lipids and beyond," *FEMS Yeast Research*, vol. 20, no. 5, p. foaa038, 2020.

[60] G. P. Kumar and P. Rajeshwarrao, "Nonionic surfactant vesicular systems for effective drug delivery—an overview," *Acta Pharmaceutica Sinica B*, vol. 1, no. 4, pp. 208–219, 2011.

[61] T. Yoshioka, B. Sternberg, and A. T. Florence, "Preparation and properties of vesicles (niosomes) of sorbitan monoesters (Span 20, 40, 60 and 80) and a sorbitan triester (Span 85)," *International Journal of Pharmaceutics*, vol. 105, no. 1, pp. 1–6, 1994.

[62] T. Fenton, K. Kanyuck, T. Mills, and E. Pelan, "Formulation and characterisation of kappa-carrageenan gels with non-ionic surfactant for melting-triggered controlled release," *Carbohydrate Polymer Technologies and Applications*, vol. 2, p. 100060, 2021.

[63] J. C. J. Bart, Emanuele Gucciardi, and S. Cavallaro, "Biolubricant product development," pp. 473-526, 2013.

[64] G. D. Galvin, "Lubricants and Lubrication," in *Mechanical Engineer's Reference Book (Eleventh Edition)*, A. Parrish, Ed., Butterworth-Heinemann, pp. 14–2, 1973

List of Bibliography (Continued

[65] C. Li *et al.*, "Increased torulene accumulation in red yeast *Sporidiobolus pararoseus* NGR as stress response to high salt conditions," *Food Chemistry*, vol. 237, pp. 1041–1047, 2017.

[66] R. Fu, Q. Fei, L. Shang, C. J. Brigham, and H. N. Chang, "Enhanced microbial lipid production by *Cryptococcus albidus* in the high-cell-density continuous cultivation with membrane cell recycling and two-stage nutrient limitation," *Journal of Industrial Microbiology and Biotechnology*, vol. 45, no. 12, pp. 1045–1051, 2018.

[67] Y. Taoka, N. Nagano, Y. Okita, H. Izumida, S. Sugimoto, and M. Hayashi, "Effect of Tween 80 on the growth, lipid accumulation and fatty acid composition of *Thraustochytrium aureum* ATCC 34304," *Journal of Bioscience and Bioengineering*, vol. 111, no. 4, pp. 420–424, 2011.

[68] J. Xu, W. Du, X. Zhao, and D. Liu, "Renewable microbial lipid production from oleaginous yeast: some surfactants greatly improved lipid production of *Rhodosporidium toruloides*," *Microbiology and Microbial Biotechnology*, vol. 32, no. 7, p. 107, 2016.

[69] G. Singh, S. Sinha, K. K. Kumar, N. A. Gaur, K. K. Bandyopadhyay, and D. Paul, "High density cultivation of oleaginous yeast isolates in 'mandi' waste for enhanced lipid production using sugarcane molasses as feed," *Fuel*, vol. 276, p. 118073, 2020.

[70] G. Singh, A. Jawed, D. Paul, K. K. Bandyopadhyay, A. Kumari, and S. Haque, "Concomitant production of lipids and carotenoids in *Rhodosporidium toruloides* under osmotic stress using response surface methodology," *Frontiers in Microbiology*, vol. 7, p. 1686, 2016.

[71] C. U. Mussagy *et al.*, "Selective recovery and purification of carotenoids and fatty acids from *Rhodotorula glutinis* using mixtures of biosolvents," *Separation and Purification Technology*, vol. 266, p. 118548, 2021.

List of Bibliography (Continued)

[72] Y. Taoka, N. Nagano, Y. Okita, H. Izumida, S. Sugimoto, and M. Hayashi, "Effect of Tween 80 on the growth, lipid accumulation and fatty acid composition of *Thraustochytrium aureum* ATCC 34304," *Journal of Bioscience and Bioengineering*, vol. 111, no. 4, pp. 420–424, 2011.

[73] L. Liu, M. Zong, Y. Hu, N. Li, W. Lou, and H. Wu, "Efficient microbial oil production on crude glycerol by *Lipomyces starkeyi* AS 2.1560 and its kinetics," *Process Biochemistry*, vol. 58, pp. 230–238, 2017.

[74] J. Xu, X. Zhao, W. Wang, W. Du, and D. Liu, "Microbial conversion of biodiesel byproduct glycerol to triacylglycerols by oleaginous yeast *Rhodosporidium toruloides* and the individual effect of some impurities on lipid production," *Biochemical Engineering Journal*, vol. 65, pp. 30–36, 2012.

[75] S. M. Choudhari, L. Ananthanarayan, and R. S. Singhal, "Use of metabolic stimulators and inhibitors for enhanced production of β-carotene and lycopene by *Blakeslea trispora* NRRL 2895 and 2896," *Bioresource Technology*, vol. 99, no. 8, pp. 3166–3173, 2008.

[76] Z. He *et al.*, "β-Carotene production promoted by ethylene in *Blakeslea trispora* and the mechanism involved in metabolic responses," *Process Biochemistry*, vol. 57, pp. 57–63, 2017.

[77] B. K. Uprety, M. Samavi, and S. K. Rakshit, "Contribution of specific impurities in crude glycerol towards improved lipid production by *Rhodosporidium toruloides* ATCC 10788," *Bioresource Technology Reports*, vol. 3, pp. 27–34, 2018.

[78] N. Bansal, D. Dasgupta, S. Hazra, T. Bhaskar, A. Ray, and D. Ghosh, "Effect of utilization of crude glycerol as substrate on fatty acid composition of an oleaginous yeast *Rhodotorula mucilagenosa* IIPL32: Assessment of nutritional indices," *Bioresource Technology*, vol. 309, p. 123330, 2020.

List of Bibliography (Continued)

[79] M. Guerfali, I. Ayadi, H.-E. Sassi, A. Belhassen, A. Gargouri, and H. Belghith, "Biodiesel-derived crude glycerol as alternative feedstock for single cell oil production by the oleaginous yeast *Candida viswanathii* Y-E4," *Industrial Crops and Products*, vol. 145, p. 112103, 2020.

[80] M. Á. Villegas-Méndez, J. Montañez, J. C. Contreras-Esquivel, I. Salmerón, A. A. Koutinas, and L. Morales-Oyervides, "Scale-up and fed-batch cultivation strategy for the enhanced co-production of microbial lipids and carotenoids using renewable waste feedstock," *Journal of Environmental Management*, vol. 339, p. 117866, 2023.

[81] A. M. Kot, S. Błażejak, M. Kieliszek, I. Gientka, K. Piwowarek, and R. Brzezińska, "Production of lipids and carotenoids by *Rhodotorula gracilis* ATCC 10788 yeast in a bioreactor using low-cost wastes," *Biocatalysis and Agricultural Biotechnology*, vol. 26, p. 101634, 2020.

[82] S. Sarantou, N. G. Stoforos, O. Kalantzi, and S. Papanikolaou, "Biotechnological valorization of biodiesel-derived glycerol: Trials with the non-conventional yeasts *Yarrowia lipolytica* and *Rhodosporidium sp*," *Carbon Resources Conversion*, vol. 4, pp. 61–75, 2021.

[83] Z. Liu, F. Natalizio, G. Dragone, and S. I. Mussatto, "Maximizing the simultaneous production of lipids and carotenoids by *Rhodosporidium toruloides* from wheat straw hydrolysate and perspectives for large-scale implementation," *Bioresource Technology*, vol. 340, p. 125598, 2021.

[84] G. Gong, X. Zhang, and T. Tan, "Simultaneously enhanced intracellular lipogenesis and β-carotene biosynthesis of *Rhodotorula glutinis* by light exposure with sodium acetate as the substrate," *Bioresource Technology*, vol. 295, p. 122274, 2020.

List of Bibliography (Continued)

[85] K. Ngernsombat, S. Khuntong, T. Samranrit, D. Kaewpa, J. Teeka, and A. Areesirisuk, "Boosting concurrent yeast oil production and secretion by *Rhodosporidium toruloides* through non-ionic surfactant addition and gene expression monitoring," *Biochemical Engineering Journal*, vol. 202, p. 109159, 2024.

[86] S. Khuntong *et al.*, "Synergistic effects of Tween 20 and ethephon on yeast oil and β-carotene co-production by *Rhodosporidium toruloides* using purified biodiesel-derived crude glycerol as an alternative carbon source," *Bioresource Technology*, vol. 422, p. 132211, 2025.

[87] C. Rakkitkanphun, J. Teeka, D. Kaewpa, and A. Areesirisuk, "Purification of biodiesel-derived crude glycerol by acidification to be used as a carbon source for microbial oil production by oleaginous yeast *Pseudozyma parantarctica* CHC28," *Biomass Conversion and Biorefinery.*, vol. 13, no. 17, pp. 15381–15391, 2023.

[88] T. Samranrit, J. Teeka, K. Ngernsombat, C.-H. Chiu, D. Kaewpa, and A. Areesirisuk, "Modulation of yeast oil production by *Pseudozyma parantarctica* CHC28 using xylose and organic acids and its conversion feasibility to bio-polyurethane foam," *Biochemical Engineering Journal*, vol. 198, p. 109025, 2023.

[89] S. Majumdar, T. Mandal, and D. Dasgupta Mandal, "Production kinetics of β-carotene from *Planococcus sp.* TRC1 with concomitant bioconversion of industrial solid waste into crystalline cellulose rich biomass," *Process Biochemistry*, vol. 92, pp. 202–213, 2020.

[90] O. Ghorbel-Bellaaj *et al.*, "Shrimp waste fermentation with *Pseudomonas aeruginosa* A2: Optimization of chitin extraction conditions through Plackett–Burman and response surface methodology approaches," *International Journal of Biological Macromolecules*, vol. 48, no. 4, pp. 596–602, 2011.

List of Bibliography (Continued)

[91] Y. Cui, J. W. Blackburn, and Y. Liang, "Fermentation optimization for the production of lipid by *Cryptococcus curvatus*: Use of response surface methodology," *Biomass and Bioenergy*, vol. 47, pp. 410–417, 2012.

[92] E. G. Bligh and W. J. Dyer, "A rapid method of total lipid extraction and purification," *Canadian Journal of Biochemistry and Physiology.*, vol. 37, no. 8, pp. 911–917, 1959.

[93] C. Rakkitkanphun, J. Teeka, D. Kaewpa, and A. Areesirisuk, "Purification of biodiesel-derived crude glycerol by acidification to be used as a carbon source for microbial oil production by oleaginous yeast *Pseudozyma parantarctica* CHC28," *Biomass Conversion and Biorefinery.*, 2021.

[94] S. Allahkarami, A. A. Sepahi, H. Hosseini, and M. R. Razavi, "Isolation and identification of carotenoid-producing *Rhodotorula sp.* from Pinaceae forest ecosystems and optimization of in vitro carotenoid production," *Biotechnology Reports*, vol. 32, p. e00687, 2021.

[95] J. L. Smith, P. M. Fratamico, and N. W. Gunther, "Shiga Toxin-Producing *Escherichia coli*," in *Advances in Applied Microbiology*, vol. 86, Elsevier, pp. 145–197, 2014.

[96] G. Wei, Y. Li, G. Du, and J. Chen, "Effect of surfactants on extracellular accumulation of glutathione by *Saccharomyces cerevisiae*," *Process Biochemistry*, vol. 38, no. 8, pp. 1133–1138, 2003.

[97] G. Singh, A. Jawed, D. Paul, K. K. Bandyopadhyay, A. Kumari, and S. Haque, "Concomitant Production of Lipids and Carotenoids in *Rhodosporidium toruloides* under Osmotic Stress Using Response Surface Methodology," *Frontiers in Microbiology.*, vol. 7, 2016.

[98] S. M. Choudhari, L. Ananthanarayan, and R. S. Singhal, "Use of metabolic stimulators and inhibitors for enhanced production of β-carotene and lycopene by *Blakeslea trispora* NRRL 2895 and 2896," *Bioresource Technology*, vol. 99, no. 8, pp. 3166–3173, 2008.

List of Bibliography (Continued)

[99] K. Vijay, R. Varunraj, U. Priyadharshini, T. Ramya, and S. Balamurugan, "Sodium oleate potentiates the concurrent overproduction of lipids and carotenoids in *Chlorella vulgaris* towards biofuel and nutraceutical applications," *Fuel*, vol. 346, p. 128307, 2023.

[100] Z. He *et al.*, "β-Carotene production promoted by ethylene in *Blakeslea trispora* and the mechanism involved in metabolic responses," *Process Biochemistry*, vol. 57, pp. 57–63, 2017.

[101] J. Hurter, M. Manser, and B. Zimmerli, "A rapid and simple method for the determination of residues of 2-chloroethylphosphonic acid (ethephon) in tomatoes, cherries, and apples," *Journal of Agricultural and Food Chemistry.*, vol. 26, no. 2, pp. 472–475, 1978.

[102] I. Marova, A. Haronikova, S. Petrik, T. Dvorakova, and E. Breierova, "Production of enriched biomass by red yeasts of *Sporobolomyces sp*. grown on waste substrates," *Journal of Microbiology, Biotechnology and Food Sciences*, vol. 1, no. 4, pp. 534–551, 2012.

[103] P. P. Pawar, A. A. Odaneth, R. N. Vadgama, and A. M. Lali, "Simultaneous lipid biosynthesis and recovery for oleaginous yeast *Yarrowia lipolytica*," *Biotechnology for Biofuels*, vol. 12, no. 1, p. 237, 2019.

[104] X.-F. Huang, Y.-H. Wang, Y. Shen, K.-M. Peng, L.-J. Lu, and J. Liu, "Using non-ionic surfactant as an accelerator to increase extracellular lipid production by oleaginous yeast *Cryptococcus curvatus* MUCL 29819," *Bioresource Technology*, vol. 274, pp. 272–280, 2019.

[105] P. Xiaowei and C. Hongzhang, "Hemicellulose sugar recovery from steam-exploded wheat straw for microbial oil production," *Process Biochemistry*, vol. 47, no. 2, pp. 209–215, 2012.

List of Bibliography (Continued)

[106] M. Á. Villegas-Méndez, J. Montañez, J. C. Contreras-Esquivel, I. Salmerón, A. A. Koutinas, and L. Morales-Oyervides, "Scale-up and fed-batch cultivation strategy for the enhanced co-production of microbial lipids and carotenoids using renewable waste feedstock," *Journal of Environmental Management*, vol. 339, p. 117866, 2023.

[107] T. M. Parreira, C. Freitas, A. Reis, J. Roseiro, and T. L. Da Silva, "Carbon concentration and oxygen availability affect lipid and carotenoid production by carob pulp syrup-grown *Rhodosporidium toruloides* NCYC 921," *Engineering in Life Sciences*, vol. 15, no. 8, pp. 815–823, 2015.

[108] Z. Wen, S. Zhang, C. K. Odoh, M. Jin, and Z. K. Zhao, "*Rhodosporidium toruloides* - A potential red yeast chassis for lipids and beyond," *FEMS Yeast Research*, vol. 20, no. 5, 2020.

[109] M. M. Don and N. F. Shoparwe, "Kinetics of hyaluronic acid production by *Streptococcus zooepidemicus* considering the effect of glucose," *Biochemical Engineering Journal*, vol. 49, no. 1, pp. 95–103, 2010.

[110] H. Li, X. Ma, Q. Zhang, W. Luo, Y. Wu, and X. Li, "Enhanced butanol production by solvent tolerance *Clostridium acetobutylicum* SE25 from cassava flour in a fibrous bed bioreactor," *Bioresource Technology*, vol. 221, pp. 412–418, 2016.

[111] J. P. López-Gómez, M. Alexandri, R. Schneider, and J. Venus, "A review on the current developments in continuous lactic acid fermentations and case studies utilising inexpensive raw materials," *Process Biochemistry*, vol. 79, pp. 1–10, Apr. 2019.

[112] Y. Tashiro, K. Takeda, G. Kobayashi, and K. Sonomoto, "High production of acetone–butanol–ethanol with high cell density culture by cell-recycling and bleeding," *Journal of Biotechnology*, vol. 120, no. 2, pp. 197–206, 2005.

[113] M. A. Abdel-Rahman, Y. Tashiro, and K. Sonomoto, "Recent advances in lactic acid production by microbial fermentation processes," *Biotechnology Advances*, vol. 31, no. 6, pp. 877–902, 2013.

List of Bibliography (Continued)

[114] T. Koga *et al.*, "Dilution rates and their transition modes influence organic acid productivity and bacterial community structure on continuous meta-fermentation using complex microorganisms," *Journal of Bioscience and Bioengineering*, vol. 136, no. 5, pp. 391–399, 2023.

[115] T. De Vrije, M. Budde, H. Van Der Wal, P. A. M. Claassen, and A. M. López-Contreras, "'In situ' removal of isopropanol, butanol and ethanol from fermentation broth by gas stripping," *Bioresource Technology*, vol. 137, pp. 153–159, 2013.

[116] J. Lipovsky, P. Patakova, L. Paulova, T. Pokorny, M. Rychtera, and K. Melzoch, "Butanol production by *Clostridium pasteurianum* NRRL B-598 in continuous culture compared to batch and fed-batch systems," *Fuel Processing Technology*, vol. 144, pp. 139–144, 2016.

[117] P. Polburee, W. Yongmanitchai, N. Lertwattanasakul, T. Ohashi, K. Fujiyama, and S. Limtong, "Characterization of oleaginous yeasts accumulating high levels of lipid when cultivated in glycerol and their potential for lipid production from biodiesel-derived crude glycerol," *Fungal Biology*, vol. 119, no. 12, pp. 1194–1204, 2015.

[118] S. H. Duarte, M. Ansolin, and F. Maugeri, "Cultivation of *Candida sp*. LEB-M3 in glycerol: Lipid accumulation and prediction of biodiesel quality parameters," *Bioresource Technology*, vol. 161, pp. 416–422, 2014.

[119] F. Spier, J. G. Buffon, and C. A. V. Burkert, "Bioconversion of raw glycerol generated from the synthesis of biodiesel by different oleaginous yeasts: Lipid content and fatty acid profile of biomass," *Indian Journal of Microbiology Research*, vol. 55, no. 4, pp. 415–422, 2015.

[120] S. K. Hoekman, A. Broch, C. Robbins, E. Ceniceros, and M. Natarajan, "Review of biodiesel composition, properties, and specifications," *Renewable and Sustainable Energy Reviews*, vol. 16, no. 1, pp. 143–169, 2012.

List of Bibliography (Continued)

[121] P. Polburee *et al.*, "Lipid production from biodiesel-derived crude glycerol by *Rhodosporidium fluviale* DMKU-RK253 using temperature shift with high cell density," *Biochemical Engineering Journal*, vol. 112, pp. 208–218, 2016.

[122] S. K. Bhatia *et al.*, "Microbial biodiesel production from oil palm biomass hydrolysate using marine *Rhodococcus sp.* YHY01," *Bioresource Technology*, vol. 233, pp. 99–109, 2017.

[123] T. Samranrit, J. Teeka, K. Ngernsombat, C.-H. Chiu, D. Kaewpa, and A. Areesirisuk, "Modulation of yeast oil production by *Pseudozyma parantarctica* CHC28 using xylose and organic acids and its conversion feasibility to bio-polyurethane foam," *Biochemical Engineering Journal*, vol. 198, p. 109025, 2023.

[124] A. Papadaki *et al.*, "Production of wax esters via microbial oil synthesis from food industry waste and by-product streams," *Bioresource Technology*, vol. 245, pp. 274–282, 2017.

[125] S. Peranginangin, H. B. Sembiring, Y. V. M. Nainggolan, N. S. Sihotang, and H. Wijoyo, "Fatty acid methyl ester (FAME) production from sludge solid waste as K_2O/SiO_2 catalyst," *Case Studies in Chemical and Environmental Engineering*, vol. 10, p. 100933, 2024.

[126] M. Wennman, M. Hellberg, A. J. Svagan, and M. S. Hedenqvist, "A biobased binder of emulsion type that provides unique and durable wet strength and hydrophobicity to paper and nonwoven," *Industrial Crops and Products*, vol. 193, p. 116126, 2023.

[127] N. Jeyakumar, B. Narayanasamy, D. Balasubramanian, and K. Viswanathan, "Characterization and effect of *Moringa Oleifera* Lam. antioxidant additive on the storage stability of Jatropha biodiesel," *Fuel*, vol. 281, p. 118614, 2020.

[128] B. K. Uprety, J. V. Reddy, S. S. Dalli, and S. K. Rakshit, "Utilization of microbial oil obtained from crude glycerol for the production of polyol and its subsequent conversion to polyurethane foams," *Bioresource Technology*, vol. 235, pp. 309–315, 2017.

List of Bibliography (Continued)

[129] A. Papadaki *et al.*, "Bioprocess development for biolubricant production using microbial oil derived via fermentation from confectionery industry wastes," *Bioresource Technology*, vol. 267, pp. 311–318, 2018.

[130] B. B. Makut, G. Goswami, and D. Das, "Evaluation of bio-crude oil through hydrothermal liquefaction of microalgae-bacteria consortium grown in open pond using wastewater," *Biomass Conversion and Biorefinery.*, vol. 12, no. 7, pp. 2567–2581, 2022.

[131] İ. Uzun, İ. Orak, Ö. Sevgili, E. Yiğit, and M. Karakaplan, "Synthesis of canthaxanthin from β-carotene and evaluation of both substances in diode construction," *Journal of Materials Science: Materials in Electronics*, vol. 33, no. 4, pp. 1888–1898, 2022.

[132] B. Y. Lamba, S. V. Shah, R. Sharma, A. K. Tiwari, S. Jain, and S. Kumar, "A pilot scale hydrothermal liquefaction of sewage water grown Chlorella sorokiniana for bio-oil production—a sustainable integrated approach," *Biomass Conversion and Biorefinery.*, vol. 14, no. 17, pp. 20321–20331, 2024.

[133] T. Samranrit *et al.*, "Sustainable production of yeast oil from rice straw hydrolysate by *Pseudozyma parantarctica* through fed-batch cultivation for bio-polyurethane foam formation," *Bioresource Technology Reports*, vol. 27, p. 101892, 2024.

[134] S. Michael, *Szycher's Handbook of Polyurethanes*. Florida: CRC Press, Taylor & Francis, 2013.

[135] C. S. Carriço, T. Fraga, and V. M. D. Pasa, "Production and characterization of polyurethane foams from a simple mixture of castor oil, crude glycerol and untreated lignin as bio-based polyols," *European Polymer Journal*, vol. 85, pp. 53–61, 2016.

[136] N. E. Marcovich, M. Kurańska, A. Prociak, E. Malewska, and K. Kulpa, "Open cell semi-rigid polyurethane foams synthesized using palm oil-based bio-polyol," *Industrial Crops and Products*, vol. 102, pp. 88–96, 2017.

[137] J. Guo, P. Li, L. Kong, and B. Xu, "Microencapsulation of curcumin by spray drying and freeze drying," *Learning with Technologies*, vol. 132, p. 109892, 2020.

List of Bibliography (Continued)

[138] J. Stabrauskiene, L. Pudziuvelyte, and J. Bernatoniene, “Optimizing encapsulation: comparative analysis of spray-drying and freeze-drying for sustainable recovery of bioactive compounds from *Citrus x paradisi* L. Peels,” *Pharmaceuticals*, vol. 17, no. 5, p. 596, 2024.

[139] B. Muhoza, H. Yuyang, A. Uriho, J. D. Harindintwali, Q. Liu, and Y. Li, “Spray- and freeze-drying of microcapsules prepared by complex coacervation method: A review,” *Food Hydrocolloids*, vol. 140, p. 108650, 2023

[140] C. K. Van, P. T. N. Nguyen, T.-T. T. Nguyen, and L. G. Bach, “Microencapsulation of *Citrus latifolia* peel essential oil by spray-drying using maltodextrin: Characterization, antimicrobial activities, and release profile,” *LWT*, vol. 197, p. 115825, 2024.

Biography

Name - Surname	Miss Sasitorn Khuntong
Date of Birth	March 10, 2000
Address	25, M. 14, Lumlukka, Lumlukka, Pathum Tani, 12150, Thailand
Education	Mater of Science (Applied Biology Program) (2022-2024)
Telephone Number	082-946-8382
Email address	sasitorn_kh@rmutt.ac.th